Theoretical Chemistry

A thesis

submitted in partial fulfilment

of the requirements for the Degree

of

Doctor of Philosophy in Chemistry

in the

University of Canterbury

by

Pravit Sudkeaw

University of Canterbury

1991

The problem with computers is that they only give answers

-attributed to P. Picasso

Contents

List of Tables

List of Figures

Abstract

Ab initio Molecular Orbital and Valence-Bond methods and the semiempirical, AM1 method are applied in the studies of:

1. The proton affinity of diacetylene

The gas-phase ion-molecule reaction between diacetylene and a proton was studied theoretically at the MP4SDQ/6-311G** level. The geometries, calculated harmonic vibrational frequencies and the proton affinity of the most stable structures are reported. The results from this study are supported by selected ion flow tube measurements and are compared with other calculations

2. The gas-phase reaction of CH_3CN and CH_3^+

The reaction between CH_3CN and CH_3^+ was studied at the MP4SDQ/6-31G* level of theory in order to determine the products and establish the multistep dissociation pathway of the reaction. The location and height of the transition states in the process is used as a criteria for the feasibility of the proposed pathway. The result is compared with the experimental and theoretical studies of the same system done by Wincel and coworkers [146].

3. The geometries and force constants of small-sized organotin compounds

The calculations on 12 small-sized organotin compounds were done at the HF/3-21G* level of theory. The objective of this study was to provide the force constants of Sn-X and X-Sn-Y types for the use in Molecular Mechanic calculations of organotin compounds. The calculated geometries and harmonic vibrational frequencies of stannane and methyl stannane are compared with experimental results in order to measure the reliability of the calculations.

4. The chemical properties of C_nO, C_nO^+, C_nHO^+, C_nS, C_nS^+ and C_nHS^+ species in the instellar clouds

C_nO and C_nS when n = 2 and 3 have been reported to be found in some interstellar clouds. These species in such environments are subjected to ionization and protonation processes. Theoretical studies of these species were done at the

MP4SDQ/6-311G** level of theory. The calculations suggest that these species are more stable in protonated forms and could be intermediates of some steady state processes.

5. Theoretical study of $C_6H_4^+$ formation in acetylenic flames

$C_6H_4^+$ has been detected as an intermediate in acetylenic flames. The semiempirical AM1 method was used to determine the most stable products and to establish a chemical mechanism of the reaction between $C_4H_2^+$ and C_2H_2. The results from AM1 method were refined by ab initio calculations at the HF/4-31G and MP4SDQ/6-31G* level. From this study, only chemical pathways involved acyclic structure isomers are feasible.

6. A Valence-Bond study of BH_2 radical

In this study a Valence-Bond program was used on IBM PC/AT microcomputer to study the correlation between the nuclear bond angle and the angle of hybrid orbitals of BH_2. The energies of BH_2 from the Valence-Bond calculations were also compared with the energies from the Molecular Orbital method at the HF, MP4SDQ and CI level with best orbital energy basis sets, 10s6p/2s1p for boron atom and 6s/1s for hydrogen atoms.

GAUSSIAN series programs, the MICROMOL package, the GAMESS program, a Valence-Bond program and the MOPAC program were used to perform the calculations.

CHAPTER 1

Theories and Computational Methods

Introduction

After nearly eighty years of development, quantum chemistry has come to play an important part in the study of chemical structures and molecular properties. The subject now has become more mature and the study of medium-sized molecules in gaseous phase is practical. Various kinds of calculation are available and can be used by a non-theorist as a guide or a complement to his experiments. Though many theories in quantum chemistry have become more and more complicated, their implementation on digital computers has allowed any chemist with a general background in quantum chemistry and some computer experience to use the calculations.

The two main theories in quantum chemistry are the Molecular Orbital theory (MO) and the Valence-Bond theory (VB). The MO theory is based on the rather physics-type point of view of free electrons moving in a potential field of fixed nuclei whereas the VB theory comes from the chemical bonding idea in which electrons from adjacent atoms use their electrons to build the chemical bonds in forming molecules. Though the VB theory has a longer history and gives better pictures of chemical bonds than the MO theory, most of molecular calculations in the past 30 years use MO theory. This stems from the difficulties in the numerical mathematics and in the finding of a complete set of electron configurations for the input which is required in the VB calculation.

Calculations in quantum chemistry are divided into ab initio methods and semiempirical methods. Ab initio methods require only the structure, geometry and basis functions for the starting parameters. The calculations then follow the relevant theory. In the semiempirical method, some required values such as one-electron integrals are deduced from experimental values, while some values like overlap integrals may be neglected on the basis of their small contribution in some types of calculation. This difference makes the ab initio method more rigorous theoretically but too expensive for molecules of medium size or larger. The semiempirical method is suitable and much cheaper for calculations on large molecules. In many cases it can yield good results when users are aware of its limitations.

This thesis is concerned with the application of both MO and VB theory. All calculation were done at the ab initio level except topic 5 in which semiempirical AM1 method was employed after convergence difficulties occurred.

The topics are:

1. The proton affinity of diacetylene.
2. The reaction of CH_3CN and CH_3^+.
3. The theoretical study of chemical properties of small-sized organotin compounds.
4. The chemical properties of C_nO, C_nO^+, C_nHO^+, C_nS, C_nS^+ and C_nHS^+ species in the interstellar clouds.
5. Theoretical study of $C_6H_4^+$ formation in acetylenic flame.
6 Valence Bond study of the BH_2 radical on an IBM PC.

Projects 1-5 used the GAUSSIAN 82 and GAUSSIAN 90 program [11,53]. Only the project 5, MOPAC version 6.0 [135] was used.

The work on BH_2 used the Micromol Mark III program [28] and a VB program written originally by Maclagan [88].

In this chapter the background and the methods in quantum chemistry that were used in this thesis are discussed only in a broad manner. The full details are avoided because there are many excellent references [26,62,81].

Though the GAUSSIAN program series is well-known, a brief description of its features is given, together with the other two programs.

1.1 Schroedinger Equation

All molecular orbital calculations are approximate solutions of the Schroedinger equation [126]. The equation has its origin in the de Broglie equation:

$$p = \frac{h}{\lambda} \qquad (1.1)$$

which applies to a photon of wavelength λ, momentum $p = mc$, and energy $E = h\nu$. De Broglie postulated that this equation should also apply to particles of matter.

Planck's constant, h, was introduced in the black-body experiment to explain the radiation curves by the equation:

$$E = h\nu \tag{1.2}$$

The frequency of radiation ν is related to the wavelength by the relation:

$$c = \nu\lambda \tag{1.3}$$

where c is the velocity of light.

The Schroedinger equation for a stationary state is the combination of the de Broglie relation and the classical differential equation of a simple harmonic three-dimensional standing wave. The general form of the equation is:

$$\mathbf{H}\Psi = E\Psi \tag{1.4}$$

The Hamiltonian operator, **H** is defined as

$$\mathbf{H} = \mathbf{T} + \mathbf{V} \tag{1.5}$$

The kinetic energy operator, **T**, is a sum of differential operators,

$$\mathbf{T} = -\frac{h^2}{8\pi^2} \sum_i \frac{1}{m_i} \left(\frac{\partial^2}{\partial x_i^2} + \frac{\partial^2}{\partial y_i^2} + \frac{\partial^2}{\partial z_i^2} \right) \tag{1.6}$$

The sum is over all particles i, which here are electrons and nuclei, and m_i is the mass of each particle.

The potential energy operator, **V** is the coulomb interaction operator,

$$\mathbf{V} = \sum_{i<} \sum_j \left(\frac{e_i e_j}{r_{ij}} \right) \tag{1.7}$$

The sum is over distinct pairs of particles (i,j) with electric charges e_i and e_j. The parameter r_{ij} is the distance between the two particles. The Hamiltonian in this equation is classified as a non-relativistic one.

The Schroedinger equation for any molecule will have many solutions, corresponding to different stationary states. The ground state is the state with lowest energy. From these solutions the information about energies and other properties of molecules can be obtained.

Born-Oppenheimer approximation [14] is used to simplify the Schroedinger equation as

$$\mathbf{H}^{elec}\,\Psi^{elec}(\mathbf{r},\mathbf{R}) = E^{eff}(\mathbf{R})\,\Psi^{elec}(\mathbf{r},\mathbf{R}) \tag{1.8}$$

which corresponds to the motion of electrons in the field of fixed nuclei.

Ψ^{elec} is the electronic wavefunction and the Hamiltonian, $\mathbf{H}^{elec}$, is defined as

$$\mathbf{H}^{elec} = \mathbf{T}^{elec} + \mathbf{V} \tag{1.9}$$

where $\mathbf{T}^{elec}$ is the electronic kinetic energy,

$$\mathbf{T}^{elec} = -\left(\frac{h^2}{8\pi^2 m_e}\right) \sum_{i}^{electrons} \left(\frac{\partial^2}{\partial x_i^2} + \frac{\partial^2}{\partial y_i^2} + \frac{\partial^2}{\partial z_i^2}\right) \tag{1.10}$$

and $\mathbf{V}$ is the coulomb potential energy,

$$\mathbf{V} = -\sum_{i}^{electrons}\sum_{s}^{nuclei}\left(\frac{Z_s e^2}{r_{is}}\right) + \sum_{i<j}^{electrons}\left(\frac{e^2}{r_{ij}}\right) + \sum_{s<t}^{nuclei}\left(\frac{Z_s Z_t e^2}{R_{st}}\right) \tag{1.11}$$

In practice, the units of parameter in the Schroedinger equation are changed to atomic unit which makes the equation take a more simple form.

The Bohr radius is defined unit of length as

$$a_0 = \frac{4\pi\varepsilon_0 h^2}{(4\pi^2 m_e e^2)} = 0.529177\ \text{Å} \tag{1.12}$$

and new coordinates (x', y', z') are written as the,

$$x' = \frac{x}{a_0} \tag{1.13}$$

In similar way, a new unit of energy, the hartree, is defined as

$$E_H = \frac{e^2}{4\pi\varepsilon_0 a_0} = 27.2114\ \text{eV}. \tag{1.14}$$

The new energy is given by

$$E' = \frac{E}{E_H} \tag{1.15}$$

The Schroedinger equation in atomic units is

$$\mathbf{H}'\,\Psi' = E'\,\Psi' \tag{1.16}$$

where the Hamiltonian, $\mathbf{H}'$, in the atomic unit, is

$$\mathbf{H}' = -\frac{1}{2}\sum_{i}^{\text{electrons}}\left(\frac{\partial^2}{\partial x'^2_i}+\frac{\partial^2}{\partial y'^2_i}+\frac{\partial^2}{\partial z'^2_i}\right)$$

$$-\sum_{i}^{\text{electrons}}\sum_{s}^{\text{nuclei}}\left(\frac{Z_s}{r'_{is}}\right)+\sum_{i<j}^{\text{electrons}}\left(\frac{1}{r'_{ij}}\right)+\sum_{s<t}^{\text{nuclei}}\left(\frac{Z_s Z_t}{R'_{st}}\right) \qquad (1.17)$$

1.2 Molecular Orbital Theory

In the Molecular Orbital theory, the full wavefunction is approximated by products of one-electron functions (or orbitals). A Cartesian coordinate function for a single electron is assigned as $\psi(x,y,z)$. The spin coordinate, ξ, is included in each molecular orbital to give a complete description. Each spin function can have two spin values $+\frac{1}{2}$ or $-\frac{1}{2}$ in units of $h/2\pi$ with the spin function, $\alpha(\xi)$ align along the positive z axis and $\beta(\xi)$ align along the negative z axis. This will give the equations,

$$\alpha(+\tfrac{1}{2}) = 1 \qquad \alpha(-\tfrac{1}{2}) = 0$$

$$\beta(+\tfrac{1}{2}) = 0 \qquad \beta(-\tfrac{1}{2}) = 1. \qquad (1.18)$$

The combination of a spin function and a Cartesian coordinate function gives a spin orbital, $\chi(x, y, z, \xi)$.

The spin orbitals of n electrons are combined in a determinant which is a wavefunction of the system and also has the required antisymmetric property.

$$\Psi_{\text{determinant}} = (n!)^{-1/2}\begin{vmatrix} \chi_1(1) & \chi_2(1) & \cdots & \chi_n(1) \\ \chi_1(2) & \chi_2(2) & \cdots & \chi_n(2) \\ & & \vdots & \\ \chi_1(n) & \chi_2(n) & \cdots & \chi_n(n) \end{vmatrix} \qquad (1.19)$$

In the usual practice, a set of orthonormal molecular orbitals, $\psi_1, \psi_2, \psi_3, \ldots$, are obtained and then electrons with particular spin functions are assigned to these orbitals. A molecular orbital can accommodate two electrons of different spin, due to the Pauli exclusion principle [100].

The orthonormal molecular orbitals have the properties:

$$S_{ij} = \int \psi_i^* \psi_j \, dxdydz = 0 \quad \text{for } i \neq j$$

and

$$S_{ii} = \int \psi_i^* \psi_i \, dxdydz = 1 \tag{1.20}$$

A full wavefunction for a closed-shell molecule with n (even) electrons, doubly occupying $\frac{n}{2}$ orbitals at the ground state is then represented as:

$$\Psi = (n!)^{-1/2} \begin{vmatrix} \psi_1(1)\alpha(1) & \psi_1(1)\beta(1) & \psi_2(1)\alpha(1) & \dots & \psi_{n/2}(1)\beta(1) \\ \psi_1(2)\alpha(2) & \psi_1(2)\beta(2) & \psi_2(2)\alpha(2) & \dots & \psi_{n/2}(2)\beta(2) \\ & & & \cdot & \\ & & & \cdot & \\ \psi_1(n)\alpha(n) & \psi_1(n)\beta(n) & \psi_2(n)\alpha(n) & \dots & \psi_{n/2}(n)\beta(n) \end{vmatrix} \tag{1.21}$$

This determinant is always referred to as a Slater determinant. $(n!)^{-1/2}$ is the normalizing factor which is added to ensure that,

$$\int \dots \int \Psi^* \Psi \, d\tau_1 d\tau_2 \dots d\tau_n = 1 \tag{1.22}$$

1.3 Basis set

The basis set is a set of functions such that each one is used to represent one electron orbital. A molecular orbital can be built from the basis set, ϕ_1, ϕ_2, ϕ_3.....ϕ_n, as

$$\psi_i = \sum_{\mu=1}^{N} c_{\mu i} \phi_i \tag{1.23}$$

where $c_{\mu i}$ are molecular orbital expansion coefficients.

In the case that atomic orbitals are used as basis functions, the method is called the Linear Combination of Atomic Orbital (LCAO) method.

Two types of basis sets are used in the molecular calculations: Slater-type atomic orbitals (STOs) and Gaussian-type atomic functions (GTFs).

STOs are mostly used for the calculations of wavefunction for atoms or small molecules. They are found to be not suitable for usual molecular calculations because of numerical difficulties. The functions in STOs are labeled like hydrogen atomic orbitals, 1s, 2s, $2p_x$... and have a normalized form,

$$\phi_{1s} = \left(\frac{\zeta_1^3}{\pi}\right)^{1/2} \exp(-\zeta_1 r)$$

$$\phi_{2s} = \left(\frac{\zeta_2^5}{96\pi}\right)^{1/2} r \exp\left(\frac{-\zeta_2 r}{2}\right)$$

$$\phi_{2px} = \left(\frac{\zeta_2^5}{32\pi}\right)^{1/2} x \exp\left(\frac{-\zeta_2 r}{2}\right) \qquad (1.24)$$

.
.
.

where ζ_i are constants called the orbital exponents.

The GTFs functions are powers of x, y and z multiplied by $\exp(-\alpha r^2)$. The constant, α, determines the size of the functions. The first ten normalized GTFs functions are

$$g_s(\alpha, r) = \left(\frac{2\alpha}{\pi}\right)^{3/4} \exp(-\alpha r^2)$$

$$g_x(\alpha, r) = \left(\frac{128\alpha^5}{\pi^3}\right)^{1/4} x \exp(-\alpha r^2)$$

$$g_y(\alpha, r) = \left(\frac{128\alpha^5}{\pi^3}\right)^{1/4} y \exp(-\alpha r^2)$$

$$g_z(\alpha, r) = \left(\frac{128\alpha^5}{\pi^3}\right)^{1/4} z \exp(-\alpha r^2)$$

$$g_{xx}(\alpha, r) = \left(\frac{2048\alpha^7}{9\pi^3}\right)^{1/4} x^2 \exp(-\alpha r^2)$$

$$g_{yy}(\alpha, r) = \left(\frac{2048\alpha^7}{9\pi^3}\right)^{1/4} y^2 \exp(-\alpha r^2)$$

$$g_{zz}(\alpha, r) = \left(\frac{2048\alpha^7}{9\pi^3}\right)^{1/4} z^2 \exp(-\alpha r^2)$$

$$g_{xy}(\alpha, r) = \left(\frac{2048\alpha^7}{\pi^3}\right)^{1/4} xy \exp(-\alpha r^2)$$

$$g_{xz(}\alpha, r) = \left(\frac{2048\alpha^7}{\pi^3}\right)^{1/4} xz \exp(-\alpha r^2)$$

$$g_{yz}(\alpha, r) = \left(\frac{2048\alpha^7}{\pi^3}\right)^{1/4} yz \exp(-\alpha r^2) \qquad (1.25)$$

GTFs functions cannot fully represent atomic orbitals because they do not have a cusp at the origin. It needs a linear combination of several GTFs functions (so-called 'primitive gaussian') to give more suitable basis functions, which are termed as 'contracted gaussians'. An s-type basis function ϕ_μ can be expanded in terms of s-type GTFs as:

$$\phi_\mu = \sum_s d_{\mu s} g_s \qquad (1.26)$$

where the coefficients, $d_{\mu s}$, are fixed.

The three types of basis set that were used in this thesis are:

1. A contracted basis sets 10s6p/2s1p for boron atom and 6s/1s for hydrogen atom were used in the VB calculation of BH_2 molecule. This basis set was taken from Poirier et al. [104] and F.B.v. Duijneveldt [46]. The basis set consists of best-energy -orbital atomic orbitals in term of K primitive gaussian functions:

$$\phi_{nl}(\zeta=1, r) = \sum_{k=1}^{K} d_{nl,k}\, g_l(\alpha_{n,k}, r) \qquad (1.27)$$

For Boron 1s, 2s and 2p orbitals, K = 10, 10 and 6. The scaling factor, ζ was taken as 1.00. The scaling factor, ζ = 1.340 was used for a hydrogen 1s orbital with K = 6.

2. Split-valence basis sets 3-21G, 4-31G and 6-31G which are provided as standard basis sets and used in the calculations on GAUSSIAN 82. Functions in this basis sets are separated into two groups, inner shells and valence shells. Each inner shell is represented by a single function which is composes of K primitive gaussian functions. The general expression for an inner shell function is:

$$\phi_{nl}(r) = \sum_{k=1}^{K} d_{nl,k}\, g_l(\alpha_{n,k}, r) \qquad (1.28)$$

where K = 3, 4, and 6 for the basis sets, 3-21G, 4-31G and 6-31G. The subscripts, n and l are used to specify atomic functions, for example, ϕ_{2s}.

The valence shell is represented by two functions which are expanded in K' and K" gaussian primitives. The general expression for these functions are:

$$\phi_{nl}(r) = \sum_{k=1}^{K'} d_{nl,k} g_l(\alpha_{n,k}, r) \qquad (1.29)$$

and

$$\phi'_{nl}(r) = \sum_{k=1}^{K''} d'_{nl,k}\, g_l(\alpha'_{n,k}, r) \qquad (1.30)$$

where K'=2 and K"=1 in the basis set 3-21G, and so forth.

3. Polarization basis sets 6-31G* and 6-31G**. These basis sets are split-valence type including polarization function which are also provided in GAUSSIAN 82 as standard basis sets. In 6-31G* basis set, a set of polarization functions, of higher angular momentum quantum number (d-type for the first-row heavy atoms, not hydrogen) are added to the split-valence 6-31G basis set. When p-type functions are added to hydrogen in the polarization 6-31G* basis set, it becomes more complete basis set and is termed 6-31G**.

1.4 The Variation method and Hartree-Fock theory

Hartree-Fock theory is used to determine the values of the expansion coefficients of the basis functions in molecular orbitals. The theory is based on the variation method in

quantum mechanics [82]. An expectation value of energy corresponding to Φ which is any antisymmetric normalized function of the electronic co-ordinate, can be written as:

$$E' = \int \Phi^* \mathbf{H} \Phi \, d\tau \tag{1.31}$$

If Φ is the exact wavefunction, Ψ, for the electronic ground state, the energy will be

$$E' = E \int \Psi^* \Psi \, d\tau = E \tag{1.32}$$

In the case that Φ is any other normalized antisymmetric function, it can be shown that

$$E' = \int \Phi^* \mathbf{H} \Phi \, d\tau > E \tag{1.33}$$

In the variation method, the expansion coefficients, $c_{\mu i}$, are adjusted until the lowest value of energy , E', is obtained. This energy will be the closest upper bound to the exact energy within the limitation of the single-determinant wavefunction and the chosen basis set. With this process, it will give the optimum orbitals and the best single-determinant wavefunction, in the energy sense. The variational equation is

$$\frac{\partial E'}{\partial c_{\mu i}} = 0 \qquad \text{for all } \mu \text{ and } i \tag{1.34}$$

1.5 Closed-shell Systems

A consequence of applying the variational condition to the closed-shell wavefunctions (1.21) is the Roothann-Hall equations [60,118]:

$$\sum_{\nu=1}^{N} (F_{\mu\nu} - \varepsilon_i S_{\mu\nu}) c_{\nu i} = 0 \qquad \mu = 1, 2, \ldots N \tag{1.35}$$

with the orthonormality conditions:

$$\sum_{\mu=1}^{N} \sum_{\nu=1}^{N} c^*_{\mu i} S_{\mu\nu} c_{\nu i} = \delta_{\mu\nu} \tag{1.36}$$

The value, ε_i, is the one-electron energy or orbital energy of the molecular orbital, ψ_i.

$S_{\mu\nu}$ are the elements of an N by N overlap matrix:

$$S_{\mu\nu} = \int \phi^*_\mu(1)\phi_\nu(1)\, dx_1 dy_1 dz_1 \tag{1.37}$$

$F_{\mu\nu}$ are the elements of the N x N Fock matrix:

$$F_{\mu\nu} = H^{core}_{\mu\nu} + \sum_{\lambda=1}^{N}\sum_{\sigma=1}^{N} P_{\lambda\sigma}\left[(\mu\nu|\lambda\sigma) - \tfrac{1}{2}(\mu\lambda|\nu\sigma)\right] \tag{1.38}$$

$H^{core}_{\mu\nu}$ is the matrix of the single electron energy in a field of 'bare' nuclei. It is defined as:

$$H^{core}_{\mu\nu} = \int \Phi^* \mathbf{H}\, \Phi d\tau \tag{1.39}$$

where

$$\mathbf{H}(1) = -\frac{1}{2}\left(\frac{\partial^2}{\partial x_1^2} + \frac{\partial^2}{\partial y_1^2} + \frac{\partial^2}{\partial y_1^2}\right) - \sum_{A=1}^{M}\frac{Z_A}{r_{1A}} \tag{1.40}$$

Z_A is the atomic number of atom A and M is a number of atoms in a molecule.

The terms, $(\mu\nu|\lambda\sigma)$, are two-electron integrals,

$$(\mu\nu|\lambda\sigma) = \int\int \phi^*_\mu(1)\phi_\nu(1)\left(\frac{1}{r_{12}}\right)\phi^*_\lambda(2)\phi_\sigma(2)\, dx_1 dy_1 dz_1 dx_2 dy_2 dz_2 \tag{1.41}$$

The density matrix, $P_{\lambda\sigma}$, is defined as:

$$P_{\lambda\sigma} = 2\sum_{i=1}^{occ} c_{\lambda i}\, c^*_{\sigma i} \tag{1.42}$$

The final formula for the molecular electronic energy, E^{ee}, is

$$E^{ee} = \frac{1}{2}\sum_{\mu=1}^{N}\sum_{\nu=1}^{N} P_{\mu\nu}\,(F_{\mu\nu} + H^{core}_{\mu\nu}) \tag{1.43}$$

The electronic energy when added to the nuclear repulsion energy, E_{nr}, will give the total energy of the molecule.

$$E_{nr} = \sum_{A<B}^{M} \sum^{M} \frac{Z_A Z_B}{R_{AB}} \qquad (1.44)$$

An iterative process is needed to solve the Roothaan-Hall equation because the Fock-matrix depends on the molecular orbital coefficients, $c_{\mu i}$, which are also the solutions of the equation. A set of coefficients is first guessed or calculated by a semiempirical method. These values are used as the beginning of a calculation which will generate a new set of coefficients and the energy of the system. The new wavefunction is used for the next iteration until there is no change in either energy value or the density matrix. This give the term 'self-consistent field (SCF) ' to the method.

The full single determinantal wavefunction from the Hartree-Fock method will be improved by using a more complete basis set. This makes the calculated energy lower, approaching the Hartree-Fock limit which lies above the true energy. The limit cannot reach the true energy because a single determinantal wavefunction fails to describe the correlated motion of the electrons and the exchange term in Hartree-Fock Hamiltonian can only be described in terms of correlation. The energy difference between the Hartree-Fock limit and the true energy is termed the correlation energy.

To do a calculation beyond the Hartree-Fock limit, more Slater determinants of other electron configurations must be included in a wavefunction. Configuration Interaction (CI) and Møller-Plesset (MP) [97] are two main methods that are used to obtained multiple determinant wavefunction.

1.6 Open-Shell systems

An open-shell molecule is a molecule that has unpaired electrons, for example, a doublet free radical with one unpaired electron or a triplet molecule with two unpaired electrons. The Roothaan-Hall equations that are used with the closed-shell system need to be modified for the use in the calculation of wavefuctions for open-shell molecules.

Two main methods for the open-shell systems are spin-restricted Hartree-Fock method (RHF) [119] and spin-unrestricted Hartree-Fock method (UHF) [109]. In RHF method, a single set of molecular orbitals is used. Some of the molecular orbitals are doubly-occupied and some are singly-occupied. The electrons in these two sets of molecular orbitals are treated differently in the calculations but the optimization of the system is still based on the variation condition (1.34).

In the UHF method, two different sets of molecular orbitals, ψ_i^α and ψ_i^β, (i = 1,.....,N), are used for α and β electrons. They are defined as:

$$\psi_i^\alpha = \sum_{\mu=1}^{N} c_{\mu i}^{\alpha} \phi_\mu ; \qquad \psi_i^\beta = \sum_{\mu=1}^{N} c_{\mu i}^{\beta} \phi_\mu \qquad (1.45) .$$

This leads to the UHF generalization of the Roothaan-Hall equation:

$$\sum_{\nu=1}^{N} (F_{\mu\nu}^{\alpha} - \varepsilon_i^{\alpha} S_{\mu\nu}) c_{\nu i}^{\alpha} = 0 \qquad i = 1, 2, \ldots, K$$

$$\sum_{\nu=1}^{N} (F_{\mu\nu}^{\beta} - \varepsilon_i^{\beta} S_{\mu\nu}) c_{\nu i}^{\beta} = 0 \qquad \mu = 1,2, \ldots, N. \qquad (1.46)$$

The Fock matrices are now defined by

$$F_{\mu\nu}^{\alpha} = H_{\mu\nu}^{core} + \sum_{\lambda=1}^{N} \sum_{\sigma=1}^{N} [(P_{\lambda\sigma}^{\alpha} + P_{\lambda\sigma}^{\beta})(\mu\nu|\sigma\lambda) - P_{\lambda\sigma}^{\alpha}(\mu\lambda|\sigma\nu)]$$

$$F_{\mu\nu}^{\beta} = H_{\mu\nu}^{core} + \sum_{\lambda=1}^{N} \sum_{\sigma=1}^{N} [(P_{\lambda\sigma}^{\alpha} + P_{\lambda\sigma}^{\beta})(\mu\nu|\sigma\lambda) - P_{\lambda\sigma}^{\beta}(\mu\lambda|\sigma\nu)] \qquad (1.47)$$

The density matrices, $P_{\lambda\sigma}^{\alpha}$ and $P_{\lambda\sigma}^{\beta}$ are:

$$P_{\lambda\sigma}^{\alpha} = \sum_{i=1}^{\alpha occ} c_{\lambda i}^{\alpha *} c_{\sigma i}^{\alpha} ; \qquad P_{\lambda\sigma}^{\beta} = \sum_{i=1}^{\beta occ} c_{\lambda i}^{\beta *} c_{\sigma i}^{\beta} \qquad (1.48)$$

The integrals $S_{\mu\nu}$, $H^{core}_{\mu\nu}$ and $(\mu\nu|\lambda\sigma)$ are defined the same as in the Roothaan-Hall equations for the closed-shell systems.

1.7 Configuration Interaction

If a system of n electrons is described by a basis set of N functions, there will be N each of α and of β spin orbitals. Only n spin orbitals will be filled while 2N - n spin orbitals remain empty. The single-determinant wavefunction for the ground state is:

$$\Psi_0 = (n!)^{-1/2} | \chi_1\chi_2 ...\chi_n| \qquad (1.49)$$

$\chi_1, \chi_2....., \chi_n$ are occupied spin orbitals which are labeled by i, j, k.. subscripts. The unoccupied or virtual spin orbitals, χ_a(a = n+1, n+2, ...2N) are labeled with the subscripts a, b, c...

Determinants other than Ψ_0 can be built by replacing one or more occupied spin orbitals, χ_i, χ_j,.. by virtual orbitals, χ_a, χ_b,.... These new determinants are denoted as Ψ_s with s > 0 and can be classified into single-substitution functions (Ψ^a_i) double-substitution functions (Ψ^{ab}_{ij}), triple-substitution functions (Ψ^{abc}_{ijk}) and so forth due to the number of the replacement of occupied orbitals by virtual ones.

In the full configuration method, a multiple determinant wavefunction can be written as:

$$\Psi = a_0\Psi_0 + \sum_{s>0} a_s\Psi_s \qquad (1.50)$$

The unknown coefficients, a_s, can also be determined by the linear variation method in the equation:

$$\sum_s (H_{st} - E_i\delta_{st})a_{si} = 0 \quad t = 0, 1, 2,.... \qquad (1.51)$$

where H_{st} is a configuration matrix element,

$$H_{st} = \int \int \Psi_s H \Psi_t \, d\tau_1 d\tau_2 .. d\tau_n \qquad (1.52)$$

The full configuration interaction method is usually not practical because a huge number of determinants, (2N!)/[n!(2N - n)!], are involved. This can be resolved by truncating the series at a given level of substitution. If only single substitutions are included, it will be referred as 'Configuration Interaction, Singles' or CIS,

$$\Psi_{CIS} = a_0 \Psi_0 + \sum_{i}^{occ} \sum_{a}^{virt} a_i^a \Psi_i^a \qquad (1.53)$$

This will lead to no improvement to the Hartree-Fock wavefunction because there is no interaction between the ground state wavefunction and the singly-excited state wavefunction due to Brillouin's theorem [19].

The next improvement is Configuration Interaction, Doubles or CID in which only double substitutions are included. The CID wavefunction is,

$$\Psi_{CID} = a_0 \Psi_0 + \sum_{i<}^{occ} \sum_{j}^{} \sum_{a<b}^{virt} \sum a_{ij}^{ab} \Psi_{ij}^{ab} \qquad (1.54)$$

If both single and double substitutions are included, the model is termed Configuration Interaction, Singles and Doubles, or CISD. The wavefunction for CISD is:

$$\Psi_{CISD} = a_0 \Psi_0 + \sum_{i}^{occ} \sum_{a}^{virt} a_i^a \Psi_i^a + \sum_{i<}^{occ} \sum_{j}^{} \sum_{a<b}^{virt} \sum a_{ij}^{ab} \Psi_{ij}^{ab} \qquad (1.55)$$

The calculation process can be reduced further by limiting the number of spin orbitals that are involved. This leads to the terms ' minimum sized window' and 'frozen core approximation' [62].

1.8 Møller-Plesset Perturbation Theory

Perturbation theory is an alternative approach to the correlation problem. In this method the generalized electronic Hamiltonian of the wavefunction is separated into unperturbed and perturbed parts:

$$\mathbf{H}_\lambda = \mathbf{H}_0 + \lambda \mathbf{V} \qquad (1.56)$$

$\mathbf{H}_0$ is the sum of one-electron Fock operators that will give the diagonal matrix with elements,

$$\int \ldots \int \Psi_s \mathbf{H}_0 \Psi_t \, d\tau_1 d\tau_2 \ldots . d\tau_n \tag{1.57}$$

The perturbation, λV, is defined as

$$\lambda V = \lambda(\mathbf{H} - \mathbf{H}_0) \tag{1.58}$$

where $\mathbf{H}$ is the correct Hamiltonian.

If $\lambda = 0$, $\mathbf{H}_\lambda$ is the unperturbed $\mathbf{H}_0$ but if the $\lambda = 1$, $\mathbf{H}_\lambda$ will become the correct Hamiltonian, $\mathbf{H}$. The zero-order Hamiltonian, $\mathbf{H}_0$ is defined as a sum of the one-electron Fock operators in Mϕller-Plesset theory. The value, E_s, is a sum of one-electron energies, ε_i, for the spin orbitals which are occupied in a particular determinant Ψ_s.

According to Rayleigh-Schroedinger perturbation theory [63], the full CI ground state wavefunction and energy of the Hamiltonian $\mathbf{H}_\lambda$ can be expanded in terms of λ as:

$$\Psi_\lambda = \Psi^{(0)} + \lambda\Psi^{(1)} + \lambda^2\Psi^{(2)} + \ldots \tag{1.59}$$

$$E_\lambda = E^{(0)} + \lambda E^{(1)} + \lambda^2 E^{(2)} + \ldots . \tag{1.60}$$

The mixing from other configurations into the ground state appears in the perturbation terms. The limitation of the mixing is due to the highest order energy term allowed in the calculation and is termed as MP2, MP3, ..MPn. This is different from the limited CI method which directly truncates the matrix involved.

The zero-order terms in (1.55) and (1.56) are,

$$\Psi^{(0)} = \Psi_0 \tag{1.61}$$

$$E^{(0)} = \sum_{i}^{occ} \varepsilon_i \tag{1.62}$$

The Mϕller-Plesset energy to first-order is thus the Hartree-Fock energy,

$$E^{(0)} + E^{(1)} = \int \ldots \int \Psi_0 \mathbf{H} \, \Psi_0 d\tau_1 d\tau_2 \ldots . d\tau_n \tag{1.63}$$

and the contribution to the wavefunction is

$$\Psi^{(1)} = \sum_{s>0} (E_0 - E_s)^{-1} V_{s0} \tag{1.64}$$

where V_{s0} are the matrix elements:

$$\int \cdots \int \Psi_s H \Psi_0 \, d\tau_1 d\tau_2 \ldots d\tau_n \tag{1.65}$$

The contributions of the first-order perturbation to the coefficients, a_s, for the wavefunction,

$$\Psi^{(1)} = \sum_{s>0} a_s \Psi_s^{(0)} \tag{1.66}$$

provided that the $\Psi^{(0)}$ is orhogonal to every $\Psi^{(k)}$, are given by

$$a_s^{(1)} = (E_0 - E_s)^{-1} V_{s0} \tag{1.67}$$

As in the CI method, the contribution is non-zero only when s corresponds to a double substitution.

The second-order contribution to the Mϕller-Plesset energy is

$$E^{(2)} = \sum_{s}^{D} (E_0 - E_s)^{-1} |V_{s0}|^2 \tag{1.68}$$

The $E^{(2)}$ is the summation over all double substitutions. V_{s0} is defined as the two-electron integral:

$$V_{s0} = (ij|\,ab) \tag{1.69}$$

and

$$(ij|\,ab) = \int\int \chi_i^*(1)\chi_j^*(2) \left(\frac{1}{r_{12}}\right) [\chi_a(1)\chi_b(2) - \chi_b(1)\chi_a(2)] \, d\tau_1 d\tau_2. \tag{1.70}$$

The second-order contribution to the energy is

$$E^{(2)} = \sum_{i<}^{occ} \sum_{j}^{} \sum_{a<b}^{virt} (\varepsilon_a + \varepsilon_b - \varepsilon_i - \varepsilon_j)^{-1} |(ij|\,ab)|^2 \tag{1.71}$$

and the third-order contribution to the energy is

$$E^{(3)} = \sum_{s}^{D} \sum_{t}^{D} (E_0 - E_s)^{-1}(E_0 - E_t)^{-1} V_{0s}(V_{st} - V_{00}\delta_{st})V_{t0} \tag{1.72}$$

MP4SDQ is the term for the partial fourth-order perturbation calculation that uses single, double and quadruple substitutions only.

The Mϕller-Plesset perturbation method is reliable and effective in most cases but it should be mentioned that the theory, terminated at any order, is no longer variational. This means that the method can give energies that lower than the true one.

1.9 GAUSSIAN Program

GAUSSIAN 70 developed by the group of J.A. Pople at the Carnegie-Mellon Institute, was introduced in 1970 by Quantum Chemistry Program Exchange (QCPE) as the first ab initio program of the GAUSSIAN series. Though there are many limitations in the program, its speed and simplicity of the input structure made it widely used and it quickly gained acceptance among users. Since then the program has been changed, improved and retitled as: GAUSSIAN 76, GAUSSIAN 80, GAUSSIAN 82, GAUSSIAN 85, GAUSSIAN 86, GAUSSIAN 88 and GAUSSIAN90. Since most of the work in this thesis was performed on GAUSSIAN 82, the following discussion of the program structure relates mostly to GAUSSIAN 82 [11].

All programs in GAUSSIAN series share the same essential feature of the calculation processes. The basic input is comprised of three main sections:

1. Geometries written in z-matrix together with charge and spin multiplicity of a molecule.

2. Basis set specification.

3. The type of calculation with the required level of theory.

The calculation then will start at Hartree-Fock level. After the full molecular wavefunction is obtained, the energy gradients are calculated to find the optimized geometry. If the optimization process fails, the calculation process has to go back to the beginning again with a new geometry (see Figure 1.1).

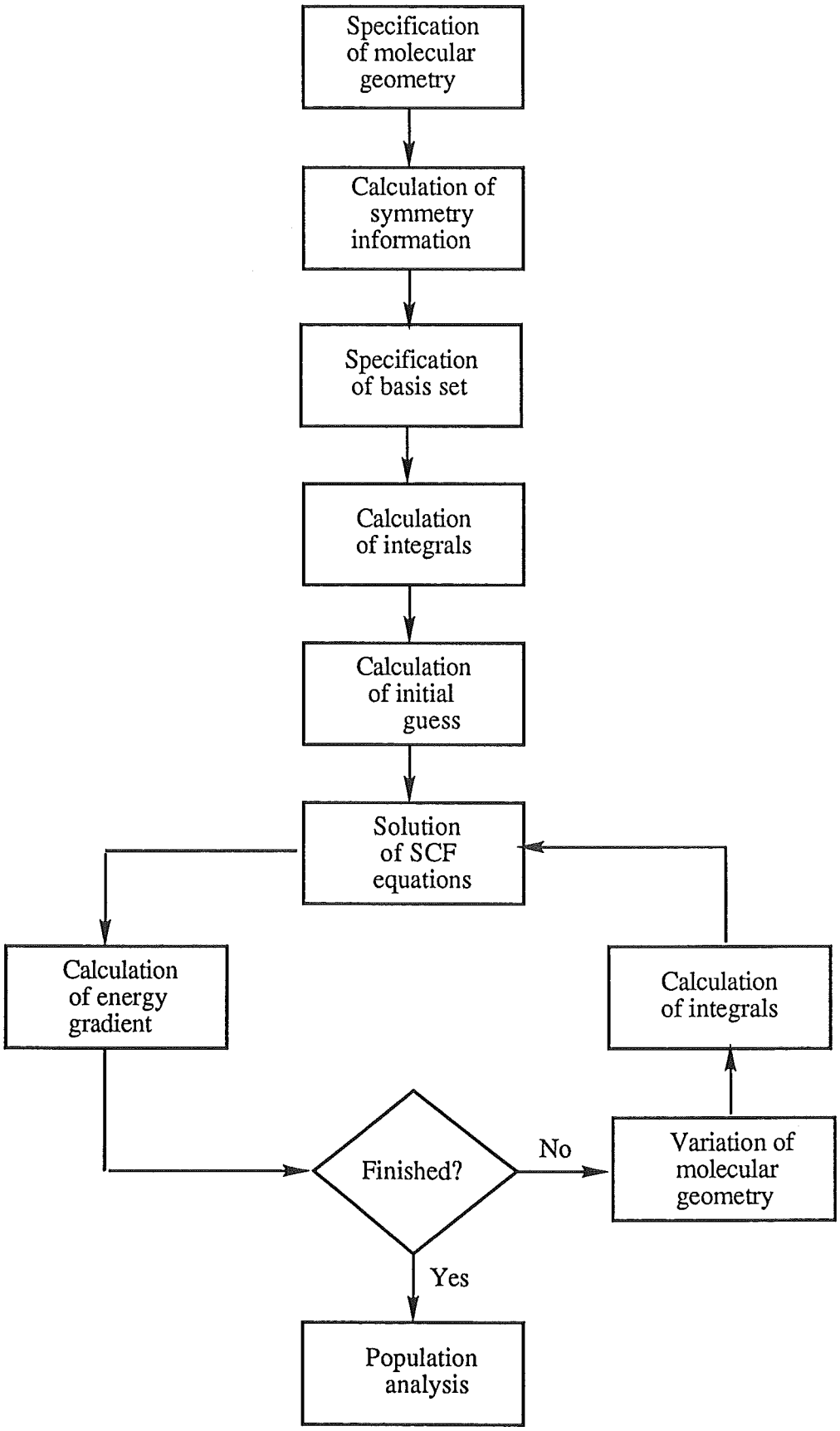

Figure 1.1 Flow diagram for the SCF calculation

GAUSSIAN 82 was developed from its predecessor, GAUSSIAN 80, by including more post-SCF procedures, a new package for calculating electrostatic properties and more standard built-in basis sets. The cutoffs for integrals, SCF convergence criteria and other tolerances were made smaller. This made GAUSSIAN 82 more precise than its predecessor.

GAUSSIAN 82 is made up of 12 overlays in which each one is a group of links. Each link works on a specific task for a part of the whole calculation and has an assigned number for each one. The numbers could be 3 or 4 digits of which the first one or two comprise the overlay number and the last two are the link number. Thus link 301 means that it is link 1 in overlay 3. The overlays in GAUSSIAN 82 are organized as follows:

Overlay 0

The overlay reads the route card then sets up the machine for running the job and defines the sequences of links that are required in the calculation.

Overlay 1

This one is used to set up the geometry and control the optimization procedure. The links in this overlay are

Link 101; reads inputs.

Link 102; controls Fletcher-Powell optimization.

Link 103; controls Berny optimization.

Link 104; controls Murtagh-Sargent optimization.

Link 105; calculates force-constant matrix by finite-difference method.

Overlay 2

This overlay converts the z-matrix produced by overlay 1 to standard cartesian coordinates with the center of mass at the origin and assigns the symmetry of the molecule. This is done by the only link in this overlay, Link 202.

Overlay 3

Overlay 3 is used for assigning the basis set and calculating integrals and their first derivatives by the following links.

Link 301; assigns the basis set from the built-in basis sets or from the supplied input to the atomic centers.

Link 302; calculates one-electron integrals.

Link 303; calculates dipole integrals.

Link 307; calculates one-electron integral derivatives.

Link 310; primitives two-electron integral program.

Link 311; calculates two-electron integrals for s- and p-orbitals.

Link 312; calculates two-electron integrals for s-, p-, and d-orbitals.

Link 314; calculates two-electron integrals for s-,p-,d-, and f-orbitals.

Link 316; calculates two-electron integral derivatives.

Overlay 4

This overlay contains only one link, link 401.

Link 401; produces an initial guess for the SCF procedure by an INDO or extended Huckel calculation.

Overlay 5

The overlay contains links that perform different types of SCF calculation.

Link 501; RHF for closed-shell system.

Link 502; UHF for open-shell system.

Link 503; Direct minimization SCF (SCFDM) for RHF and UHF.

Link 505; RHF for open-shell system (ROHF). This link will be used in the case that link 502 is unreliable because of spin contamination.

Overlay 6

This overlay will analyse the wavefunction, produced from the overlay 5.

Link 601; calculates Mulliken population analysis, Fermi contact analysis for the open-shell system and the dipole moment.

Link 602; calculates one-electron properties such as multiple moments, electric potential, field and field gradient.

Overlay 7

This overlay is used for the first-, second-derivative force constant calculation.

Link 701; calculates first derivatives of one-electron integrals.

Link 702; calculates first derivatives of two-electron integrals for sp functions.

Link 703; calculates first derivatives of two-electron integrals for spd functions.

Link 707; calculates second derivatives of one-electron integrals and sum their contribution into the Hartree-Fock force-constants.

Link 708; calculates second derivatives of two-electron integrals and sum their contribution into the Hartree-Fock force-constants.

Link 716; converts cartesian forces and second derivatives to internal coordinates and communicates with optimization control programs.

Overlay 8

This overlay is used for integral transformations which are required for post-SCF calculations.

Link 801; setup program for transformation of two-electron integrals, produces molecular orbital coefficient matrix and eigenvalues.

Link 802; transforms integrals for closed- and open-shell using N^3 'in-core' algorithm.

Overlay 9

This overlay performs the post-SCF calculations by using the results from overlay 8.

Link 901; forms anti-symmetrized two-electron integrals and computes MP2 energy and first-order MP wavefunction.

Link 902; tests the stability of the Hartree-Fock wavefunction with respect to relaxing of various constraints.

Link 903; is 'in-core' program for closed-shell MP2 calculation.

Link 904; is 'in-core' program for open-shell MP2 calculation.

Link 905: is 'in-core' program for closed-shell complex MP2 calculation.

Link 909; is a setup program for MP3, MP4 or CI calculations.

Link 910-912; perform perturbation calculations or one CI iteration.

Link 913; calculates energies, perform MP4 and test the convergence in the case of CI calculation.

link 918; produces a new and initial guess for less constrained wavefunction if an instability is detected.

Overlay 10

This overlay is used for calculation of the derivatives of the MP2 and CI energies for optimizations.

Link 1001; calculates the two-electron contribution to the MP2 or CI gradients.

Link 1002; produces the derivatives of the MO coefficients from CPHF equation and adds the contribution from CPHF to analytic HF frequencies, CI and MP2 gradients.

Overlay 99

This is the final overlay in any GAUSSIAN 82 job. It produces a summary of the results of the calculation for archiving and reformats arrays for input to other programs.

The schematic diagram, Figure 1.2, shows the route for a closed-shell optimization on GAUSSIAN 82. More detail about this program is available and well documented [26,62].

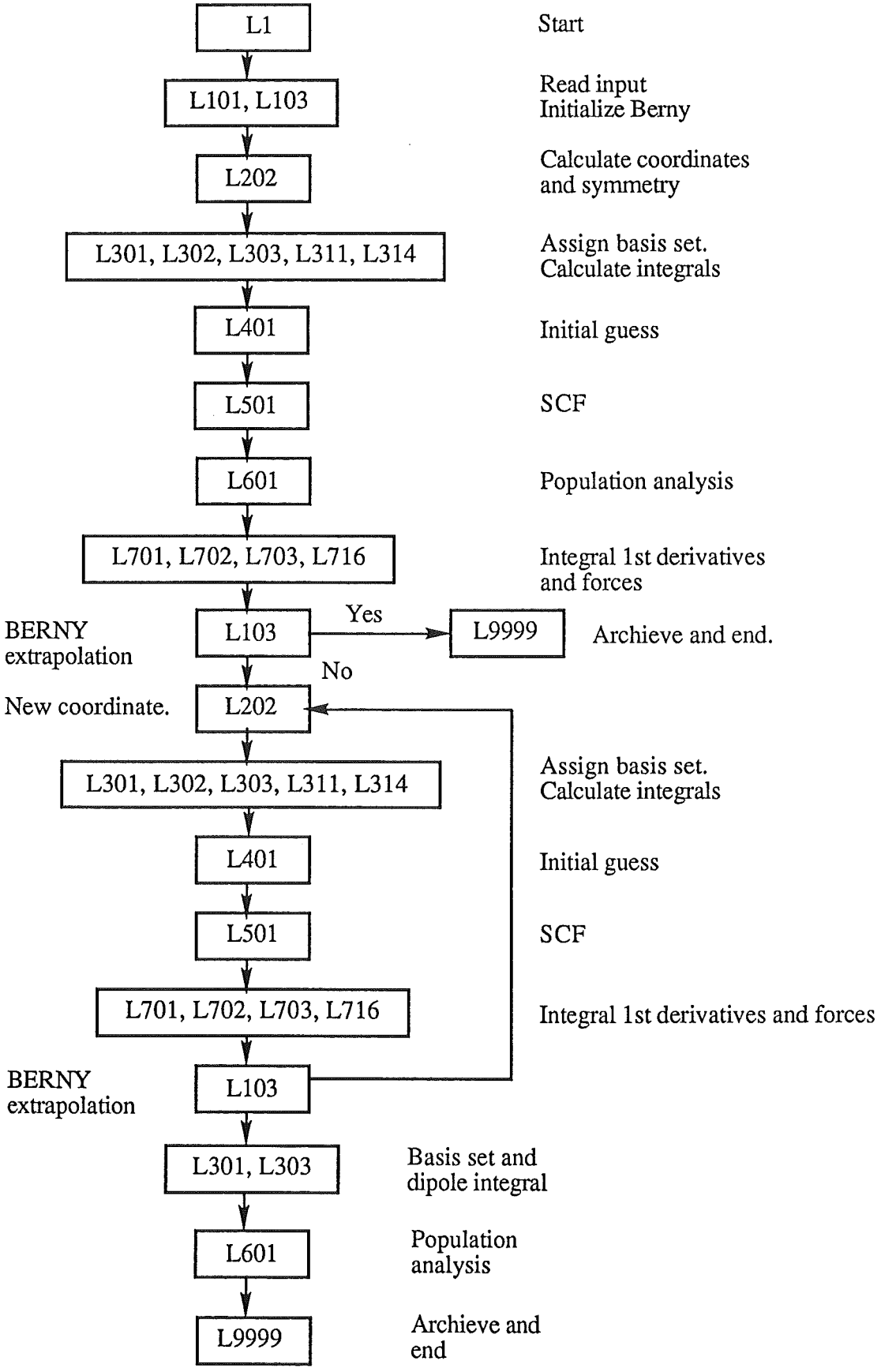

Figure 1.2: Sequence of Links in a Hartree-Fock Optimization

1.10 Micromol Program

This program has been developed in the Department of Theoretical Chemistry, University of Cambridge by S.M. Cowell with the assistance from R.D. Amos, N.C. Handy and A.R. Marshall. It was adapted from the Cambridge Analytic Derivative Package (CADPAC) which itself originated from a version of Dupuis and King's HONDO program [47]. The program was developed on IBM PC/XT and designed to work on microcomputers with 640Kb of accessible memory.

Micromol Mark III, Micromol Mark V and Micromol Mark VI are the three available versions of the program currently. In this work, Micromol Mark III was used for the calculation of one-electron and two-electron integrals which were required as an input for the Valence Bond program.

The capabilities of Micromol Mark III are:

1. the evaluation of one-electron and two-electron integrals over contracted cartesian gaussian basis functions of type s, p and d.

2. SCF calculations for closed-shell wavefunctions.

3. calculation of gradients of the energy.

4. use of the gradients for geometry optimization, and for the calculation of force constants by numerical differentiation.

The principal limitations of the program are:

1. a maximum of 63 basis functions.

2. a maximum of 12 shells.

3. a maximum of 12 atoms

4. a maximum of 10 primitive gaussians in any contracted function.

5. a maximum of 110 unique primitives in total.

1.11 The Valence-Bond method

This method is based on VB theory which was first formulated by Heitler and London [65]. The simple model of this theory is when atoms from infinity come close to form a molecule, the wavefunctions on each atoms will distort from their normal states in isolated atoms in order to provide bonding orbitals. The changes of the wavefunctions can

be interpreted as charge-transfer, spin pairing, promotion into a valence state etc. The deformation of wavefunctions mostly involves the electrons in the valence shell which are able to take part in the bonding process, the orbitals in this method are constructed in order to give physical meaning to how atoms interact to form a molecule rather than to be confined in pure mathematical constraint of orthogonality. Thus the VB orbitals are non-orthogonal, which generates some complicated computational problems, particularly in evaluation of the cofactors of determinant formed in evaluating the overlap integrals between wavefunctions. The 'non-orthogonality' problem was resolved when Prosser and Hagstrom [115] introduced the biorthogonalization technique which directly and efficiently works on non-orthonormal basis orbitals.

In the VB calculation, the eigenvalue equation

$$(\mathbf{H} - ES)\mathbf{C} = 0 \qquad (1.73)$$

has to be solved only once. This is different from Molecular-Orbital theory where one has to performed iterations to solve the eigenvalue equation

$$(\mathbf{F} - \varepsilon S)\mathbf{C} = 0 \qquad (1.74)$$

The eigenvalues E in the VB calculation correspond to spectroscopic states while the ε in MO theory are orbital energies.

Though many efficient matrix methods have been applied to ease the difficulties in the VB method, the MO method is still far more convenient to use and this is the main reason for the domination of the MO theory in the past three decades. The advantage of the VB method emerges when the electron correlation is considered. In the MO-CI method the full expansion limit can be reached only very rarely and very high cost in computation time and for a total number of electrons ranging up to about eight. The use of non-orthogonal orbitals in the most accurate wavefunction which is obtained from the truncate CI expansion, permits a dramatic reduction in the number of terms [27,54,116]. With the advantage of more compact, easily interpretable and accurate wavefunctions, the VB theory has become a serious alternative to molecular orbital calculations.

In this study, the VB theory was used to determine the optimized structure of BH_2.

The aims for working with the Valence-Bond program are:

1. To verify the Valence-Bond calculation on IBM personal computer.

2. To study the concept of computation with the Valence-Bond theory.

1.12 The Valence-Bond program

The package that used in this study originated from Maclagan and Schnuelle's work [88]. It originally was designed to work on main frame computer and was transferred with small changes to fit in IBM personal computer.

In the calculation process in this program, one-electron and two-electron integrals over atomic basis functions, are the same as those used in the MO method but molecular orbitals are never formed. Instead, all the significant Slater determinant wavefunctions involving atomic orbitals are used to construct the Hamiltonian, **H**, and overlap, **S**, matrices. The Hamiltonian operator, **H**, is defined in atomics units as the equation (1.17):

$$\mathbf{H} = -\frac{1}{2}\sum_{i}^{\text{electrons}}\left(\frac{\partial^2}{\partial x'^2_i}+\frac{\partial^2}{\partial y'^2_i}+\frac{\partial^2}{\partial z'^2_i}\right) - \sum_{i}^{\text{electrons}}\sum_{s}^{\text{nuclei}}\left(\frac{Z_s}{r'_{is}}\right)+\sum_{i<j}^{\text{electrons}}\sum\left(\frac{1}{r'_{ij}}\right)+\sum_{s<t}^{\text{nuclei}}\sum\left(\frac{Z_sZ_t}{R'_{st}}\right)$$

The computational scheme was as follow:

1. Evaluation of one-electron and two-electron integrals. This part of calculation was done the program Micromol Mark III which had been described above.

2. Input of details of most important configuration determinants required in the calculation.

3. Evaluation of H and S matrices between all input determinants by using the Presser-Hagstrom biorthogonalization method to evaluate cofactors and then applying Lowdin's formulae [87].

4. Input of details of which input determinants are to be used in the study

5. Solution of eigenvalue equation (H-ES)C = 0.

The computational scheme is shown in Figure 1.3

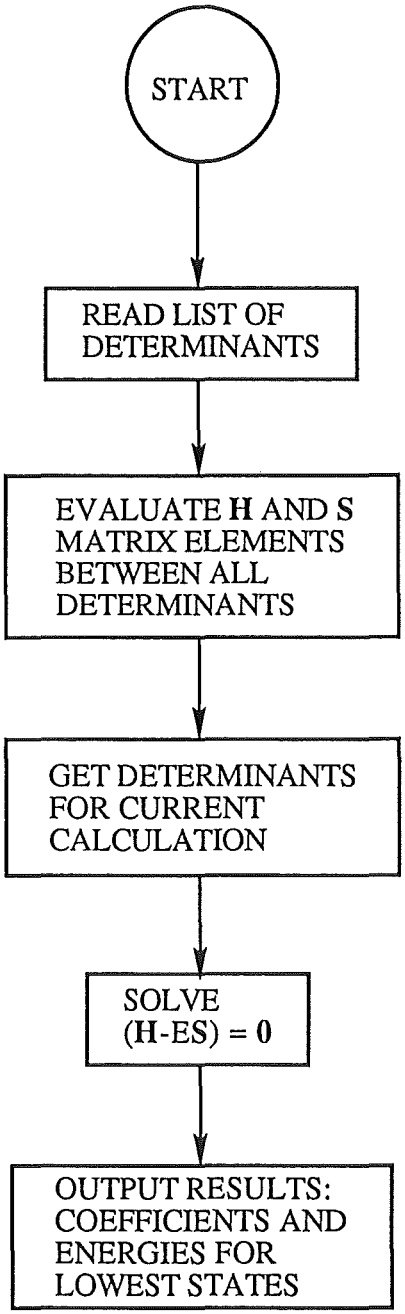

Figure 1.3 Flow diagram for the Valence-Bond program

1.13 Semiempirical methods

The first semiempirical methods were the qualitative π-molecular orbital methods, usually termed 'Huckel theory', which existed before 1965. Later this approach was

superseded by the all-valence-electron methods, but meanwhile its principle was developed by Dewar [36] to give a more quantitative PMO method. Modern semiempirical methods was initiated when the ab initio methods was found to be impractical for the large polyatomic systems. In the semiempirical approach, the complicated integrals used by ab initio theory were estimated on the basis of empirical data. A mixture of functions based on atomic spectra and on formal theory was used to approximate one- and two-center terms, while three- and four-center integrals were ignored. At present time, the parameters of the semiempirical method which were formerly based on atomic spectral data and ab initio results are usually replaced by parameters based on molecular data, to give better performance. The various levels of semiempirical molecular orbital theory are as follows:

1.13.1 Complete Neglect of Differential Overlap (CNDO)

The CNDO method is the first widely used semiempirical self consistent field method [106,107]. It ignores most of the integrals used in ab initio calculations and approximates the energy in terms of some simple parameters and the retained integrals. Many of the quantities used in this method, such as the two-electron one-center integrals, are derived from experimental data. The approximations of the CNDO method are:

1. All overlap integrals involving different atomic orbitals are set to zero. The secular equation:

$$| \mathbf{F} - \mathbf{ES} | = 0 \tag{1.74}$$

is thus reduced to

$$| \mathbf{F} - \mathbf{E} | = 0 \tag{1.75}$$

The Fock matrix, **F**, is a sum of one- and two-electron contributions

$$\mathbf{F} = \mathbf{H} + \mathbf{G} \tag{1.76}$$

Here E is the one dimensional array of orbital energies and S is the overlap matrix.

2. All charge clouds resulting from overlap of different atomic orbitals, ϕ_μ, are ignored. Most multicenter two-electron integrals are eliminated by this constraint since we now have

$$(\mu\nu \mid \lambda\sigma) = \delta_{\mu\nu}\delta_{\lambda\sigma}\,(\mu\nu \mid \lambda\sigma) \tag{1.77}$$

where

$$(\mu\nu|\lambda\sigma) = \int\int \phi^*_\mu(1)\phi_\nu(1)\left(\frac{1}{r_{12}}\right)\phi^*_\lambda(2)\phi_\sigma(2)\,dx_1dy_1dz_1dx_2dy_2dz_2 \tag{1.41}$$

and $\delta_{\mu\nu} = 1$ if $\mu = \nu$, otherwise $\delta_{\mu\nu} = 0$.

3. All two-center two-electron integrals between a pair of atoms are set equal to one another, i.e.,

$$(\mu\mu \mid \lambda\lambda) = \gamma_{AB} \begin{cases} \text{all } \mu \text{ on atom A} \\ \text{all } \lambda \text{ on atom B} \end{cases} \tag{1.78}$$

where γ_{AB} is a function of atoms A and B and the interatomic distance R_{AB}.

4. All electron-core interactions for a given pair of atoms are set equal, i.e.,

$$(\mu \mid V_B \mid \nu) = \delta_{\mu\nu}\, V_{AB} \tag{1.79}$$

5. The off-diagonal one-electron or resonance integrals are scaled in proportion to the overlap integrals as

$$H_{\mu\nu} = \beta_{AB}S_{\mu\nu} \tag{1.80}$$

These approximations reduce the Fock equation:

$$F_{\mu\nu} = H^{core}_{\mu\nu} + \sum_{\lambda=1}^{N}\sum_{\sigma=1}^{N} P_{\lambda\sigma}\,[(\mu\nu|\lambda\sigma) - \tfrac{1}{2}(\mu\lambda|\nu\sigma)] \tag{1.38}$$

where the density matrix P is

$$P_{\lambda\sigma} = 2\sum_{i=1}^{occ} c_{\lambda i}\, c^*_{\sigma i} \tag{1.42}$$

to

$$F_{\mu\mu} = U_{\mu\mu} - \sum_{B\neq A} V_{AB} \qquad \text{(one-electron)}$$

$$+ (P_{AA} - \frac{1}{2} P_{\mu\mu})\, \gamma_{AA} + \sum_{B\neq A} P_{BB}\gamma_{AB} \qquad \text{(two-electron)} \qquad (1.81)$$

for diagonal terms.

The off-diagonal terms, where $\mu \neq \nu$, are now

$$F_{\mu\nu} = \beta_{AB}\, S_{\mu\nu} - \frac{1}{2}\, P_{\mu\nu}\, \gamma_{AB} \qquad (1.82)$$

The total electron density on atom A is defined as:

$$P_{AA} = \sum_{\mu}^{A} P_{\mu\mu} \qquad (1.83)$$

Although the CNDO method was a significant advance in semiempirical computational methods, it had many technical difficulties. For example, in the energy expression

$$E^{elec} = \frac{1}{2} \sum_{\lambda\sigma} P_{\lambda\sigma}\, (H_{\lambda\sigma} + F_{\lambda\sigma}) \qquad (1.84)$$

E^{elect} is required to be minimum, but there is no guarantee of the convergence when the Fock matrix is iterated.

1.13.2 Complete Neglect of Differential Overlap, Version 2 (CNDO/2)

Inequality of the electron-core attraction and electron-electron repulsion in CNDO was found to lead to an excess attraction for two separated neutral atoms. This error was corrected by changing the electron-core attraction term to

$$V_{AB} = Z_B\, \gamma_{AB} \qquad (1.85)$$

A second change was the re-definition of $U_{\mu\mu}$, which in CNDO was obtained from the ionization potential, I_μ, as

$$U_{\mu\mu} = -I_\mu - (Z_A - 1)\,\gamma_{AA} \qquad (1.86).$$

$U_{\mu\mu}$ can be also derived from the electron affinity, A_μ as

$$U_{\mu\mu} = -A_\mu - Z_A\,\gamma_{AA} \qquad (1.86)$$

which in CNDO/2 was combined with (1.86), to give an average value for the one electron integral $U_{\mu\mu}$ as

$$U_{\mu\mu} = -\frac{1}{2}(I_\mu + A_\mu) - (Z_A - \frac{1}{2})\,\gamma_{AA} \qquad (1.87).$$

With the above changes, the diagonal element for CNDO/2 became

$$F_{\mu\mu} = -\frac{1}{2}(I_\mu + A_\mu) - (Z_A - \frac{1}{2})\,\gamma_{AA} - \sum_{B\neq A} Z_B\gamma_{AB} \qquad \text{(one-electron)}$$

$$+ (P_{AA} - \frac{1}{2}P_{\mu\mu})\,\gamma_{AA} + \sum_{B\neq A} P_{BB}\gamma_{AB} \qquad \text{(two-electron)}$$

(1.88)

where the off-diagonal term became

$$F_{\mu\nu} = \beta_{AB}S_{\mu\nu} - \frac{1}{2}P_{\mu\nu}\,\gamma_{AB} \qquad (1.89)$$

1.13.3 Intermediate Neglect of Differential Overlap (INDO)

In the INDO method [108] the constraint in CNDO that monocentric two-electron integrals must be equal was lifted. Five unique two-electron one-center integrals per heavy atom were introduced and used in all INDO methods. These integrals are $G_{ss} = (ss \mid ss)$, $G_{sp} = (ss \mid pp)$, $G_{pp} = (pp \mid pp)$, $G_P^2 = (pp \mid p'p')$, $p \neq p'$, and $H_{sp} = (sp \mid sp)$.

The diagonal Fock matrix element in INDO is

$$F_{\mu\mu} = U_{\mu\mu} \qquad \text{(one-electron)}$$

$$+ \sum_{\lambda}^{A} [\, P_{\lambda\lambda}(\mu\mu \mid \lambda\lambda) - P^{\alpha}_{\lambda\lambda}\,(\mu\lambda \mid \mu\lambda)\,]$$

$$\text{(two-electron)}$$

$$+ \sum_{B \neq A} (P_{BB} - Z_B)\,\gamma_{AB} \qquad (1.90)$$

where P^{α} is the density matrix element of α-spin orbitals.

The off-diagonal monocentric Fock matrix element is

$$F^{\alpha}_{\mu\nu} = (2P_{\mu\nu} - P^{\alpha}_{\mu\nu})\,(\mu\nu \mid \mu\nu) - P^{\alpha}_{\mu\nu}\,(\mu\mu \mid \nu\nu) \qquad (1.91)$$

The off-diagonal two center Fock matrix element in INDO is the same as the corresponding element in CNDO/2. The resonance integral in INDO is derived from the average β terms of the two contributing atomics orbitals:

$$F^{\alpha}_{\mu\nu} = \frac{1}{2}(\beta_{\mu} + \beta_{\nu})S_{\mu\nu} - P^{\alpha}_{\mu\nu}\,(\mu\mu \mid \nu\nu) \qquad (1.92)$$

1.13.4 Neglect of Diatomic Differential Overlap (NDDO)

In the NDDO method [106], all interactions except those arising from diatomic differential overlaps were considered. The matrix elements of the Hartree-Fock Hamiltonian operator are

$$F_{\mu\nu} = H_{\mu\nu} \qquad \text{(one-electron)}$$

$$+ \sum_{B} \sum_{\lambda}^{B} \sum_{\sigma}^{B} P_{\lambda\sigma}\,(\mu\nu \mid \lambda\sigma) \qquad \text{(two-electron)}$$

$$\mu, \nu \text{ both on A}$$

$$- \frac{1}{2} \sum_{\lambda}^{A} \sum_{\sigma}^{A} P_{\lambda\sigma}\,(\mu\sigma \mid \nu\lambda)$$

$$(1.93)$$

The Fock matrix of two-center two-electron integral in this method is

$$F_{\mu\nu} = H_{\mu\nu} - \frac{1}{2}\sum_{\sigma}^{A}\sum_{\lambda}^{B} P_{\lambda\sigma}\,(\mu\sigma \mid \nu\lambda) \qquad \mu \text{ on A and } \nu \text{ on B} \qquad (1.94)$$

1.13.5 Modified Intermediate Neglect of Differential Overlap (MINDO)

In 1975 Dewar and his co-workers published the MINDO/3 method [10]. The basic form of the equations was similar to those in INDO but the origin of the parameters in MINDO/3 and INDO is different i.e. $U_{\mu\mu}$ in MINDO/3 was made an adjustable parameter rather than derived from atomic spectral data. Several other parameters in this method were adjusted to give the best fit to experimental data for molecules. This is the main feature of MINDO/3 adjusting the parameters to fit the molecular data rather than theory and made it different from its predecessors.

The Fock matrix of MINDO/3 has the basic form

$$F_{\mu\mu} = U_{\mu\mu} - \sum_{B\neq A} Z_B\gamma_{AB} \qquad \text{(one-electron)}$$

$$+ \sum_{\nu}^{A} (P_{\nu\nu}G_{\mu\nu} - \frac{1}{2}P_{\mu\nu}H_{\mu\nu}) + \sum_{B\neq A} P_{BB}\gamma_{AB} \qquad \text{(two-electron)} \qquad (1.95)$$

and

$$F_{\mu\nu} = \beta_{AB}S_{\mu\nu} - \frac{1}{2}P_{\mu\nu}\,\gamma_{AB} \qquad (1.96)$$

$G_{\mu\nu}$ in this method is a one-center two-electron integral of type $(\mu\mu \mid \nu\nu)$, and $H_{\mu\nu}$ is the corresponding exchange integral, $(\mu\nu \mid \mu\nu)$.

In the INDO method, when electron-core attraction is set equal to electron-electron repulsion, triplet hydrogen atoms repel each other at all distances. This error was corrected in MINDO/3 by making the core-core repulsion term a function of the electron-electron repulsion integral:

$$E_{AB} = (1 - a)Z_AZ_B\gamma_{AB} + a(Z_AZ_B/R_{AB}) \qquad (1.97)$$

where a is a function of the interatomic distance, R_{AB} and a diatomic constant α_{AB}

$$a = \alpha_{AB} \exp(-R_{AB}) \qquad (1.98)$$

1.13.6 Modified Neglect of Diatomic Overlap (MNDO)

Since MINDO/3 had difficulty with systems which contained lone pairs of electron, Dewar and Thiel [37] developed and published a new method, MNDO, in 1977. The Fock matrix in MNDO has the following form:

1. Diagonal terms

$$F_{\mu\mu} = U_{\mu\mu} - \sum_{B \neq A} Z_B(\mu\mu \mid ss) \qquad \text{(one-electron)}$$

$$+ \sum_{\nu}^{A} P_{\nu\nu} \left[(\mu\mu \mid \nu\nu) - \frac{1}{2}(\mu\nu \mid \mu\nu)\right]$$

$$\text{(two-electron)}$$

$$+ \sum_{B} \sum_{\lambda}^{B} \sum_{\sigma}^{B} P_{\lambda\sigma} (\mu\mu \mid \lambda\sigma) \qquad (1.99)$$

2. Off-diagonal terms on the same atom

$$F_{\mu\nu} = - \sum_{B \neq A} Z_B(\mu\nu \mid ss) \qquad \text{(one-electron)}$$

$$+ \frac{1}{2} P_{\mu\nu}[3(\mu\nu \mid \mu\nu) - (\mu\mu \mid \nu\nu)]$$

$$\text{(two-electron)}$$

$$+ \sum_{B} \sum_{\lambda}^{B} \sum_{\sigma}^{B} P_{\lambda\sigma}(\mu\nu \mid \lambda\sigma) \qquad (1.100)$$

3. Term between orbitals on different atoms

$$F_{\mu\nu} = \frac{1}{2}(\beta_\mu + \beta_\nu) S_{\mu\nu} - \frac{1}{2} \sum_{\lambda}^{A} \sum_{\sigma}^{B} P_{\mu\nu} (\mu\lambda \mid \nu\sigma) \qquad (1.101)$$

In this method the core-core repulsion term was also made a function of the electron-electron repulsion integral:

$$E_{AB} = Z_A Z_B (s_A s_A \mid s_B s_B) \qquad (1.102)$$

By using experimental data on 34 compounds the parameters used in MNDO were optimized to reproduce observed heats of formation, dipole moment, ionization potentials and molecular geometries. The unique feature that made MNDO more versatile is the used of entirely monoatomic parameters for the resonance integrals and core-core repulsion instead of using diatomic parameters.

1.13.7 Austin Model 1 (AM1)

A problem with MNDO is that it gives excessive repulsion at van der Waals' distances, which makes it unable to reproduce hydrogen bonding. This error was corrected in AM1 by assigning a number of spherical Gaussians to each atom in order to mimic correlation effects. The core-core term in AM1 becomes

$$E_{AB} = Z_A Z_B (s_A s_A \mid s_B s_B) + Z_A Z_B / R_{AB} \sum_{i}^{4} [a_i(A) e^{-b_i(A)[R_{AB} - c_i(A)]^2} + a_i(B) e^{-b_i(B)[R_{AB} - c_i(B)]^2}] \quad (1.103)$$

in which the $a_i(A)$, $b_i(A)$, and $c_i(A)$ are parameters.

In 1985 parameters were derived for the four elements, C, H, N, and O in this method [38]. Only the two-electron one-center integrals were still based on atomic spectra.

1.13.8 Parametric Method Number 3 (MNDO-PM3)

In this method, the latest development in semiempirical methods, all one-center two-electron integrals, plus the seven parameters of MNDO and two AM1-type Gaussians are optimized. In the resulting method, called MNDO-PM3 [132], the parameters are optimized using an automatic optimization routine [133] based on a large set of reference molecular data.

1.13.9 MOPAC

MOPAC is a general-propose, semiempirical molecular orbital program for the study of chemical reactions involving molecules, ions and linear polymers. It implements the semiempirical Hamiltonians of MNDO, AM1, MINDO/3, and MNDO-PM3, and combines calculations of vibrational spectra, thermodynamic quantities, isotropic substitution effects, and force constants in a fully integrated program. Elements parameterized at the MNDO level include H, Li, Be, B, C, N, O, F, Al, Si, P, S, Cl, Ge, Br, Sn, Hg, Pb, and I while at the PM3 level the elements H, C, N, O, F, Al, Si, P, S, Cl, Br, and I are available. Within the electronic part of the calculation, molecular and localized orbitals, excited states up to sextets, chemical bond indices, charges, etc. are computed. Both intrinsic and dynamic reaction coordinates can be calculated. A transition-state location routine and two transition-state optimizing routine are available for studying chemical reactions [134].

Table 1.1 shows the parameters that used in the four main methods and their nature. Parameters optimized for a given method are indicated by *. A + indicates that the value of parameter was obtained from experiment (not optimized). The blanks mean that the associated parameter is not used in that method.

Table 1.1 Parameters used in the four main semiempirical methods and their natures

Parameter	Description	MNDO/3	MNDO	AM1	PM3
U_s and U_p	s and p atomic orbital one-electron one-center integrals	+	*	*	*
β_s and β_p	s and p atomic orbital one-electron two-resonance integral terms		*	*	*
Is	s atomic orbital ionization potential for two-center resonance integral term	+			
Ip	p atomic orbital ionization potential for two-center resonance integral term	+			
β_{AB}	diatomic two-center one-electron resonance integral multiplier	*			
ξ_s	s-type Slater atomic orbital exponent	*	*	*	*
ξ_p	p-type Slater atomic orbital exponent	*	*	*	*
α_A	atom A core-core repulsion term		*	*	*
α_{AB}	atom A and B core-core repulsion term	*			
G_{ss}	s-s atomic orbital one-center two-electron repulsion integral	+	+	+	*
G_{sp}	s-p atomic orbital one-center two-electron repulsion integral	+	+	+	*
G_{pp}	p-p atomic orbital one-center two-electron repulsion integral	+	+	+	*
G_{p2}	p-p' atomic orbital one-center two-electron repulsion integral	+	+	+	*
H_{sp}	s-p atomic orbital one-center two-electron exchange integral	+	+	+	*
K_{nA} or a_{nA}	Gaussian multiplier for nth Gaussian of atom A			*	*
L_{nA} or b_{nA}	Gaussian exponent multiplier for nth Gaussian of atom A			*	*
M_{nA} or c_{nA}	radius of center of nth Gaussian of atom A			*	*

CHAPTER 2

The Proton Affinity Study of Diacetylene

2.1 Introduction

Protonated diacetylene, $C_4H_3^+$, has been found as a carbocation in acetylenic flame as a result of the reaction:

$$HCCH + HCCH \rightarrow HCCCCH_2^+ + H + \text{other products} \quad (1)$$

The molecule C_4H_2 was also identified as one of the polyacetylenes which are constituents of interstellar clouds and primitive planetary atmospheres [79]. This molecule is likely to be protonated by H_3^+ and HCO^+, which are abundant in these ionizing environments and can transfer protons to molecules with higher proton affinities (PAs).

$$HCCCCH + H_3^+ \rightarrow HCCCCH_2^+ + H_2 \quad (2)$$

$$HCCCCH + HCO^+ \rightarrow HCCCCH_2^+ + CO \quad (3)$$

The protonated diacetylene may then recombine with electrons or undergo ion-molecule reactions, including proton transfer to other molecules having higher proton affinities. Thus the proton affinity is an important property for deciding subsequent chemical processes of diacetylene in the gas phase.

In the present study we used the Gaussian 82 [11] program to calculate a theoretical value of the proton affinity of diacetylene at the MP4SDQ level with a 6-311G** basis set. The calculated results were supported by selected ion flow tube (SIFT) measurements of proton transfer equilibria between diacetylene and C_2H_5I, BrCN and CH_3NO_2 [101]. We also compare our results with the other calculations on diacetylene at different levels of theory by Deakyne et al. [29] and Botschwina et al. [15]. Deakyne et al. [29] also performed experimental ion cycloton resonance (ICR) studies to confirm their theoretical results.

2.2 Theory

The gas phase proton affinity (PA) of a molecule, B, is defined as the negative value of the room temperature (298 K) enthalpy change for the reaction

$$B + H^+ \rightarrow BH^+ ; \quad PA = -(\Delta H) \qquad (4)$$

while gas phase basicity is defined as:

$$-\Delta G(298) = -\Delta H(298) + T\Delta S(298) \qquad (5)$$

In our study we compute the PA , using the formulae:

$$PA = -\Delta H(298)_{calcd} \qquad (6)$$

$$\Delta H(298)_{calcd} = \Delta U(298)_{calcd} + \Delta(PV) \qquad (7)$$

$$\Delta U(298)_{calcd} = \Delta U^0_e + \Delta(\Delta U_e)^{298} + \Delta U^0_v + \Delta(\Delta U_v)^{298} + \Delta U_r^{298} + \Delta U_t^{298} \qquad (8)$$

Definitions:

ΔU_e^0 is the computed difference in the electronic energies of reactants and products at 0 K, including the correlation energy correction to the Hartree-Fock energy.

$\Delta(\Delta U_e)^{298}$ is the change in the electronic energy difference between 298 K and 0 K. This term should be negligible for our study.

ΔU_v^0 is the difference between the zero-point vibrational energies of reactants and product at 0 K.

$\Delta(\Delta U_v)^{298}$ is the change in the vibrational energy difference between 298 and 0 K.

ΔU_r^{298} is the difference in rotational energies of reactants and product. Classically, this is equal to (-1/2)RT for each degree of rotational freedom lost during to the complex formation [84]. This value is equal to 0.0 in this study.

ΔU_t^{298} is the translational energy change due to the change in the number of degrees of freedom. In our study, three degree of freedom are lost by the hydrogen atom, so that this term is equal to (-3/2)RT.

$\Delta(PV)$, which is the PV work term at constant pressure, is the difference between ΔH and ΔU. Assuming ideal gas behaviour, this term is equal to (-RT), since 1 mole of gas is lost in the protonation reaction.

2.3 Method of Calculation

In order to calculate PA of C_4H_2, we need to identify the most stable structural isomer of $C_4H_3^+$. The three lowest energies structures for C_4H_2 : vinylacetylene, methylene cyclopropane and cyclobutadiene were taken as starting species [68] . The structures (2) and (5) are generated by removal of hydrogen out of vinyl acetylene and ionizing the products. Methylenecyclopropene, after removal of methylene hydrogen and ionization, will give structure (3). The four-membered carbon ring isomer for $C_4H_3^+$ is the bent structure (4). The planar four-membered ring structure (6) is a transition state and so gives one imaginary frequency in our calculations.

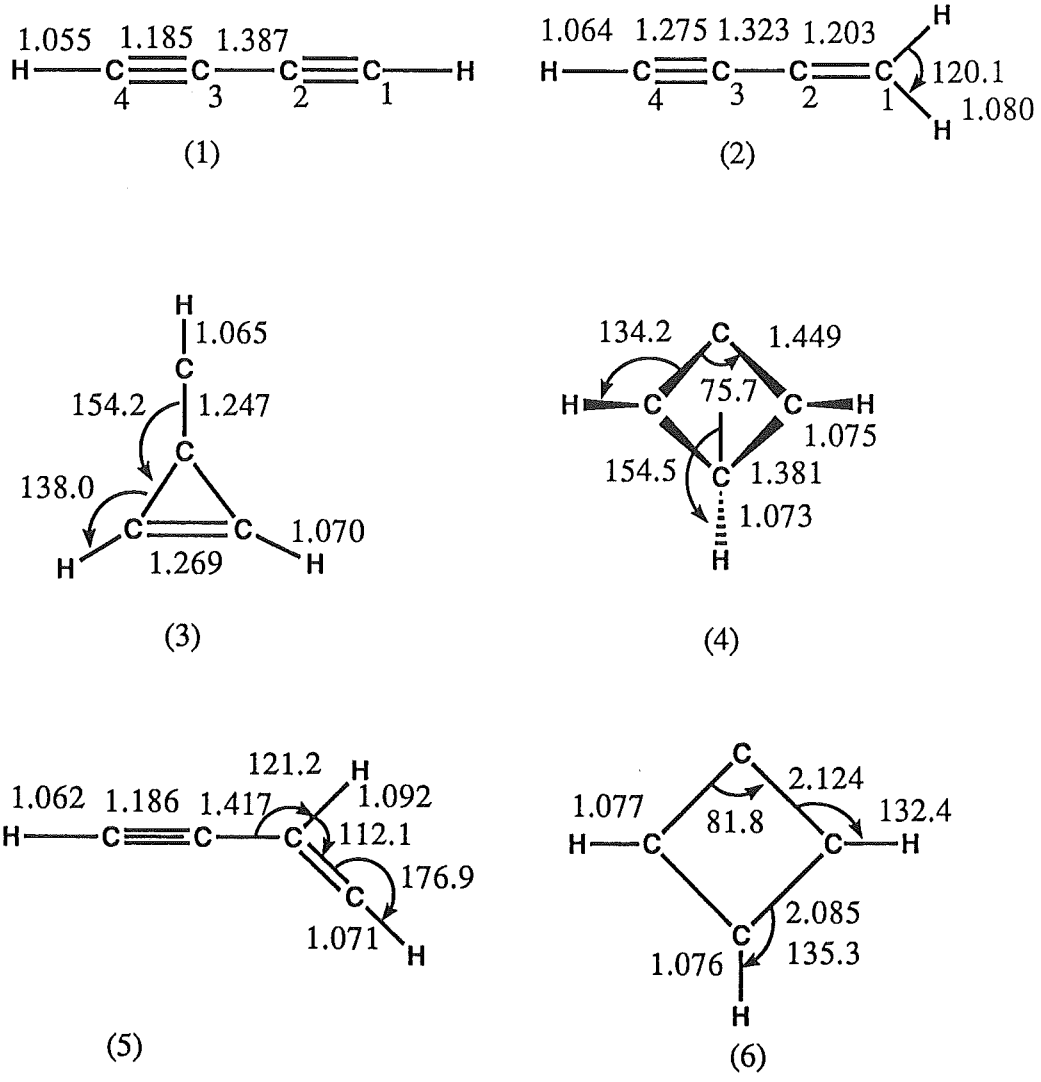

Figure 2.1 6-311G** optimized geometries of C_4H_2 and $C_4H_3^+$ (Ångstroms and degrees)

The optimized geometries and electronic energies (U_e) of these isomers and C_4H_2 were calculated at RHF level using the Gaussian 82 program with 6-31G* and 6-311G** basis sets. The correlation energies were calculated with fourth order Mϕller-Plesset perturbation theory, MP4SDQ, which includes contributions from single, double and quadruple excitations. The Harmonic vibration frequencies were calculated at the HF/6-31G* level and zero-point vibrational energies were determined. Following Pitzer [103], the contribution of the harmonically approximated, low-frequency vibrational modes at 298 K was evaluated as

$$\Delta(\Delta U_v)^{298} = 298R[\ \Sigma_i\ (u_i/(e^{u_i} - 1)) - \Sigma_j\ (u_j/(e^{u_j} - 1))\ ] \tag{9}$$

where

$$u = 4.826 \times 10^{-3}\ \nu. \tag{10}$$

R = gas constant

Here ν is the frequency (in cm^{-1}) of the normal mode, and i and j range over product and reactant normal modes respectively. The zero-point vibrational energies $\Delta(\Delta U_v)$ value are multiplied by a scale factor of 0.89 as suggested by DeFrees and Pople [109].

2.4 Results

The optimized geometries for C_4H_2 and isomers of $C_4H_3^+$ are given in Table 2.1. The Hartree-Fock and correlated energies of C_2H_4 and five structure isomers of $C_4H_3^+$ are shown in Table 2.2. The $\Delta U_e^0(ZPE_{cor})$ values are given in Table 2.3. The calculated and experimental PAs are given in Table 2.4, while the theoretical vibrational frequencies are given in Table 2.5.

Table 2.1 Calculated equilibrium geometries of C_4H_2 and $C_4H_3^+$ (Ångstroms and degrees)

parameters	HF 6-311G**[a]	HF 6-31G**[b]	CEPA-1 n-cGTOs[c]	HF n-cGTOs[d]
C_4H_2				
r_{12}	1.185	1.188	1.211	
r_{23}	1.387	1.389	1.380	
r_{CH}	1.055	1.057	1.060	
$C_4H_3^+$				
r_{12}	1.203	1.207	1.230	1.200
r_{23}	1.323	1.325	1.321	1.321
r_{34}	1.275	1.278	1.292	1.271
r_{1H}	1.081	1.081	1.088	1.079
r_{4H}	1.064	1.066	1.070	1.062
A_{HCH}	120.1	120.0	119.1	120.1

a This work, using GAUSSIAN 82.

b Deakyne et al. [29], using GAUSSIAN 82.

c Botschwina et al. [15], using Meyer's Coupled Electron Pair Approximation method, 96 cGTOs for C_4H_2 and 102 cGTOs for $C_4H_3^+$

d Botschwina et al. [15], using Hartree-Fock method with 102 cGTOs for $C_4H_3^+$ but C_4H_2 was not reported.

Table 2.2 Calculated total electronic energies for C_4H_2 and $C_4H_3^+$.

Structure	HF	MP2	MP4SDQ	ZPVE
		Hartree		
6-31G* Basis set				
(1) C_4H_2	-152.49793	-153.00760	-153.00602	0.042006
(2) $C_4H_3^+$	-152.79842	-153.28728	-153.29621	0.050784
(3)	-152.77082	-153.25617	-153.26555	0.050265
(4)	-152.76789	-153.24629	-153.25724	0.053400
(5)	-152.75413	-153.23287	-153.24548	0.050209
(6)	-152.73325	-153.19350	-153.26555	0.050265
6-311G** Basis set				
(1) C_4H_2	-152.53525		-153.07111	
(2) $C_4H_3^+$	-153.83117		-153.35909	

Table 2.3 Calculated electronic energies with zero-point vibrational energies correction (kJ mol^{-1}).

Structure	ΔU_e^0 ($ZPVE_{cor}$)
6-31G* Basis set	
(1).C_4H_2	0.0
(2) $C_4H_3^+$	-738.8
(3)	-659.7
(4)	-629.7
(5)	-607.2
(6)	-506.0
6-311G** Basis set	
(1) C_4H_2	0.0
(2) $C_4H_3^+$	-733.0[a]

[a] used zero-point vibrational energy from harmonic vibration frequencies calculation of structure (2) with 6-31G* basis set

Table 2.4 Proton affinity of C_4H_2 (kJ mol^{-1})

Theory	ΔU_e^0	$\Delta U_e^0(ZPVE_{cor})$	Temperature contribution[a]	PA_{cal} (PA_{exp})
MP4SDQ 6-311G**[b]	-756.08092	-733.03428	-3.54666	736.58093
with 0.89[d] correction	-756.08092	-735.56941	-3.82310[e]	739.39251 (741 ± 4)[c]
MP3 6-31G**[f]	-777.3872	-759.8144	-5.0208	764.8352 (753 ± 4)
CEPA-1[g]	-756.5	-736.7	-4.5	741 (------)

a temperature contribution = $\Delta(\Delta U_v)^{298} + \Delta U_t^{298} + \Delta U_r^{298} + \Delta PV$

b This work.

c Reference101

d 0.89 factor for calculated vibrational results suggested by Defrees and Pople [110].

e In this value, only $\Delta(\Delta U_v)^{298}$ was multiplied by 0.89.

f Work done by Deakyne et al. [29], experiment done on Ion Cycloton Resonance method.

g Work done by Botschwina et al.[15], 130 and 124 contracted GTOs were used for $C_4H_3^+$ and C_4H_2 respectively, temperature contribution, -4.5 kJ mol^{-1}, was taken from reference 29, by multiplying -5.0 kJ mol^{-1} by 0.9.

Table 2.5 Calculated vibrational frequencies for $C_4H_3^+$ (cm^{-1}).

Hartree-Fock 6-31G* basis[a]		Hartree-Fock 3-21G basis[b]		CEPA-1 potential with vibrational Hamiltonian[c]	
(b_2)	215	(b_1)	219		
(b_1)	233	(b_2)	224		
(b_2)	473	(b_2)	535		
(b_1)	573	(b_1)	587		
(b_1)	786	(b_1)	880		
(a_1)	960 (854)	(a_1)	963	(a_1)	889
(b_2)	997	(b_2)	1059		
(b_2)	1032	(b_2)	1107		
(b_1)	1075	(b_1)	1122		
(a_1)	1475 (1313)	(a_1)	1501	(a_1)	1331
(a_1)	1975 (1758)	(a_1)	1971	(a_1)	1789
(a_1)	2330 (2074)	(a_1)	2261	(a_1)	2030
(a_1)	3294 (2932)	(a_1)	3249	(a_1)	3045
(b_2)	3392	(b_2)	3336		
(a_1)	3581 (3187)	(a_1)	3547	(a_1)	3286

[a] This work, in bracket are the calculated vibrational frequencies multiplied by 0.89 factor.

[b] Reference 29, the values were also suggested to multiplied with 0.89 factor to be compare with experiment.

[c] Reference 15,using 102 contracted GTOs, only total symmetric vibrational modes were reported. This values had been include anharmonic correction.

2.5 Discussion

In this study we used the valence-double-split polarized basis 6-31G* and the valence-triple-split polarized 6-311G** basis in the molecular orbital theory calculations. These basis sets should be suitable for neutral molecule like C_4H_2. The larger basis sets which include diffuse functions will give more accurate electronic energies but the proton affinity study of 13 small molecules, by D.J. DeFrees and A.D. McLean [31], has shown that the mean error was 3.9 kJ mol^{-1} between MP4/6-311++G(3df,3pd) and MP4/6-311G(d,p). So the error from the lack of diffuse functions in the basis set we used, is likely to be small and should not cause any serious problem. The errors from the basis set superposition error (BSSE) [17] are not included in this study because of the size of the molecules and because the error is likely to be partly cancelled by other deficiencies in the theoretical model. For these reasons, the basis sets we used are practical and reliable when considering of the size diacetylene and the cost of computations.

The optimized results for protonated diacetylene isomers from Deakyne et al. [29] and the present work show that the C_1 protonated linear structure isomer is the most stable product. The 24 kJ mol^{-1} difference in $\Delta U_e^0(ZPE_{cor})$ between this study and the work of Deakyne et al. [29] is due to the different size of basis set and the different level of theory used in the calculations. On the other hand, our $\Delta U_e^0(ZPE_{cor})$ value agrees very well with the value from Botschwina et al. [15], which use nearly the same size of basis set (130 cGTOs for $C_4H_3^+$, our is 148) but used a different theoretical approach, namely, Meyer's Coupled Electron Pair Approximation [95].

Our temperature contribution is different from those of Deakyne et al. [29] and Botschwina et al. [15] because they took the value ΔU_r^{298} = (-1/2RT) whereas we took ΔU_r^{298} = 0.0. We believe the value should be zero, because there is no change in the number of degrees of rotational freedom in the protonation process. This view is supported by Del Bene et al. [34]. The PA value from our calculations fits very well with the PA value from selected ion flow tube experiment and if we use our ΔU_r^{298} value in Botschwina's calculation we get nearly the same PA value.

The factor 0.89 has been suggested by Pople et al. [110] to scale all calculated values of harmonic vibrational frequencies. It was derived by comparing theoretical and experimental frequencies for a number of neutral molecules. When we use this factor to scale our calculated vibrational frequencies, the scaled frequencies agree very well with the results of Botschwina's work, which included anharmonicity in the calculation and reported only total symmetric vibrational modes.

The optimized geometries are not significantly different among the calculations which used different size of basis sets and different levels of molecular orbital theory, and it is well-known that equilibrium geometric parameters are not affected much by the size of basis sets or the level of theory, whereas the energies are strongly affected by both factors. The optimized geometries from CEPA-1 calculation which is not a variational method, show systematic differences from the rest, although the authors had shown that this method gave very good geometrical results with reference molecules such as ethylene.

In all calculations, the bond length r_{12} increase and bond length r_{23} decrease significantly after diacetylene is protonated. Electron densities from a Mulliken population analysis shows that most electron density change occurs in the Y-axis.

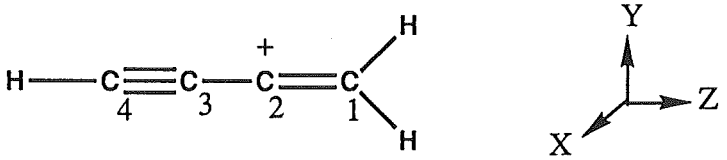

	H	C4	C3	C2	C1	H
		0.135	-0.036	0.104	-0.102	
ΔED(s)		0.135	-0.036	0.104	-0.102	
$\Delta ED(p_x)$		0.062	-0.064	0.180	0.167	
$\Delta ED(p_y)$		-0.466	0.171	-0.595	0.167	
$\Delta ED(p_z)$		0.033	-0.194	0.136	0.118	
ΔE(tot)	-0.083	-0.236	-0.123	-0.175	-0.008	0.120

Figure 2.2.The change in electron population on each atom after an addition of a proton to a terminal of C_4H_2

Deakyne et al. [29] explained the change of bond length by suggesting the change in molecular orbitals in HOMO which affects the bonding between C_1 and C_2 decreased bonding while the bonding between C_2 and C_3 changes from anti-bonding to bonding, as a diagram below.

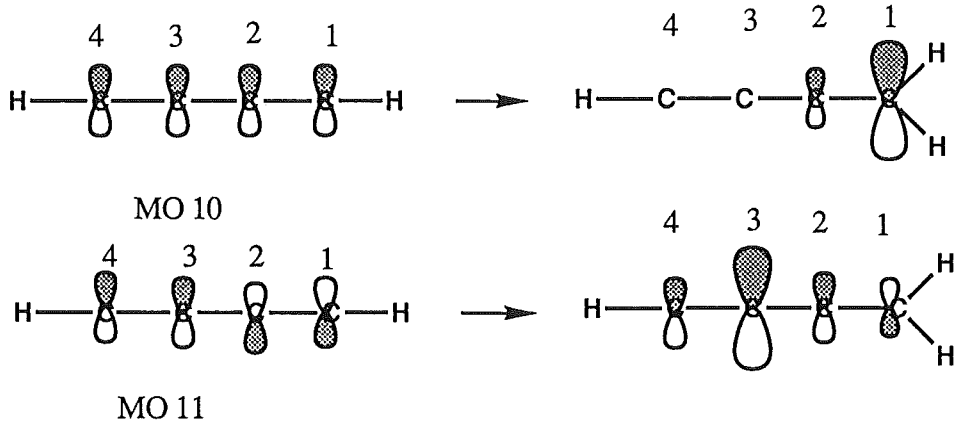

Figure 2.3 The changes of HOMO of C_4H_2 after protonation process

2.6 Conclusion

As shown in Table 2.4, our calculated PA of diacetylene is 739.4 kJ mol^{-1} which agrees very well with the value 741 ± 4 kJ mol^{-1} from the selected ion flow tube experiment and the value 741 kJ mol^{-1} from the work of Botschwina et al. [15]. There are a 25.6 kJ mol^{-1} and a 13.6 kJ mol^{-1} difference between our and Deakyne et al.'s calculated values and the ICR experiment value [29]. This means that, as might have been predicted, larger basis sets and higher level of theory are needed to obtain a more accurate PA value and improve the agreement between theory and experiment.

CHAPTER 3

Ab Initio Study of the Reaction between CH_3CN and CH_3^+

3.1 Introduction

Acetonitrile, CH_3CN which has been detected in the atmosphere recently, is considered to be an important chemical compound in the chemistry of the atmosphere [123]. The reaction of acetonitrile and CH_3^+ is fast and exothermic. It gives an addition product of a nitrilium compound CH_3CNCH_3 (1) with a high energy of reaction (ΔH = -427 kJ mol^{-1}) [145]. The chemistry of CH_3CN has been studied extensively in both theoretical and experimental aspects [5,24,52,57,77,92-94,117,141]. With the high energy of the association , $CH_3CNCH_3^+$ is expected to be in an excited state [146]. It can decompose directly to give CH_3CN, CH_3NC and CH_3^+ or it can decompose via a multistep sequence involving intermediates within which hydrogen atom shifts and ring-closure processes can occur before dissociation. In this study we use ab initio molecular orbital calculations to establish a possible chemical pathway and predict the most stable products for the multistep dissociation reaction of $CH_3CNCH_3^+$. From the calculated electronic energies, $HCNH^+$ and C_2H_4 are likely to be the most stable products for the multistep pathway. We proposed a mechanism in which the most important step is the shift of hydrogen atom from the adjacent methyl group to nitrogen atom. While our work was in progress, the same work on this reaction by H. Wincel and coworkers was published with both theoretical and experimental results [146]. $HCNH^+$ and C_2H_4 were confirmed to be the most stable products in a gas collision experiment on CH_3^+ and CH_3CN. They also used an ab inito calculation results from a work of G. Bouchoux and co-workers [16] to establish another chemical mechanism. Their proposed pathway agrees very well with 90 percent of the amount of labelled $H^{13}CNH^+$ produced in their experiment which used radioactive labelled technique. Their proposed mechanism and experimental results are different from our proposed mechanism.

3.2 Method

Ab initio molecular calculations were done at the restricted (RHF) and unrestricted (UHF) Hartree-Fock levels using the Gaussian 82 program [11]. First the split-valence 4-31G basis set was used in the optimization of molecular structures and energy calculations at the second order of Mϕller-Plesset perturbation theory (MP2). The optimized structures were then reoptimized with the polarization basis set, 6-31G*. The new optimized structures then were used in a calculation with fourth-order the Mϕller-Plesset perturbation theory including single, double and quadruple excitations (MP4SDQ) to take account of correlation energy. The transition-state structures were obtained by minimizing the gradient norm while ensuring that the matrix of the second derivatives of the energy had one negative eigenvalue.

The results are presented in Table 3.1-3.4 and in Figure 3.1-3.3. In Figure 3.3 a part of the calculation from this study is put into the mechanism which was proposed by Wincel et al. [146] for comparison. The transition state structures (7) and (14) are for our suggested pathway and the work of Wincel and coworkers respectively.

Table 3.1 Calculated energies of compounds (hartree) at different levels of theory and basis sets.

Molecule	HF/4-31G	HF/6-31G*	MP2/4-31G	MP4SDQ/6-31G*
(1)	-39.175125	-39.230640	-39.242048	-39.344672
(2)	-131.728271	-131.927534	-132.027910	-132.354473
(3)	-171.041061	-171.294020	-171.423611	-171.855741
(4)	-170.926879	-171.180413	-171.273799	-171.727569
(5)	-170.965890	-171.233882	-171.344340	-171.800551
(6)	-170.948505	-171.216517	-171.330169	-171.784795
(7)	-170.827087	-171.087322	-171.210000	-171.662026
(8)	-78.198801	-78.311232	-78.362026	-78.574161
(9)	-92.731929	-92.875198	-92.944545	-93.163683
(10)	-77.922157	-78031718	-78.104769	-78.310549
(11)	-93.022352	-93.159042	-93.229229	-93.443359
(12)	-170.926138	-171.181581	-171.287652	-171.736863
(13)	-171.011686	-171.271916	-171.384258	-171.837806
(14)	-170.889539	-171.150492	-171.260140	-171.771095
(15)	-171.024240	-171.271590	-171.396982	-171.836009

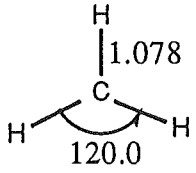

(1)

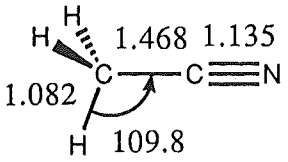

(2)

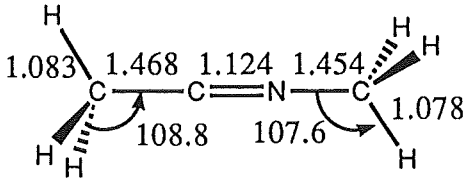

(3)

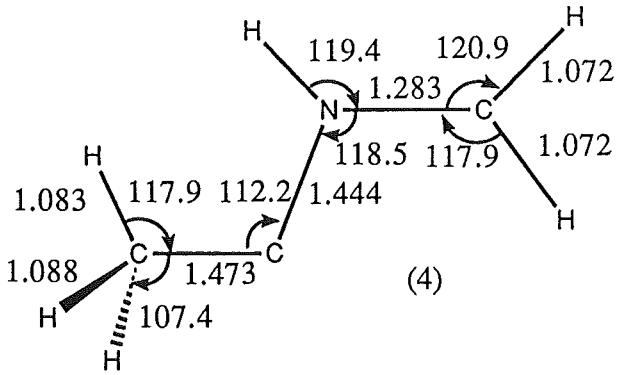

(4)

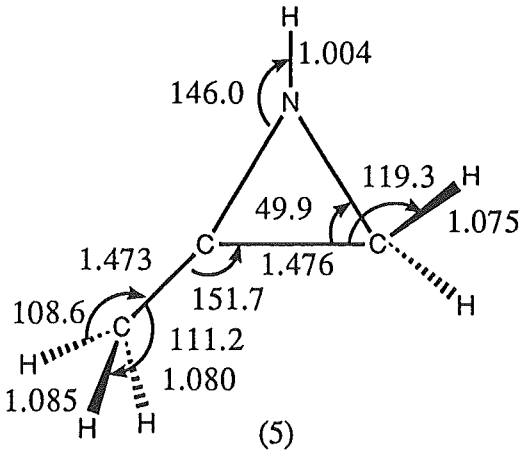

(5)

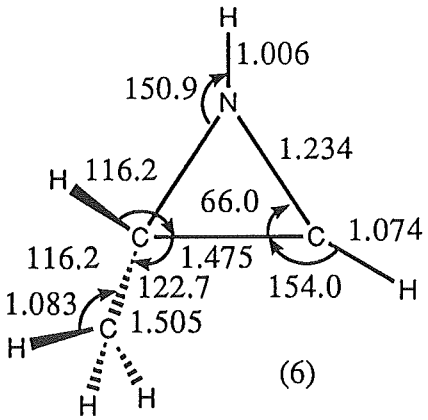

(6)

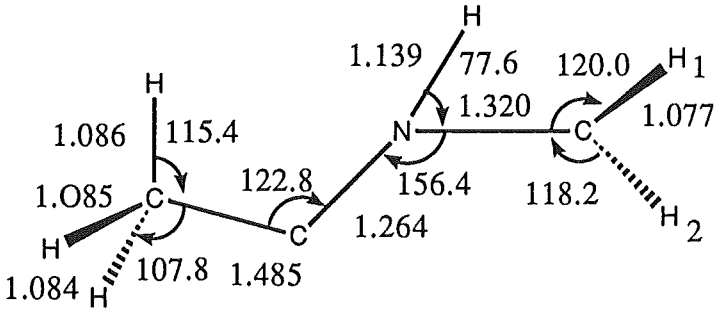

DCNCH1 = 73.8

DCNCH2 = -118.2 (7)

Figure 3.1 Optimized structures of compounds with 6-31G* basis set

(Ångstroms and degrees)

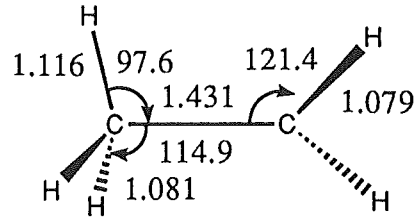

DHCCH = 87.4

(8)

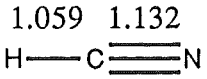

(9)

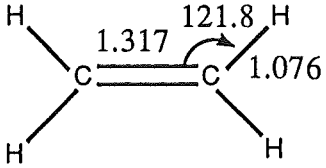

(10)

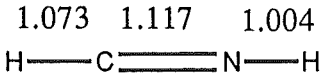

(11)

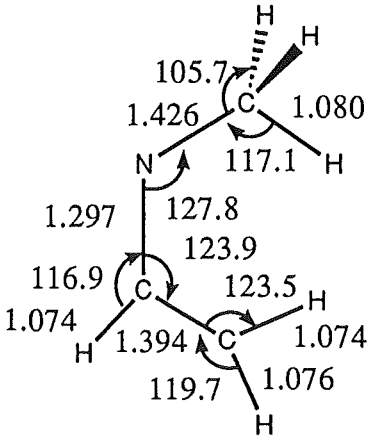

(12)

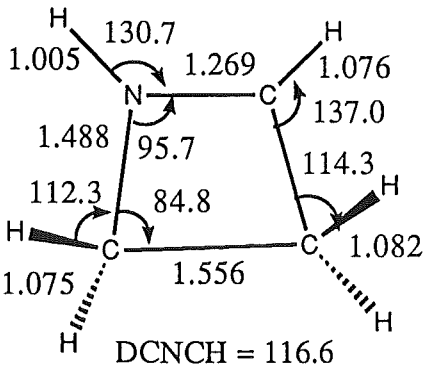

DCNCH = 116.6

DNCCH = 115.9

(13)

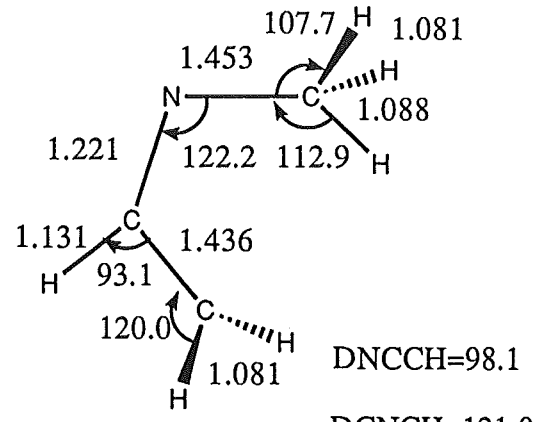

DNCCH=98.1

DCNCH=121.0

(14)

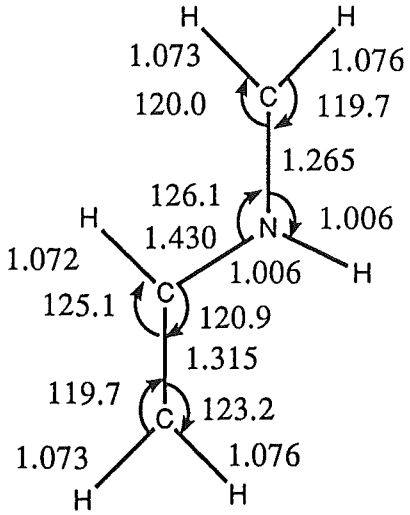

(15)

Figure 3.1 (continued)

Table 3.2 Calculated harmonic vibrational frequencies and zero-point vibrational energies of molecules with the 4-31G basis set.

Molecule	Harmonic vibrational frequencies (cm^{-1})			ZPVE (kJ mol^{-1})
(1)	(a_2'') 1516	(e') 1542	(e') 1542	88.0
	(a_1') 3228	(e') 3438	(e') 3438	
(2)	(e) 430	(e) 430	(a_1) 984	128.6
	(e) 1213	(e) 1213	(a_1) 1599	
	(e) 1637	(e) 1637	(a_1) 2581	
	(a_1) 3209	(e) 3289	(e) 3289	
(3)	11	221	221	241.5
	529	529	695	
	1075	1214	1214	
	1285	1285	1588	
	1602	1602	1610	
	1630	1630	2685	
	3203	3241	3300	
	3300	3354	3354	
(4)	185i	199	345	237.6
	576	680	877	
	928	1146	1178	
	1219	1309	1371	
	1527	1548	1620	
	1625	1672	1799	
	3125	3185	3334	
	3335	3463	3666	
(5)	99	368	384	243.3
	680	811	961	
	1080	1083	1208	
	1240	1265	1328	
	1386	1570	1603	
	1616	1654	1948	
	3190	3260	3315	
	3338	3461	3833	

(6)	192	404	445	242.8
	619	753	907	
	1096	1100	1175	
	1242	1256	1311	
	1374	1525	1600	
	1633	1646	1846	
	3208	3286	3303	
	3383	3459	3813	
(7)	1371i	113	175	219.7
	266	541	660	
	810	993	1167	
	1173	1271	1290	
	1336	1564	1605	
	1627	1638	1755	
	2257	3180	3266	
	3276	3307	3459	
(8)	212	726	941	169.7
	1183	1338	1411	
	1504	1526	1618	
	1667	2976	3243	
(9)	(π) 905	(π) 905	(σ) 2382	47.2
	(σ) 3693			
(10)	(b_{2u}) 935	(b_{3u}) 1125	(b_{2g}) 1162	144.8
	(a_u) 1167	(b_{3g}) 1386	(a_g) 1521	
	(a_{1u}) 1639	(a_g) 1856	(b_{1u}) 3305	
	(a_g) 3329	(b_{3g}) 3376	(b_{2u}) 3407	
(11)	(π) 862	(π) 862	(π) 1012	81.0
	(π) 1012	(σ) 2391	(σ) 3521	
	(σ) 3881			

(12)	(a") 192	(a") 291	(a') 342	238.1
	(a") 540	(a') 618	(a') 923	
	(a") 1079	(a') 1131	(a") 1208	
	(a') 1287	(a") 1315	(a') 1342	
	(a') 1483	(a') 1581	(a") 1585	
	(a') 1601	(a') 1654	(a') 1695	
	(a') 3178	(a") 3245	(a') 3312	
	(a') 3339	(a') 3413	(a') 3446	
(13)	(a") 365	(a") 782	(a') 866	252.6
	(a') 945	(a") 971	(a') 1037	
	(a') 1041	(a") 1110	(a") 1238	
	(a") 1276	(a') 1310	(a") 1323	
	(a') 1407	(a') 1434	(a') 1565	
	(a') 1604	(a') 1646	(a') 1801	
	(a') 3266	(a') 3300	(a") 3327	
	(a") 3383	(a') 3427	(a') 3810	
(14)	270i	174	182	225.4
	383	518	773	
	872	925	1156	
	1217	1256	1272	
	1352	1592	1600	
	1624	1652	2064	
	2581	3193	3270	
	3304	3331	3394	
(15)	(a") 143	(a') 360	(a") 595	249.4
	(a") 1079	(a") 1188	(a') 1189	
	(a") 1198	(a") 1304	(a') 1373	
	(a') 1481	(a')1590	(a')1597	
	(a') 1695	(a') 1846	(a') 1899	
	(a') 3345	(a') 3351	(a') 3414	
	(a') 3448	(a') 3472	(a') 3724	

Table 3.3 The relative energies between reactants, CH_3^+ and CH_3CN and products. These were calculated at equilibrium geometries using the 4-31G and 6-31G* basis sets.

Molecules	HF/4-31G	HF/6-31G*	MP2/4-31G	MP4SDQ/6-31G*
		kJ mol^{-1}		
(1) + (2)	0.0	0.0	0.0	0.0
(3)	-336.6	-331.8	-378.6	-386.3
(4)	-39.7	-36.4	11.9	-52.7
(5)	-137.4	-172.1	-168.6	-239.5
(6)	-92.3	-127.0	-131.9	-198.7
(7)	203.4	189.1	160.5	100.5
(8) + (9)	-71.5	-73.9	-95.8	-101.3
(10) + (11)	-98.8	-76.4	-158.9	-134.6
(12)	-38.3	-40.0	-25.0	-77.6
(13)	-248.3	-262.6	-264.1	-328.1
(14)	45.2	29.0	34.6	-22.6
(15)	-317.3	-297.8	-333.5	-358.7

Table 3.4 The zero-point vibrational corrected energies of relevant molecules and possible intermediates, relative to $CH_3CNCH_3^+$.

Molecules	HF/4-31G	HF/6-31G*	MP2/4-31G	MP4SDQ/6-31G*
		kJ mol^{-1}		
(3)	0.0	0.0	0.0	0.0
(1) + (2)	336.6	331.8	378.5	386.3
(4)	296.9	295.4	390.4	333.6
(5)	199.2	159.8	210.0	146.8
(6)	244.3	204.8	246.6	187.6
(7)	540.0	520.9	539.1	486.8
(8) + (9)	265.1	257.9	282.8	285.0
(10) + (11)	237.8	255.4	219.6	251.7
(12)	298.3	291.8	353.6	308.7
(13)	88.3	69.2	114.5	58.2
(14)	381.8	360.8	413.2	372.5
(15)	52.1	66.8	77.8	59.7

3.3 Results and Discussion

Most molecules were optimized and local minima were obtained with no negative eigenvalue in the computed force constant matrix. Only $CH_3CNCH_3^+$ (3) gave one negative eigenvalue in the harmonic vibrational calculation, due to the low energy barrier of the mutual rotation of the two methyl groups. The calculation also shows that the eclipsed structure of $CH_3CNCH_3^+$ is more stable than the staggered structure by 9.2 kJ mol^{-1}.

Two possible groups of end products in the multistep dissociation process of $CH_3CNCH_3^+$ are C_2H_4 and $HCNH^+$ and C_2H_5 and HCN. The reactions are:

$$CH_3CNCH_3^+ \rightarrow [\text{intermediates}]^+ \rightarrow C_2H_4 + HCNH^+$$

and

$$CH_3CNCH_3^+ \rightarrow [\text{intermediates}]^+ \rightarrow C_2H_5^+ + HCN$$

From our calculations at the MP4SDQ/6-31G* level shown in Table 3.4, the products, C_2H_4 and $HCNH^+$ are more stable than the products $C_2H_5^+$ and HCN by 33.3 kJ mol^{-1}.

For $CH_3CNCH_3^+$, the electron densities obtained from a Mulliken population analysis showed that the charge on nitrogen atom is -0.427 while the cyanide carbon atom charge is +0.559. This might suggest that a hydrogen atom on N-methyl group prefers to shift to nitrogen atom rather than the carbon atom in cyanide group. Later, detailed calculations on these two possible intermediates were done in order to compare the work of H. Wincel et al. with this study. It was then found that the hydrogen shift process preferred the carbon centre more than the nitrogen centre by 24.9 kJ mol^{-1} at the MP4SDQ/6-31G* level.

In our initially proposed pathway, after a hydrogen from N-methyl group shifts to nitrogen atom and forms a bent isomer (4), electrons from methylene group will form a bond with α–carbon atom to give a three membered ring structure (5). Then a hydrogen atom from methylene group will shift to carbon atom of the C-CH_3 apex to give structure (6) in which the the ring will break and yield the proposed products (scheme 1).

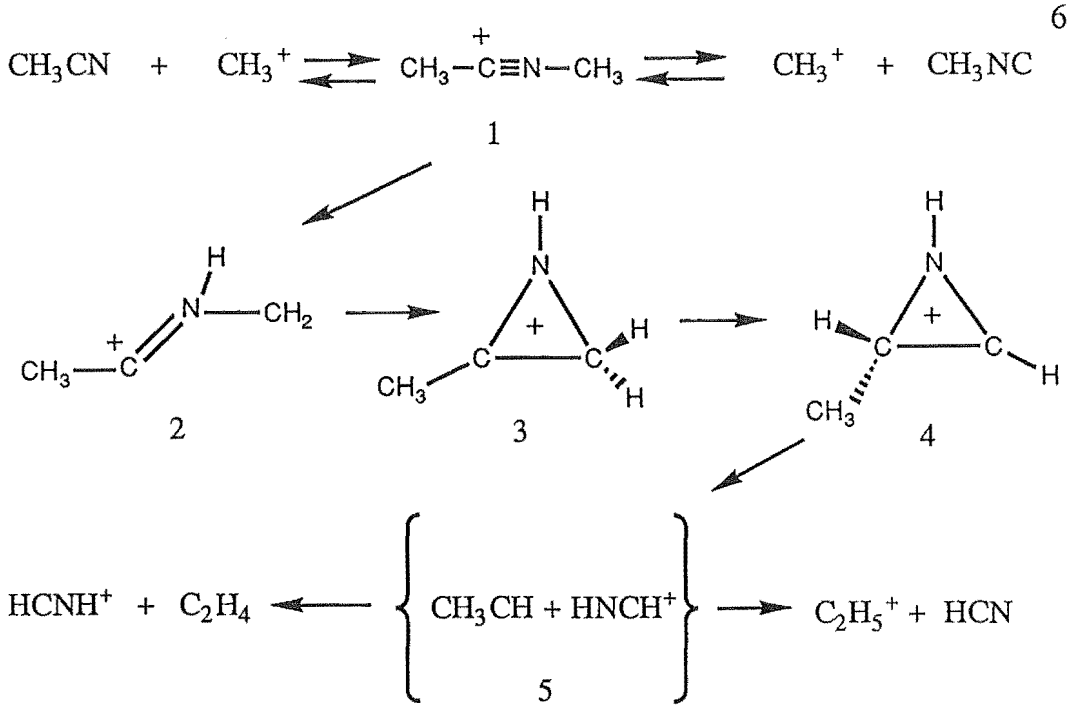

Scheme 1

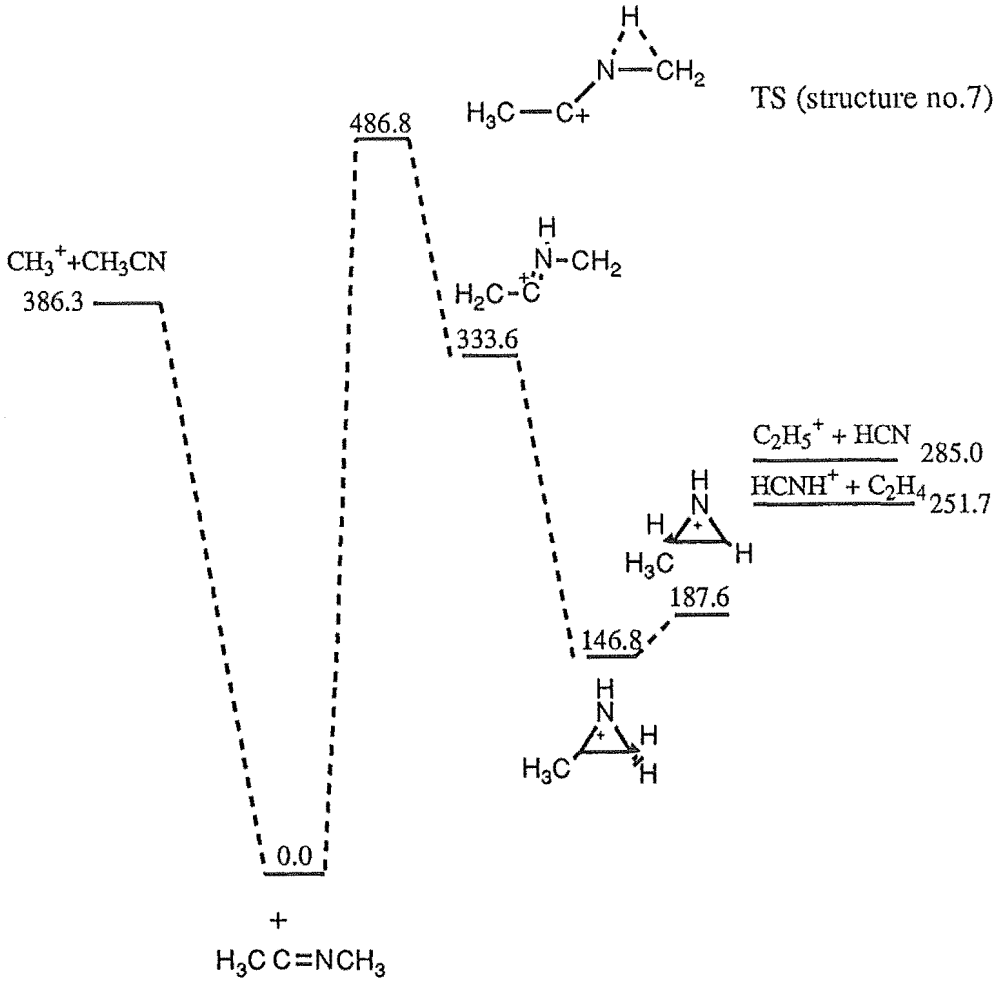

Figure 3.2 Energy diagram (kJ mol^{-1}) for $C_3H_6N^+$ isomers from this study (with scheme 1)

These proposed products and intermediates are consistent with the idea of multistep dissociation of $CH_3CNCH_3^+$, because all those energies of the proposed intermediates and products are lower than the energy that required for the direct dissociation process. However the calculations for the transition state (7) were made at the end of the series of calculations for scheme 1. The energy of this transition state is 100.5 kJ mol^{-1} higher than the energy sum of the reactants, which makes our proposed pathway kinetically unfavourable. H. Wincel et al. [146] proposed another pathway which involves the hydrogen shift from C-methyl group to the adjacent carbon atom. This yields a four-membered ring intermediate (scheme 2). We repeated the calculations for some intermediates which they proposed and also did a calculation for their transition state structure which had not been reported. Our results agree very well with their work. The energy of their transition state at the MP4SDQ/6-31G* level is lower than the energy for the direct dissociation by 22.6 kJ mol^{-1}. The relative energies of this transition state, compare with the sum of reactants' energies range from +45.2 to -22.6 kJ mol^{-1}, the inconsistency in the calculated energies arise from the different levels of theory that were used .

The study by H. Wincel and co-workers on CID/MIKE (the collisionally induced dissociation/ the mass analyzed ion kinetic energy) spectral [146] provides important evidence about the mechanism. In experiments starting with $(CH_3)^{13}CNCH_3$, the MIKE spectral of dissociative products show that 90% of ^{13}C is retained in the $^{13}CH_2N^+$, there is only 10 % of unlabelled CH_2N^+ ion in the products. This result strongly supports their proposed pathway. Though it is possible to explain the 10% unlabelled CH_2N^+ in the products by our proposed pathway, the previous discussion would indicate that this is unlikely. Wincel et al. also suggested an alternative mechanism to account for the 10% unlabelled CH_2N^+ in the same paper [146] but it has not so far been tested by any calculation or experiment.

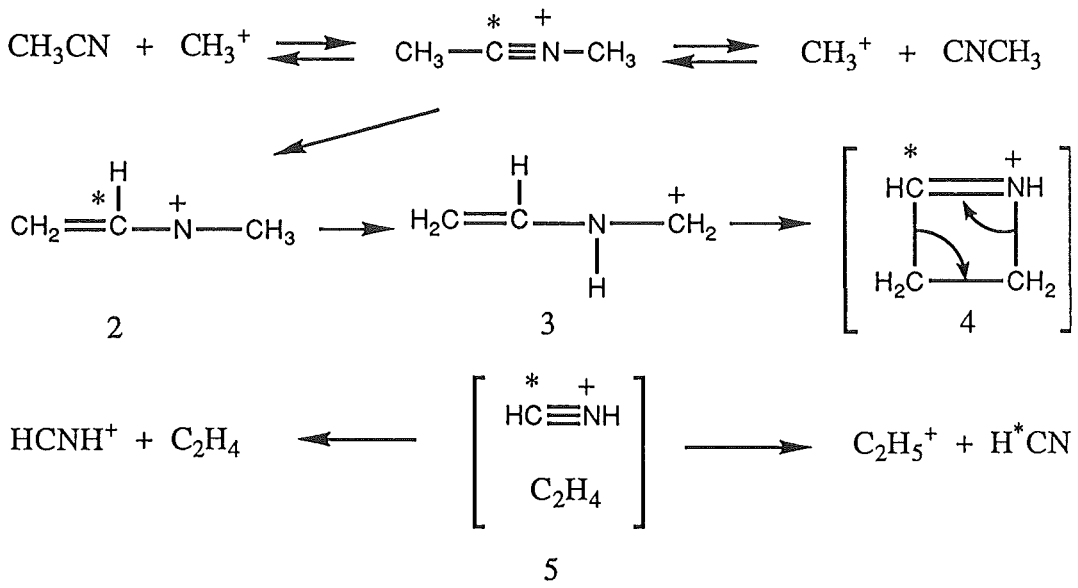

Scheme 2

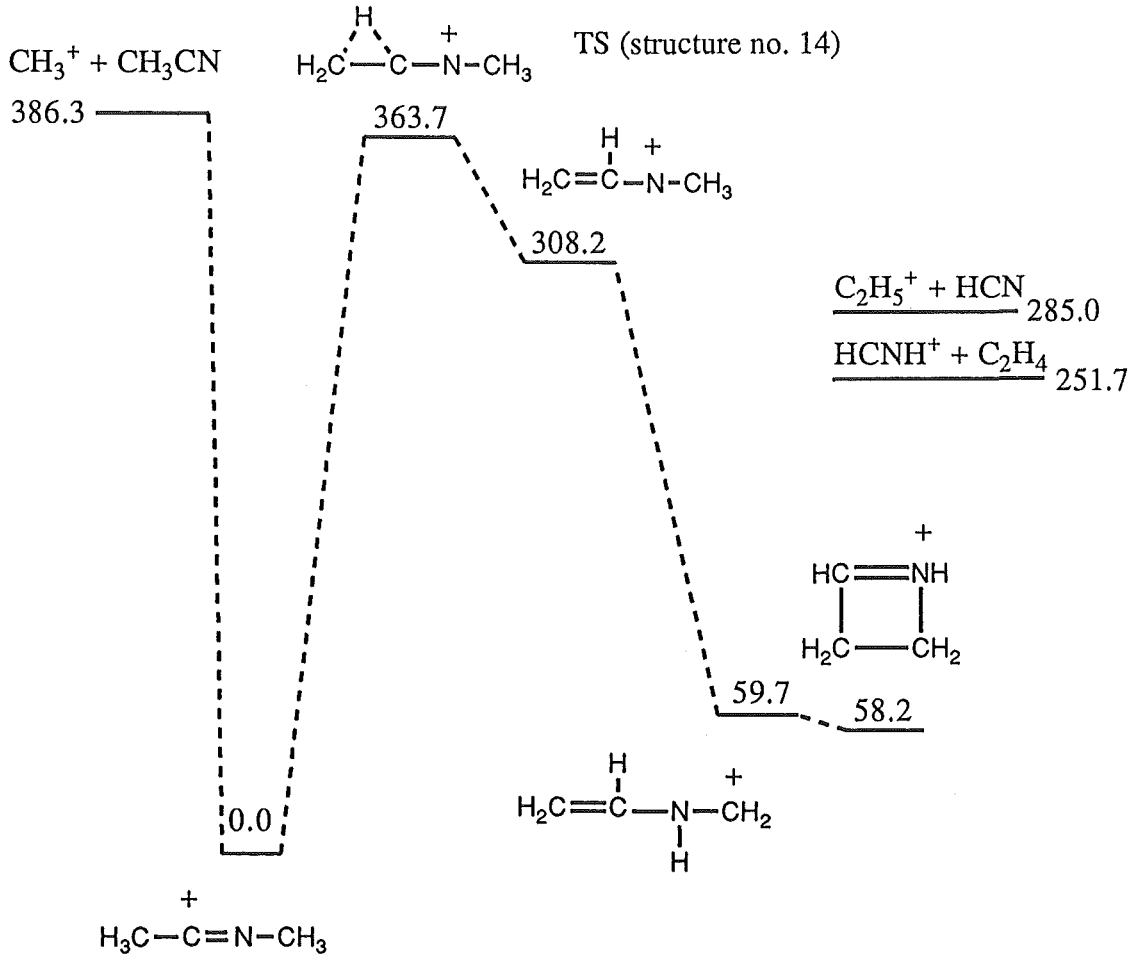

Figure 3.3 Energy diagram (kJ mol^{-1}) for $C_3H_6N^+$ suggested by ref. [145] (with scheme 2)

3.4 Conclusion

In this study the multistep pathway of the reaction between CH_3CN and CH_3^+ has been established by ab initio calculation. The calculated energy of the transition state is higher than the energies of reactant species, which suggest that the proposed pathway is unlikely to be correct. Wincel et al. [146] conducted a study of this chemical system by examining collisionally induced dissociations (CID) / mass-analyzed ion kinetic energy (MIKE) spectra. Our predicted products from the multistep process agree with their experimental results. They also established a chemical pathway for this reaction by using calculated data at the MP4/6-31G*//3-21G from a work of Bouchoux et al. [16]. We repeated and extended their calculations at the MP4SDQ/6-31G*//4-31G in order to compare their proposed pathway with our one. Their proposed pathway was confirmed to be more favourable and agree with the ^{13}C labelling experiments.

CHAPTER 4

Ab Initio Study of Organotin Compounds

4.1. Introduction

The chemistry of tin compounds has recently been of increasing interest because of their role in organic synthesis. However very few ab initio calculations on these compounds have been done. Dewar et al. [39,40] have applied the semi-empirical, Modified Neglect of Diatomic Overlap (MNDO) method to study organotin compounds with sufficient success to interpret the structures of cyclopentadienyl-tin complexes, multiple bonding involving tin, and the mechanism of hydrostannylation. Relativistic effects for a series of main group methyl derivatives and hydrides including tin have been investigated by Almof et al. [3] . More recently Pouchan et al. [112] claimed to have developed the " most complete" force field for methylstannane using Hartree-Fock and Mϕller-Plesset perturbation methods with a double zeta basis set. Their parameters agree very well with the experimental ones except for the calculated force constants.

Considering the industrial importance and utility of tin compounds in organic synthesis it is surprising that the geometries, energies and force constants remain largely uncharacterized by ab initio methods.

In this study we have used ab initio computations to provide equilibrium geometries, energies and force constants for a range of organotin compounds which can be used in the force field programs to give more information about molecular conformations and intra-molecular interactions within a variety of tin species, leading to a greater understanding of tin chemistry.

4.2. Method

All ab initio molecular orbital calculations in this study, were performed with the Gaussian 82 system of programs [11] . The supplemented split valence, 3-21G*, basis sets which had been recommended for third- and fourth-row, main group elements were used. Coefficients and exponents for carbon, hydrogen and oxygen, excluding their polarization functions, were taken from the work of Binkley, Pople and Hehre [12]. Coefficients and

exponents for tin were taken from the work of Dobbs and Hehre [43]. The uncontracted polarization function exponents used for carbon [58], oxygen [58] and tin [70] were 0.636, 0.8 and 0.183, respectively. The scale factors for all exponents were set to be 1.0.

Energies of the compounds studied were optimized at the Hartree-Fock level of theory with respect to the internal coordinates, to obtain bond lengths and bond angles. The structures of twelve organotin compounds were optimized and seven of these optimized molecular structures were used in vibrational frequency calculations to provide force constant values.

The vibrational frequencies had to be calculated from force constants provided by Gaussian 82 because the algorithm in the Gaussian 82 program we use produces an incorrect reduced mass for tin. Vibrational analyses for stannane (1) and methyl stannane (2) were performed within the FG formalism of Wilson et al. [144], involving equation (1).

$$| \mathbf{FG} - \mathbf{E}\lambda | = 0 \qquad (1)$$

where **F** is a matrix of force constants, **G** is a matrix which involves the mass and certain spatial relationships of the atoms and **E** is a unit matrix.

λ which brings the frequency, ν, into the equation (1), is defined by

$$\lambda = 4\pi^2 c^2 \nu^2 \qquad (2)$$

By solving equation (1) using scaled force constants deduced from our calculations on Gaussian 82 as elements of **F**, we obtained the eigenvalues λ which gave the vibrational frequencies of molecules.

Because of the use of dummy co-ordinates in specifying the z-matrix as the inputs for Gaussian 82, the calculated force constants of other five organotin compounds could not be used in Wilson et al.'s formula above.

Later, when Gaussian 90 [53] was available, the calculations for harmonic vibrational frequencies of these molecules including stannane and methyl stannane were done. The calculated vibrational frequencies for stannane and methyl stannane given by the algorithm in Gaussian 90 agree with the results obtained from Wilson et al.'s formulae.

Because simple organotin compounds tend to be unstable, there are a few published structures of these compounds. Only the structures of stannane (1) and methyl stannane (2) have been determined.

4.3 Results

Optimized structure of 12 organotin compounds at the HF/ 3-21G* level of theory are shown in Figure 4.1. In Table 4.1, the calculated total energies of these organotin compounds are reported. Table 4.2 shows the calculated harmonic vibrational frequencies that were obtained from the calculations with Gaussian 90. The calculated force constants of 7 selected organotin compounds are in Table 4.3. The geometries, force constants and total energies of stannane from different methods and experiment are compared in Table 4.4 to 4.7 respectively. The results for methyl stannane are similarly compared in Table 4.8 to 4.10.

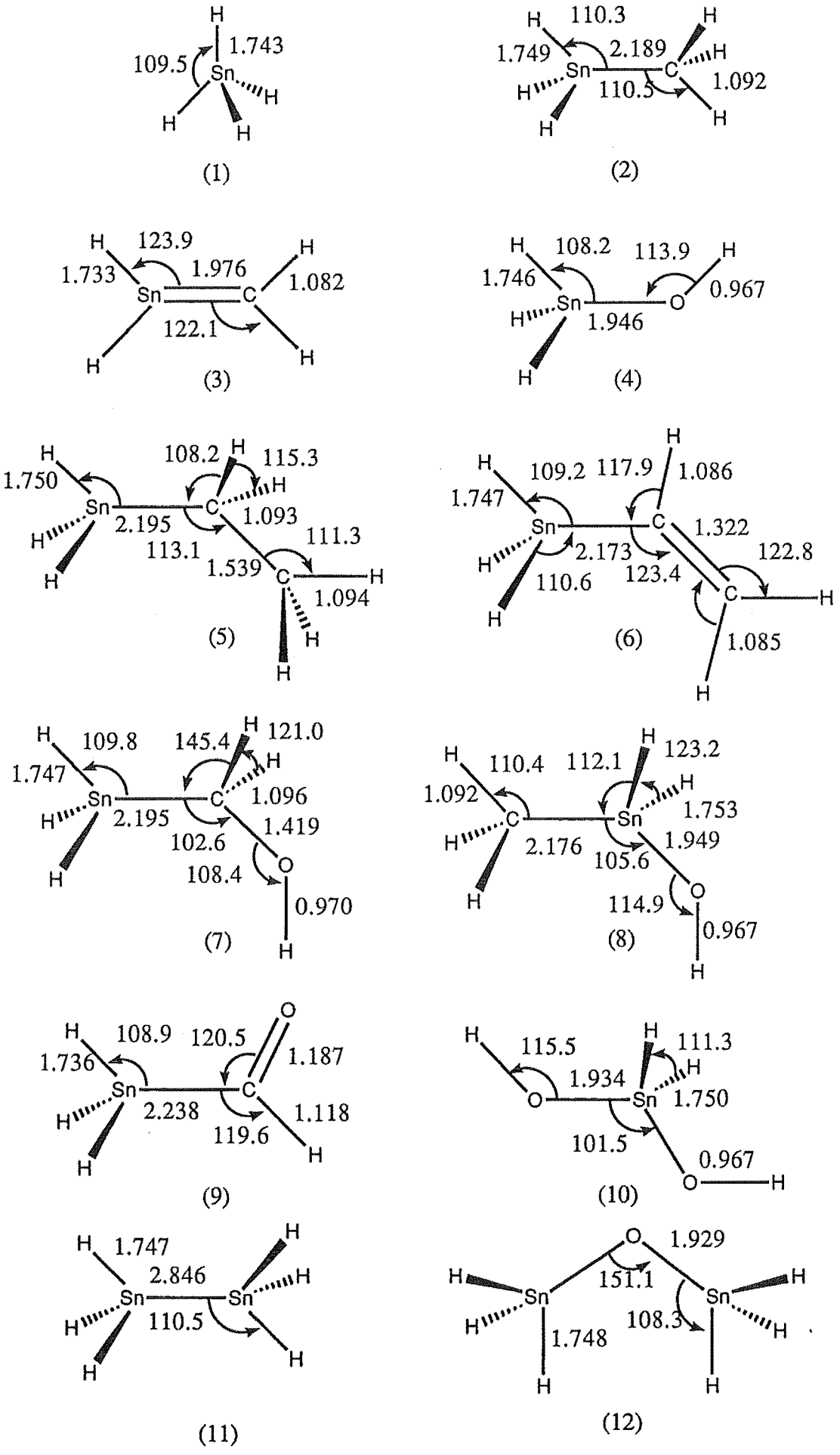

Figure 4.1 Optimized structures of organotin compounds (Ångstroms and degrees)

Table 4.1 The calculated total energies (hartree) of organotin compounds at the Hartree-Fock level with the 3-21G* basis set.

	Molecule	Energy
(1)	SnH_4	-5999.03529
(2)	H_3SnCH_3	-6037.89316
(3)	H_2SnCH_2	-6036.65480
(4)	H_3SnOH	-6073.54286
(5)	$H_3SnCH_2CH_3$	-6076.73902
(6)	$H_3SnCHCH_2$	-6075.55372
(7)	H_3SnCH_2OH	-6112.34754
(8)	H_3CSnH_2OH	-6112.40416
(9)	H_3SnCHO	-6111.19053
(10)	$H_2Sn(OH)_2$	-6148.05501
(11)	H_3SnSnH_3	-11996.96539
(12)	$H_3SnOSnH_3$	-12071.48371

Table 4.2 The calculated harmonic vibrational frequencies (cm^{-1}) and zero-point vibrational energies (kJ mol^{-1}) for organotin compounds .

Molecule	Harmonic vibrational frequencies						ZPVE
(1) SnH_4	(t_2)	763	(t_2)	763	(t_2)	763	71.01
	(e)	806	(e)	806	(e)	806	
	(t_2)	1988	(t_2)	1988	(t_2)	1988	
	(a_1)	2008					
(2) $SnCH_6$	(a_2)	85	(e)	435	(e)	435	153.69
	(a_1)	552	(a_1)	763	(e)	790	
	(e)	790	(e)	846	(e)	846	
	(a_1)	1388	(e)	1594	(e)	1594	
	(e)	1967	(e)	1967	(a_1)	1985	
	(a_1)	3169	(e)	3245	(e)	3245	
(3) $SnCH_4$	(b_1)	256	(b_2)	408	(a_2)	687	100.24
	(a_1)	754	(b_2)	795	(b_1)	800	
	(a_1)	808	(a_1)	1516	(b_2)	2018	
	(a_1)	2030	(a_1)	3295	(b_2)	3392	
(4) H_3SnOH	(a")	78i	(a')	530	(a")	558	89.57
	(a')	705	(a')	771	(a")	773	
	(a')	790	(a')	888	(a")	1984	
	(a")	1984	(a')	2006	(a")	3986	
(5) SnC_2H_8	(a")	67	(a')	199	(a")	239	234.55
	(a")	436	(a')	461	(a')	565	
	(a")	741	(a')	756	(a")	790	
	(a')	791	(a')	1032	(a")	1037	
	(a')	1106	(a')	1355	(a")	1369	
	(a')	1551	(a')	1592	(a')	1631	
	(a")	1638	(a")	1964	(a')	1964	
	(a')	1980	(a')	3155	(a')	3168	
	(a")	3197	(a')	3208	(a")	3221	

(9) H_3SnCHO	(a")	33i	(a')	230	(a")	400	103.27
	(a')	437	(a')	629	(a')	743	
	(a")	783	(a')	784	(a")	906	
	(a')	1488	(a')	1936	(a")	1985	
	(a')	1987	(a')	2000	(a')	2955	
(10) H_2SnOH_2	(a_2)	208i	(b_1)	129i	(a_1)	203	106.84
	(b_1)	507	(a_2)	554	(b_2)	686	
	(a_1)	717	(b_2)	736	(a_1)	780	
	(b_2)	854	(a_1)	869	(b_1)	1971	
	(a_1)	1998	(a_1)	3993	(b_2)	3993	

Table 4.3 The calculated force constants of organotin compounds at the Hartree-Fock level with the 3-21G* basis set.

	Molecule	Force constants[a]	
(1)	SnH_4	k_{Sn-H} : 2.34	k_{H-Sn-H} : 0.68
(2)	H_3SnCH_3	k_{Sn-H} : 2.29	k_{Sn-C} : 2.41
		k_{Sn-C-H} : 0.82	k_{C-Sn-H} : 0.68
(3)	H_2SnCH_2	k_{Sn-H} : 2.41	k_{Sn-C} : 4.71
		k_{Sn-C-H} : 0.89	k_{C-Sn-H} : 0.70
(4)	H_3SnOH	k_{Sn-H} : 2.34	k_{Sn-O} : 4.48
		k_{Sn-O-H} : 0.39	k_{O-Sn-H} : 0.74
(9)	H_3SnCHO	k_{Sn-H} : 2.33	k_{Sn-C} : 2.02
		k_{Sn-C-O} : 1.57	k_{C-Sn-H} : 0.62
		k_{H-C-Sn} : 1.38	
(10)	$H_2Sn(OH)_2$	k_{Sn-H} : 2.32	k_{Sn-O} : 4.68
		k_{Sn-O-H} : 0.37	k_{O-Sn-O} : 0.90
		k_{H-Sn-H} : 0.74	

[a] $aJÅ^{-2}$ for stretching and $aJÅ^{-1}$ for deforming force constants (aJ = atto Joule). atto = 10^{-8}.

Table 4.4 The comparison of geometries (Ångstrom and degrees) of stannane in this study with other works.

Parameter	This work	MNDO[a]	DISCO[b]	OCE[c]	Expt[d]
1. r_{Sn-H}	1.744	1.586	1.705	1.762	1.701
2.H-Sn-H	109.5				109.5

[a] reference 39 [b] Reference 3
[c] Reference 30 [d] Reference 143

Table 4.5 Calculated force constants for stannane[a], compare with experimental results and with other works.

Parameter	This work	DISCO[b]	OCE[c]	Expt[d]
1. Sn-H str	2.34	2.74	2.0	2.27
2. H-Sn-H def	0.68			

[a] aJÅ^{-2} for stretching and aJÅ^{-1} for deforming force constants.
[b] Reference 3 [c] Reference 30 [d] Reference 83

Table 4.6 The calculated and experimental harmonic vibrational frequencies (cm^{-1}) for stannane.

Assign	This work		Experiment[a]
	Wilson formulae	Gaussian 90	
(t_2)	763	763	677
(e)	806	806	758
(t_2)	1987	1988	1901

[a] Reference 83

Table 4.7 Calculated energies of stannane (hartree) as obtained by different methods.

	This work	DISCO[a] (non-relativistic)	OCE[b]
Energy	-5999.04	-6024.56	-6024.27

[a] Reference 3 [b] Reference 30

Table 4.8 Comparison of geometries of methyl stannane (Ångstroms and degrees) with other works.

Parameter	This work	SCF[a]	MP2[a]	Expt[b]
1. r_{Sn-C}	2.189	2.108	2.148	2.143
2. r_{C-H}	1.092	1.085	1.108	1.083
3. r_{Sn-H}	1.749	1.719	1.730	1.708
4. H-Sn-C	110.3	110.8	110.6	109.4
5. Sn-C-H	110.5	110.7	110.2	110.4

[a] Reference 112 [b] Reference 76

Table 4.9 Comparison of force constants found for methyl stannane[a]

Parameter	This work	SCF[b]	MP2[b]	Expt[c]
1. Sn-H str	2.29	2.52	2.46	2.24
2. Sn-C str	2.41	2.87	2.90	2.12
3. C-H str	5.72	5.90	5.76	5.39
4. Sn-C-H def	0.82			
5. C-Sn-H def	0.68			

[a] aJÅ^{-2} for stretching and aJÅ^{-1} for deforming force constants.
[b] Reference 112 [c] Reference 76

Table 4.10 The calculated harmonic vibrational frequencies (cm^{-1}) for methylstannane; values from Gaussian 90 are in parenthesis.

Assign	This work	SCF[a]	MP2[a]	Adj[a]	Expt[b]
(a_1)					
CH_3 str	3169 (3169)	3195	3156	3062	3058
SnH_3 str	1985 (1985)	2066	2038	1944	1935
CH_3 def	1388 (1388)	1455	1354	1236	1242
SnH_3 def	762 (763)	827	780	719	716
SnC str	552 (552)	600	603	516	527
(e)					
CH_3 str	3245 (3245)	3291	3276	3156	3157
SnH_3 str	1967 (1967)	2038	2020	1943	1935
CH_3 def	1594 (1594)	1613	1526	1466	1481
CH_3 rock	789 (790)	872	827	806	796
SnH_3 def	762 (790)	820	766	741	755
SnH_3 rock	435 (435)	454	430	431	430
(a_2)					
torsion	86 (85)	134	118	109	110

[a] Reference 112 [b] Reference 125

4.4 Discussion

In Table 4.4 the tetrahedral stannane structure is compared with the data deduced by Wilkinson and Wilson [143] from the infrared spectrum. The agreement between our calculated Sn-H bond length and the experimental values is a significant improvement on Dewar's MNDO calculation [39]. The result also agrees with Declaux and Pyykko's work [30], which was a Dirac-Fock calculation using the One Center Expansion (OCE) method, but it is inferior to Almlof and Faegri's work [3], which used the Direct SCF Code (DISCO) method, including relativistic effects.

As is evident from Table 4.5, our calculated force constant for SnH stretching is closer to the experimental value than the results from the OCE [30] and DISCO [3] methods.

In Table 4.7, our calculated molecular energy of stannane is about 25 hartree higher than the values from the OCE [30] and DISCO [3] methods. The vibrational frequencies for stannane in Table 4.6 agree with the experimental results by Levine and Schiffer [83].

From Table 4.8 and 4.9, our results for methylstannane are in good agreement with experimental data. Force constants correspond well with the available values; however, bond lengths and bond angles are less accurate (as expected) than those of Pouchan et al. [112], whose calculations included electron correlation at the MP2 level with a double-zeta basis set.

The calculated harmonic vibrational frequencies are expected to be too large due to the harmonic approximation and to a lesser extent of the neglect of electron correlation. They are between 10 to 15 percent higher than the experimental values, in the case of the calculations with double zeta basis set [13,113,147]. Pouchan et al. [112] corrected for the electron correlation effect by performing their calculation at MP2 level and replacing the diagonal elements in **F** matrix in Wilson formalism [144] with the force constant values from a least-squares fit between their ab initio calculation and experimental data, so it is not surprising that their adjusted results agree very well with the experimental ones.

Without any adjustments, our calculated vibrational frequencies show an average error of 4.8 percent when compare with the experimental data. The imaginary frequencies found for H_3SnOH and $H_2Sn(OH)_2$ are likely to be the results of low rotational energy barriers of Sn-O-H bonds. The use of larger basis sets should resolve this problem.

There are no available calculated or spectroscopic data for the rest organotin compounds in this study. We consider, by extrapolation from the results for stannane and methylstannane that our results are sufficiently reliable to use as a basis for further study of tin compounds.

CHAPTER 5

Theoretical study of C_nO, C_nO^+, C_nHO^+, C_nS, C_nS^+, and C_nHS^+ species.

5.1 Introduction

The Chemistry of the interstellar clouds has been of increasing interest recently due to the variety of newly identified molecules. Beside the abundant hydrogen molecule, astronomers have also found almost 100 other molecules, ionized molecules and radicals composed of the light elements hydrogen, carbon, oxygen, nitrogen, sulphur, silicon, chlorine and phosphorus. The densities of these molecules are as low as 100 molecules per cubic centimetre in the diffuse and translucent clouds, and up to 1000 or 10000 per cubic centimetre in the dense clouds, with temperature of 70 K in the diffuse clouds and 10 K in the dense ones. A number of clues have led astronomers to believe that large molecules containing rings of carbon atoms may exist in the interstellar medium. These large molecules are likely to be polycyclic aromatic hydrocarbons like coronene ($C_{24}H_{12}$) and napthalene ($C_{10}H_8$) [2].

Neutral and singly-ionized carbon atoms are known to be abundant in interstellar clouds. They are the starting material for all carbon-containing molecules, one of simplest of which is carbon monoxide. CO is the second most abundant interstellar molecule after hydrogen. A hypothetical mechanism for the generation of CO from C atoms is [2]:

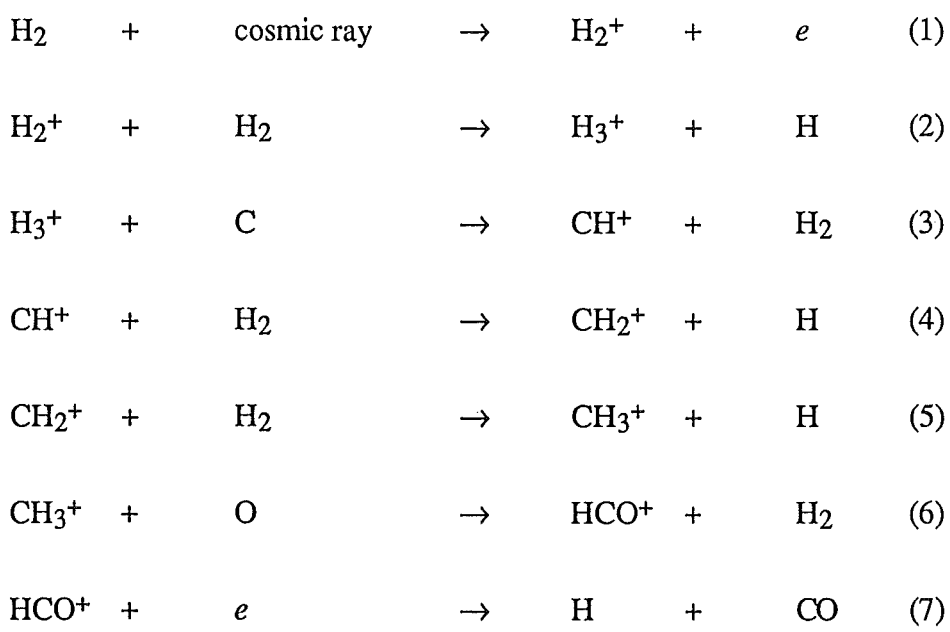

Carbon monoxide can react with H_3^+ to form HCO^+, which has been detected in various interstellar clouds:

$$H_3^+ + CO \rightarrow HCO^+ + H_2 \qquad (8)$$

The HCO^+ ion can capture an electron and regenerate CO molecule by the reaction (7) above. The CO molecule has been studied extensively, both experimentally and theoretically.

C_2O ($6\sigma^2$, $1\pi^4$, $7\sigma^2$, $2\pi_x^1$, $2\pi_y^1$ $X^3\Sigma^-$)

The radical C_2O has not been yet detected in any interstellar clouds. An upper limit for the column density, (1-2) x 10^{12} cm^{-2} in TMC-1, was calculated by Irvine et al. [71]. The abundance of this molecule is likely to be much lower than that of its sulphur analogue, C_2S. The study of C_2O has focussed mainly on its role as a reactive intermediate in chemical systems [6,44,45]. Schildcrout and Franklin [122] found this molecule among other carbon suboxide and fragments produced by electron bombardment of C_3O_2 in the ion source of a mass spectrometer. The suggested process is:

$$C_3O_2 + e \rightarrow \text{primary ions} \qquad (9)$$

where primary ions are $C_3O_2^+$, C^+, C_3^+, O^+, CO^+, C_2O^+ and C_3O^+, followed by

$$C_2O^+ + C_3O_2 \rightarrow C_3O_2^+ + C_2O \qquad (10)$$

Schildcrout and Franklin [122] concluded that the upper limit of ionization potential for C_2O was 11.5 eV. (1109.6 kJ mol^{-1}). A heat of formation of 384 ± 21 kJ mol^{-1} for C_2O an the upper limit of 1477 kJ mol^{-1} for C_2O^+ were estimated by Baker and Bayes [7].

Jacox et al. [73] photolyzed C_3O_2 in argon matrix at 4 K and observed a recurring infrared band at 2244 cm^{-1} which was assigned later to C_3O. The C_2O molecule was suggested as an intermediate of this process.

$$C + CO \rightarrow C_2O \qquad (11)$$

$$C + C_2O \rightarrow C_3O \quad (12)$$

DeKock and Weltner [33] detected an infrared spectrum of C_2O at 1928 cm^{-1} in the same system and showed that C_2O was changed to C_3O when the temperature was increased. They concluded that C_2O has different bonding system from the isoelectronic molecule, CNN: crudely C=N=N vs C-C=O.

Laser photolysis of acetylene in the present of O_2 has been used to generate C_2O which is in the $A^3\Pi_u$ state instead of the $X^3\Sigma^-$ ground state [45].

Chabalowski et al. [25] studied the low-lying electronic transition of C_3 and C_2O at HF and multiconfiguration double excitation (MRD-CI) levels. The vertical $A^3\Pi_u$ - $X^3\Sigma^-$ transition energy (T_v) between is found to be 1.479 eV.

The abundance of CO and C^+ in the interstellar medium and the experimentally known existence of C_2O^+, C_3O^+, C_4O^+ etc. led Haese and Woods [59] to do theoretical studies on COC^+ and CCO^+. These molecules were found to have unusual long bonds $C\text{-}CO^+$ and $C\text{-}OC^+$. They concluded that C^+ loosely attaches to CO in both structures, and the bond more resemble the inorganic ion-carbonyl ligand system than conventional covalent bonds. The calculation also shows that the barrier energy is low for the important chemical process:

$$C^+ + CO \rightarrow CO + C^+ \quad (13)$$

which is related to the process:

$$^{13}C^+ + O^{12}C \rightarrow {}^{12}C^+ + {}^{13}CO \quad (14)$$

The COC^+ ion also has unequal C-O bond length.

C_3O ($8\sigma^2$, $1\pi^4$, $9\sigma^2$, $2\pi^4$ $^1\Sigma^+$)

C_3O was detected in the interstellar molecular cloud TMC-1 by Mathew et al. [91]. Brown et al. [22] found that the fractional abundance of C_3O is low.

In the electron bombardment study of C_3O_2 by Schildcrout and Franklin [122], C_3O^+ was found as one of primary ions and was also formed by the reaction:

$$C_2O^+ + C_3O_2 \rightarrow C_3O^+ + 2CO \quad (15)$$

C_3O^+ is reactive and can react with C_3O_2 to give C_4O^+.

$$C_3O^+ + C_3O_2 \rightarrow C_4O^+ + 2CO \quad (16)$$

As mentioned above, in the photolysis experiments on C_3O_2 by Jacox et al. [73] they found the recurring infrared band at 2244 cm^{-1}. This frequency (2204 cm^{-1}) was re-examined and assigned to CCCO molecule by DeKock and Weltner [33]. A carbon atom is assumed to be captured by the intermediate C_2O as in the reaction (12).

A theoretical study of C_3O has been made by Brown and Rice [20] at HF and MP3 levels with STO-3G, 4-31G and 6-31G* basis sets. Their calculations show that the singlet state energy of C_3O is lower than the triplet state by 168 kJ mol^{-1}. The calculated heat of formation is 282 kJ mol^{-1}. C_3O is thermodynamically more stable than C_2 + CO by 433 kJ mol^{-1}. The calculated rotational constants and dipole moment (μ) were reported to be 4814 MHz. and 1.85 D. The predicted vibrational frequencies (cm^{-1}) are 200 (π), 720 (π), 1010 (σ), 1890 (σ)and 2200 (σ) (these have been scaled by a factor of 0.9).

A possible route to produce C_3O by the pyrolysis of the compound $C_{12}H_{12}O_8$ was examined theoretically. The hypothetical process is:

$$C_{12}H_{12}O_8 \rightarrow C_4O_2 + \text{other products} \rightarrow C_3O + CO + \text{other products} \quad (17)$$

Brown and Rice [20] also found in the calculation that C_4O_2 was stable compare with C_3O and CO at MP2/6-31G level and the energy barrier of the reaction was high, which means that the process above is not feasible.

The calculations show that some dimers of C_3O are thermodynamically stable but the energy barriers for their formation are high.

C_2S ($6\text{-}7\sigma^2, 8\sigma^2, 2\pi^4, 9\sigma^2, 3\pi^2, {}^3\Sigma^-$)

Saito et al. [121] performed an experiment on a mixture of CS_2 and He in a free-space absorption cell with a DC glow discharge for generating free radicals. The linear C_2S radical was detected with by microwave spectroscopy, and the spectrum from this experiment was used to assign unidentified lines from TMC-1 and Sgr B2. The estimated column densities of C_2S in TMC-1 and Sgr B2 are $(8\pm2) \times 10^{13}$ cm^{-2} and $(6\pm1) \times 10^{13}$ cm^{-2}, respectively.

A theoretical study of C_2S was done by Murakami [98] at the HF, MP3 and CI levels of theory with a 6-31G* basis set and with large well-tempered Gaussian basis set. The calculated rotational constant (B_e = 6438 MHz) and the dipole moment (μ = 2.8 D) were reported.

C_3S ($7\text{-}9\sigma^2, 10\sigma^2, 2\pi^4, 11\sigma^2, 3\pi^4, {}^1\Sigma^+$)

Saito et al. [148] employed the same experiment as described above to assigned the spectral lines of C_3S in TMC-1. The rotational constant (B_0 = 2890.38 MHz.) and the estimated column density (1.3×10^{13} cm^{-2}) were reported.

In the same paper, Murakami [98] reported a theoretical study of C_3S at the same levels and with the same basis sets as used for C_2S. The calculated rotational constant (B_0 = 2888 MHz) and the dipole moment (μ = 3.6 D) were reported. Murakami [98] also found that the addition of a carbon atom to the short chain monosulphides will stabilize the molecule by 418-669 kJ mol^{-1}.

These studies have shown that abundances of C_2S and C_3S are much greater than the estimated abundances of C_2O and C_3O, and that the abundances of sulphur-contained organic molecules like thioformaldehyde (H_2CS) are greater than the expected values from the steady state model [66]. Thus interstellar sulphur chemistry is not clearly understood.

In the present study, calculations have been made on C_nO, C_nO^+, C_nHO^+, C_nS, C_nS^+ and C_nHS^+ (n=2,3) species at high levels of theory. The results provide data for inonization and protonation processes and molecular properties such as geometries, dipole moment, vibrational frequencies, heat of formation and rotational constants. These data should be useful to experimentalists. A comparison between oxygen and sulphur compounds has also been made.

5.2 Computation Details.

All the calculations derived here were made with Gaussian 82 program [11]. Geometries were initially optimized at the HF level with the 6-31G* basis set. These optimized geometries were then used in calculation of harmonic vibration frequencies at MP2 and MP4SDQ level with the same basis set. This procedure was repeated with a 6-311G** basis set for the unprotonated species and for the lowest energy isomer of the protonated species.

In order to include the effects of electron correlation on geometry, we optimized C_3O and C_3O^+ at the MP2/6-311G** level and used these optimized geometries in MP2 and MP4SDQ calculations. The MP4SDQ energies quoted do not include core interactions, but MP2 (FC) energies do. The basis set superposition energy correction was taken into account in the proton affinity calculation by putting the hydrogen basis set on C_3O, C_2O, C_3S and C_2S neutral species at optimized geometries in MP2 and MP4SDQ calculations with with 6-311G** basis set. The location of the hydrogen basis set relative to C_1 was as in the corresponding optimized HC_nX^+ structure.

5.3 Results and Discussion

The structures of the compound studied are shown in Figure 5.1. Table 5.9 contains the energies of the species, calculated using the 6-31G* and 6-311G** basis sets. Only the lower-energy protonated forms were calculated with the 6-311G** basis set. In Table 5.10 and Table 5.11, the optimized geometric parameters are reported for oxygen and sulphur

species, respectively. Where no bond angles are given the molecules are linear. In Table 5.12 are given the harmonic vibrational frequencies and zero-point vibrational energies at the HF/6-31G* level of theory. Table 5.13 and 5.14 contains values of ionization potentials and proton affinities of C_nO and C_nS species, where unscaled zero-point vibrational energies were included in the calculation. In the case of the proton affinities, no basis set superposition error correction was made.

5.3.1 Optimized Geometries

In Table 5.1 the optimized geometries of oxygen and sulphur containing species in this study are presented in pairs. The optimized geometry of C_3O is close to that calculated by Brown and Rice [20] with a smaller basis set (6-31G*). The results imply that all the bonds have a bond order about two. The C_1C_2 bond length is close to that of the C_2C_3 bond in butatriene (1.283 Å) while the C_2C_3 bond length in C_3O is close to that of the CC bond in cyclopropene (1.30 Å). The CO bond is shorter than those in ketene (1.161 Å) and carbon dioxide (1.162 Å).

Both CC bond lengths in C_3S are close to those in C_3O and should be the same types. The CS bond is shorter than the double bond in carbon disulphide (1.553 Å). In ionization processes all the bonds in both molecules change by amount ranging from 0.2 to 8.8 %.

Terminal protonation process significantly affects the geometries of both molecules, giving bent structure for the x-terminal protonated species.

The CC bond length in C_2O is close to that of the CC bond in cyanoacetylene (1.378 Å) while the CC bond in C_2S is intermediate between the CC bonds in cyclopropene (1.300 Å) and allene (1.308 Å). The CS bond in C_2S evidently has a bond order less than that in C_3S.

Protonation and ionization processes change the geometries in both molecules to the same extent as for the C_3X species. Protonation on the terminal carbon atom gives a bend structure for C_2O but a linear one for C_2S.

The HF optimized bond lengths for C_2O are shorter than those (RC_1C_2 = 1.368 Å and RC_2O = 1.165 Å) obtained by Chabalowski et al. [25] from MRD-CI calculations which included correlation effects. The value $RC_1C_2 + RC_2O$ = 2.52 Ångstroms was obtained by Devillers and Ramsay [35] from spectroscopic measurements. The value from our HF/6-311G** calculations is 2.481 Ångstrom. Walch [142] obtained the larger value of 2.578 Ångstrom from POL-CI calculations.


(1)


(10)


(2)


(11)

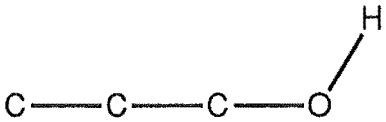
(3)

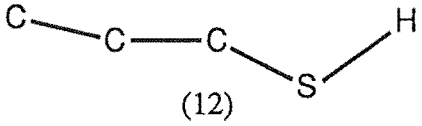
(12)

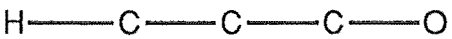
(4)

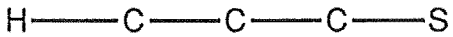
(13)

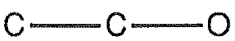
(5)

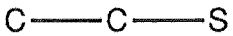
(14)

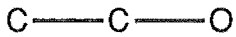
(6)

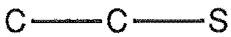
(15)


(7)

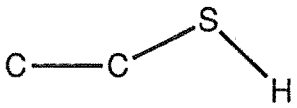
(16)

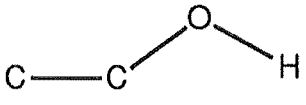
(8)


(17)

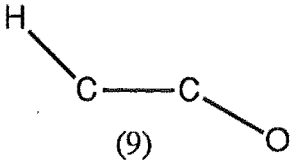
(9)

Figure 5.1. Structures found for C_nO, C_nO^+, C_nHO^+, C_nS, C_nS^+ and C_nHS^+ species.

Table 5.1 Optimized geometries (Ångstroms and degrees) of oxygen and sulphur containing species (grouped in pairs for comparison).

Molecule	Theory	C_1C_2	C_2C_3	C_1X	C_1H	XH
			Ångstrom			
C_3O	MP2/6-311G**	1.281	1.304	1.158		
	HF/6-311G**	1.251	1.294	1.119		
C_3S	HF/6-311G**	1.260	1.283	1.526		
C_3O^+	MP2/6-311G**	1.178	1.369	1.113		
	HF/6-311G**	1.233	1.337	1.098		
C_3S^+	HF/6-311G**	1.257	1.307	1.517		
C_3OH^+	HF/6-31G*	1.312	1.226	1.217		0.970
		$C_1C_2C_3 = 179.6$		$C_2C_3O = 176.4$		$C_3OH = 119.8$
C_3SH^+	HF/6-31G*	1.318	1.231	1.638		1.333
		$C_1C_2C_3 = 178.5$		$C_2C_3S = 175.5$		$C_3SH = 95.3$
HC_3O^+	HF/6-311G**	1.188	1.350	1.092	1.067	
HC_3S^+	HF/6-311G**	1.191	1.348	1.472	1.064	
C_2O	MP2/6-311G**	1.377		1.160		
	HF/6-311G**	1.351		1.130		
C_2S	HF/6-311G**	1.302		1.546		
C_2O^+	HF/6-311G**	1.581		1.086		
C_2S^+	HF/6-311G**	1.383		1.527		
C_2OH^+	HF/6-31G*	1.359		1.225		0.969
		$C_1C_2O = 146.6$		$C_1OH = 116.5$		
C_2SH^+	HF/6-31G*	1.255		1.614		1.335
		$C_1C_2S = 170.1$		$C_2SH = 98.6$		
HC_2O^+	HF/6-311G**	1.356		1.102	1.075	
		$OC_1C_2 = 176.2$		$C_2C_1H = 142.2$		
HC_2S^+	HF/6-311G**	1.264		1.547	1.067	

5.3.2 Rotational Constants

Calculated rotational constants for C_nO, C_nO^+, C_nS and C_nS^+ from this study are presented in Table 5.2. Our calculated rotational constant for C_3O is close to the value observed by Brown et al. [21], while the calculated value for C_3S agrees very well with the experimental value of Saito et al. [148]. The rotational constant found for C_2O is quite large but is supported by the value obtained by Devillers and Ramsay [35]. In this study the calculated rotational constant for C_2S differed by 4.8 % from the experiment result obtained by Saito et al. [121]. We found in our calculations that increasing the size of the basis set led to increased B_e values, making them in less agreement with the experimental results.

Table 5.2 Calculated rotational constants of C_nO, C_nO^+, C_nS and C_nS^+, comparing with available experimental values.

Molecule	Theory	B_e (MHz)	Experiment (MHz)
C_3O	MP2/6-311G**	4871.6	4810.9[a]
	HF/6-311G**	4927.0	
C_3S	HF/6-311G**	2942.5	2891.0[b]
C_3O^+	MP2/6-311G**	4871.6	
	HF/6-311G**	4884.6	
C_3S^+	HF/6-311G**	2921.5	
C_2O	MP2/6-311G**	11847.8	11545.0[c]
	HF/6-311G**	11446.1	
C_2S	HF/6-311G*	6166.6	6477.8[d]
C_2O^+	HF/6-31G**	10354.7	
C_2S^+	HF/6-311G**	6401.8	
COC^+	HF/6-311G**	9452.6	

[a] Reference 21 [b] Reference 148 [c] Reference 35 [d] Reference 121

5.3.3 Dipole Moments

In Table 5.3, calculated dipole moments of C_nO, C_nO^+, C_nS, C_nS^+ and COC^+ were reported. For the dipole moment of C_3O we found that, with the same basis set, a calculation at the HF level gave better agreement with the experimental result than a calculation at the MP2 level. For C_3S and C_2S the larger basis set gives larger dipole moments. This trend was also found in the calculations by Murakami [98]. The dipole moment of COC^+ is large compared with that of C_2O^+ because the charge distribution in COC^+ has more ionic character at the terminal atoms. The Mulliken charge of C_1 in CCO^+ is 0.4 a.u. while that of C_1 in COC^+ is 0.8 a.u..

Table 5.3 Calculated dipole moments of C_nO, C_nO^+, C_nS, C_nS^+ and COC^+ in Debye(D).

Molecule	Theory	Dipole (D)	Experiment (D)
C_3O	MP2/6-311G**	1.557	2.391[a]
	HF/6-311G**	2.134	
C_3S	HF/6-311G**	3.122	
	HF/6-31G*	2.644	
C_3O^+	MP2/6-311G**	2.319	
	HF/6-311G**	2.450	
C_3S^+	HF/6-311G**	0.298	
C_2O	MP2/6-311G**	1.409	
	HF/6-311G**	1.590	
C_2S	HF/6-311G**	3.123	
C_2O^+	HF/6-311G**	1.756	
C_2S^+	HF/6-311G**	1.528	
COC^+	HF/6-311G**	3.646	

[a] Reference 21

5.3.4 Adiabatic Ionization Energy.

As shown in the table below, the ionization energies are not affected much by using optimized geometries from an MP2 calculation instead of HF with the same basis set. Both C_3O and C_2O have considerably higher ionization energies than the sulphur analogues. This could be attributed to the greater screening effect in sulphur containing species. The value of the scale factor used in correcting the zero-point vibrational energies has only a very small effect on the calculated ionization energies.

Table 5.4 Calculated adiabatic ionization energies for C_3O, C_3S, C_2O, and C_2S at the MP4SDQ level of theory and a 6-311G** basis set.

Molecule	Theory	Ionization Energy kJ mol^{-1}
C_3O/C_3O^+	MP4SDQ/6-311G**//HF/6-311G**	
	with unscaled Z.P.V.E.	1045.2
	with scaled Z.P.V.E.	1045.6
	MP4SDQ/6-311G**//MP2/6-311G**	
	with unscaled Z.P.V.E.	1044.8
	with scaled Z.P.V.E.	1045.1
C_3S/C_3S^+	MP4SDQ/6-311G**/HF/6-311G**	
	with unscaled Z.P.V.E.	1003.4
	with scaled	1003.8
C_2O/C_2O^+	MP4SDQ/6-311G**//HF/6-311G**	
	with unscaled Z.P.V.E.	1020.4
	with scaled Z.P.V.E.	1020.8
C_2S/C_2S^+	MP4SDQ/6-311G**//HF/6-311G**	
	with unscaled Z.P.V.E.	977.2
	with scaled Z.P.V.E.	977.7

5.3.5 Proton Affinity

The proton affinity calculations show C_2S and C_3S to have significantly higher values than C_2O and C_3O. This could lead to a contradiction because from the calculated values C_2S and C_3S should be protonated easily and be observed in protonated forms. The astronomical observations have shown that C_2S and C_3S are present in the interstellar clouds in unprotonated form. Further studies are required to resolve this discrepancy.

Table 5.5 Calculated proton affinities for C_3O, C_3S, C_2O and C_2S at the MP4SDQ level of theory with 6-31G* and 6-311G** basis sets.

Molecule	Theory	Proton Affinity kJ mol^{-1}
C_3O/C_1-H	MP4SDQ/6-311G**//HF/6-311G**	
	with unscaled Z.P.V.E.	872.2
	with scaled Z.P.V.E.	876.1
	include BSSE	867.4
	at 298 K	867.7
C_3O/O-H	MP4SDQ/6-31G*//HF/6-31G*	519.1
C_3S/C_1-H	MP4SDQ/6-311G**//HF/6-311G**	
	with unscaled Z.P.V.E.	938.0
	with scaled Z.P.V.E.	941.8
	include BSSE	932.9
C_3S/S-H	MP4SDQ/6-31G*//HF/6-31G*	596.1
C_2O/C_1-H	MP4SDQ/6-311G**//HF/6-311G**	
	with scaled Z.P.V.E.	780.6
	with scale Z.P.V.E.	783.4
	include BSSE	774.9
	at 298 K	776.4
C_2O/O-H	MP4SDQ/6-31G*//HF/6-31G*	445.5
C_2S/C_1-H	MP4SDQ/6-311G**//HF/6-311G**	
	with unscaled Z.P.V.E.	874.6
	with scale Z.P.V.E.	877.3
	include BSSE	868.0
	at 298 K	869.6
C_2S/S-H	MP4SDQ/6-31G*//HF/6-31G*	565.3

5.3.6 Dissociation Energy.

The general dissociation reaction in our study is:

$$C_nX \rightarrow CX + C_{n-1} \qquad (18)$$

The dissociation energy for C_3O agrees very well with the experimental results found by Brown et al. [20]. The C_2O result is about 50 kJ mol^{-1} different from the experimental value found by Jacox et al. [73]. This error is acceptable when one considers the level of theory that has been used. Better agreement is obtained by using G1 method [105] in Gaussian 90 [53] is due to the $\Delta E(2df)$ correction and the slightly different optimized geometry when correlation terms are included.

Table 5.6 Calculated dissociation energies at different levels of theory and experimental values for C_3O, C_3S, C_2O and C_2S.

Molecule	Theory	Calculated energy kJ mol^{-1}	Experiment
C_3O	MP4SDQ/6-311G**//HF/6-311G**		
	with unscaled Z.P.V.E.	451.5	433[a]
	with scaled Z.P.V.E.	453.1	
C_3S	MP4SDQ/6-311G**//HF/6-311G**		
	with unscaled Z.P.V.E.	602.7	
	with scaled Z.P.V.E.	604.2	
C_2O	MP4SDQ/6-311G**//HF/6-311G**		
	with unscaled Z.P.V.E.	166.6	<239.2[b]
	with scaled Z.P.V.E.	167.8	
	POL-CI[c]	128.0*	
* this value is actually estimated to 226.0.			
	Becker and Bayes[c]	220.0	
	G1 in GAUSSIAN 90	212.3	
C_2S	MP4SDQ/6-311G**//HF/6-311G**		
	with unscaled Z.P.V.E.	396.7	
	with scaled Z.P.V.E.	398.1	

[a] Reference 20 [b] Reference 73 [c] Reference 142 [d] Reference 7

5.3.7 Harmonic Vibrational Frequencies.

The harmonic vibrational frequencies of all species in this study were determined at the HF/6-31G* level. The results for C_3O and C_2O are in good agreement with the experiment data. There are no experimental data available for C_2S and C_3S, but with the level of theory and the size of basis set used here the calculated vibrational frequencies for these species should be reliable enough to use for making experimental assignments.

Table 5.7 Calculated harmonic vibrational frequencies (cm^{-1}) at different levels of theory and experimental values for C_3O, C_3S, C_2O and C_2S.

Molecule	Frequencies (cm^{-1})			References
C_3O	(σ) 929	(σ) 1926	(σ) 2211	theory[a]
	(σ) 1053	(σ) 2003	(σ) 2246	experiment[b]
	(σ) 1010	(σ) 1890	(σ) 2200	theory[c]
C_3S	(π) 160	(π) 524	(σ) 795	
	(σ) 1673	(σ) 2264		theory[a]
C_2O	(π) 405	(σ) 1042	(σ) 1976	theory[a]
	(π) 379			theory[d]
		(σ) 1074	(σ) 1979	experiment[e]
			(σ) 1969	experiment[b]
C_2S	(π) 345	(σ) 955	(σ) 1889	theory[a]

[a] This work [c] Reference 14 [e] Reference 11
[b] Reference 12 [d] Reference 10

5.3.8 Standard Heat of Formation.

The standard of heat of formation, ΔH_f^0 (AX), of a molecule AX is given by

$$\Delta H_f^0 (AX) = \Delta H_f^0 (A) + \Delta H_f^0 (X) - \Delta E_{AX} \quad (18)$$

where

$$\Delta E_{AX} = -(E_{AX}) + (E_A) + (E_X) \quad (19)$$

is the energy of the reaction:

$$AX \rightarrow A + X \quad (20)$$

The standard heat of formation of C_2O, C_3O, C_2S and C_3S are calculated for the reactions,

$$C_2O \rightarrow CO + C\ (^3P) \quad (21)$$

$$C_3O \rightarrow CO + C_2\ (^3\Sigma) \quad (22)$$

$$C_2S \rightarrow CS + C\ (^3P) \quad (23)$$

$$C_3S \rightarrow CS + C_2\ (^3\Sigma) \quad (24)$$

Table 5.8 shows the values of standard heat of formation which were calculated from the MP4/6-311G**//HF/6-311G** energies and the known standard heats of formation of C, C_2, CO and CS [85]. The zero-point energies were taken from the MP2/6-31G*//HF/6-31G* calculations.

Table 5.8. Calculated heats of formation for C_3O, C_3S, C_2o and C_2S at the MP4/6-311G** level of theory compare with others' works.

Species	Total energies hartree	ZPVE kJ mol^{-1}	ΔH_f^0 kJ mol^{-1}	$\Delta H_f^0(ZPVE_{corr})$ kJ mol^{-1}
C	-37.76378	0.0	716.7	
C_2	-75.68107	14.5	831.9	
CO	-113.08174	14.6	-110.5	
CS	-435.60307	8.5	267.0	
C_2O	-150.91159	25.7	432.7	443.9
			372.4[a]	
			385.8[b]	
			393.9[c]	
C_3O	-188.93888	44.1	259.1	274.1
			282.0[d]	
C_2S	-473.50523	21.1	620.4	633.0
C_3S	-511.51881	36.5	482.8	480.9

[a] Reference142 [b] Reference 111

[c] Reference 53 (The values of E_0 for C, CO and C_2O were -37.78463, -113.17722 and -151.04269 hartrees)

[d] Reference 20

For the calculated standard heat of formation of C_2O, the value from our study is higher than the calculated value by Walch which used POL-CI wavefunction [142] and the value from experiments by Becker and Bayes [111]. The calculated value is in better agreement with those values when the G1 method [105] is used. This shows that the calculated standard heats of formation from our study are likely to be overestimated even though a large basis set and a high level of theory were used.

5.4 Conclusion

The reason for the difference between the amounts of C_nO and C_nS species in the interstellar clouds is still unknown. Although the proton affinities found in our study indicate that C_2O, C_3O, C_2S and C_3S prefer to be in protonated forms, substantial amounts of C_2S and C_3S species have been detected in the interstellar clouds, more studies are needed to explain of their existence. Our work has provided the basic chemistry data for both oxygen and sulphur containing species which would be required for further study.

Table 5.9. Energies of C_nO, C_nO^+, $H_mC_nO^+$, C_nS, C_nS^+, and $H_mC_nS^+$ species at different levels of theory and basis sets.

Molecule		HF 6-31G*	MP2(FC) 6-31G*	MP4SDQ 6-31G* hartree	HF 6-311G**	MP4SDQ 6-311G**
(1)	C_3O	-188.32616	-188.87265	-188.86299	-188.37351	-188.93888
(2)	C_3O^+	-187.99178	-188.46356	-188.46982	-188.03510	-188.53948
(3)	C_3OH^+	-188.54018	-189.07125	-189.07060		
(4)	HC_3O^+	-188.66556	-189.21608	-189.20622	-188.71239	-189.28449
(5)	C_2O	-150.46216	-150.83881	-150.84715	-150.50188	-150.91159
(6)	C_2O+	-150.08371	-150.44977	-150.46231	-150.11965	-150.52176
(7)	COC^+	-150.05396	-150.39702	-150.41659	-150.08643	-150.46917
(8)	C_2OH^+	-150.67604	-151.01490	-151.02805		
(9)	HC_2O^+	-150.77711	-151.14364	-151.15149	-150.81611	-151.21861
(10)	C_3S	-510.95172	-511.46717	-511.45458	-510.99769	-511.51881
(11)	C_3S^+	-510.65778	-511.06226	-511.07697	-510.69968	-511.13502
(12)	C_3SH^+	-511.19539	-511.68548	-511.68946		
(13)	HC_3S^+	-511.31173	-511.83394	-511.82220	-511.35788	-511.88918
(14)	C_2S	-473.10304	-473.44237	-473.45190	-473.14175	-473.50523
(15)	C_2S^+	-472.75488	-473.05925	-473.08293	-472.79030	-473.13126
(16)	C_2SH^+	-473.35701	-473.65942	-473.67555		
(17)	HC_2S^+	-473.45741	-473.77700	-473.79191	-473.49522	-473.84798

Table 5.10. Optimized geometric parameters for C_nO, C_nO^+ and C_nHO^+ species in Ångstroms and degrees.

Molecule	Theory/Basis Set						
(1) C_3O	HF/6-31G*	C_1C_2	1.256	C_2C_3	1.295	C_3O	1.129
	HF/6-311G**	C_1C_2	1.251	C_2C_3	1.294	C_3O	1.119
	MP2/6-311G**	C_1C_2	1.281	C_2C_3	1.304	C_3O	1.158
(2) C_3O^+	HF/6-31G*	C_1C_2	1.237	C_2C_3	1.340	C_3O	1.108
	HF/6-311G**	C_1C_2	1.233	C_2C_3	1.337	C_3O	1.098
	MP2/6-311G**	C_1C_2	1.178	C_1C_2	1.369	C_3O	1.113
(3) C_3OH^+	HF/6-31G*	C_1C_2	1.312	C_2C_3	1.226	C_3O	1.217
		$C_1C_2C_3$	179.6	C_2C_3O	176.4	C_3OH	119.8
						OH	0.970
(4) HC_3O^+	HF/6-31G*	C_1C_2	1.192	C_2C_3	1.353	C_3O	1.100
						C_1H	1.068
	HF/6-311G**	C_1C_2	1.188	C_2C_3	1.350	C_3O	1.092
						C_1H	1.067
(5) C_2O	HF/6-31G*	C_1C_2	1.354	C_2O	1.139		
	HF/6-311G**	C_1C_2	1.351	C_2O	1.130		
	MP2/6-311G**	C_1C_2	1.377	C_2O	1.160		
(6) C_2O^+	HF/6-31G*	C_1C_2	1.600	C_2O	1.094		
	HF/6-311G**	C_1C_2	1.581	C_2O	1.086		
(7) COC^+	HF/6-31G*	C_1O	1.746	OC_2	1.139		
	HF/6-311G**	C_1O	1.822	OC_2	1.130		
(8) C_2OH^+	HF/6-31G*	C_1C_2	1.307	C_2O	1.225	OH	0.969
		C_1C_2O	146.6	C_1OH	116.5		
(9) HC_2O^+	HF/6-31G*	C_1C_2	1.359	C_2O	1.111	C_1H	1.074
		OC_1C_2	175.9	C_2C_1H	141.5		
	HF/6-311G**	C_1C_2	1.356	C_2O	1.102	C_1H	1.075
		OC_1C_2	176.2	C_2C_1H	142.2		

Table 5.11. Optimized geometric parameters for C_nS, C_nS^+ and C_nHS^+ species at different levels of theory in Ångstroms and degrees.

Molecule	Theory/Basis Set						
(10) C_3S	HF/6-31G*	C_1C_2	1.265	C_2C_3	1.283	C_3S	1.531
	HF/6-311G**	C_1C_2	1.260	C_2C_3	1.283	C_3S	1.526
(11) C_3S^+	HF/6-31G*	C_1C_2	1.262	C_2C_3	1.309	C_2S	1.521
	HF/6-311G**	C_1C_2	1.257	C_2C_3	1.307	C_3S	1.517
(12) C_3SH	HF/6-31G*	C_1C_2	1.318	C_2C_3	1.231	C_3S	1.638
		SH	1.333	$C_1C_2C_3$	178.5	C_3SH	95.3
		C_2C_3S	175.5				
(13) HC_3S^+	HF/6-31G*	C_1C_2	1.195	C_2C_3	1.349	C_3S	1.474
						C_1H	1.065
	HF/6-311G**	C_1C_2	1.191	C_2C_3	1.348	C_3S	1.472
						C_1H	1.064
(14) C_2S	HF/6-31G*	C_1C_2	1.304	C_2S	1.549		
	HF/6-311G**	C_1C_2	1.302	C_2S	1.546		
(15) C_2S^+	HF/6-31G*	C_1C_2	1.382	C_2S	1.532		
	HF/6-311G**	C_1C_2	1.383	C_2S	1.527		
(16) C_2SH^+	HF/6-31G*	C_1C_2	1.255	C_2S	1.614	SH	1.335
		C_1C_2S	170.1	C_2SH	98.6		
(17 HC_2S^+	HF/6-31G*	C_1C_2	1.267	C_2S	1.550	C_1H	1.068
	HF/6-311G**	C_1C_2	1.464	C_2S	1.547	C_1H	1.067

Table 5.12. Harmonic vibrational frequencies and zero-point vibrational energies.

Molecule	Harmonic vibrational frequencies(cm^{-1})						ZPVE(kJ mol^{-1})
(1) C_3O	(π)	159	(π)	683	(σ)	1044	44.1
	(σ)	2164	(σ)	2485			
(2) C_3O^+	(π)	168	(π)	560	(σ)	968	40.7
	(σ)	1935	(σ)	2448			
(3) C_3OH^+	(a")	159	(a')	176	(a')	550	70.1
	(a")	634	(a')	1003	(a')	1148	
	(a')	1820	(a')	2441	(a')	3791	
(4) HC_3O^+	(π)	237	(π)	660	(π)	957	79.3
	(σ)	972	(σ)	2356	(σ)	2643	
	(σ)	3578					
(5) C_2O	(π)	455	(σ)	1171	(σ)	2221	25.7
(6) C_2O^+	(π)	346	(σ)	501	(σ)	2568	22.5
(7) COC^+	(π)	89	(σ)	272	(σ)	2189	15.8
(8) C_2OH^+	(a')	288	(a")	665	(a')	1199	55.2
	(a')	1296	(a')	1968	(a')	3810	
(9) HC_2O^+	(a')	440	(a")	505	(a')	684	51.2
	(a')	1167	(a')	2333	(a')	3426	
(10) C_3S	(π)	160	(π)	524	(σ)	795	36.5
	(σ)	1673	(σ)	2264			
(11) C_3S^+	(π)	202	(π)	384	(σ)	758	32.2
	(σ)	1577	(σ)	1884			
(12) C_3SH^+	(a")	126	(a')	159	(a')	392	57.0
	(a")	441	(a')	669	(a')	1079	
	(a')	1477	(a')	2320	(a')	2870	

(13) HC_3S^+	(π)	213	(σ)	514	(σ)	794	70.9
	(π)	912	(σ)	1803	(σ)	2377	
	(σ)	3597					
(14) C_2S	(π)	345	(σ)	955	(σ)	1889	21.1
(15) C_2S^+	(π)	252	(σ)	831	(σ)	1371	16.2
(16) C_2SH^+	(a')	187	(a'')	357	(a')	859	43.0
	(a')	1095	(a')	1847	(a')	2846	
(17) HC_2S^+	(π)	313	(π)	475	(σ)	935	46.5
	(σ)	1742	(σ)	3514			

Table 5.13. Ionization potentials of C_nO and C_nS species calculated including unscaled zero-point vibrational energies.

Molecules	HF /6-31G*	MP2 /6-31G*	MP4SDQ /6-31G* kJ mol^{-1}	HF /6-311G**	MP4SDQ /6-311G**
C_3O/C_3O^+	874.5	1070.6	1028.8	885.1	1045.2
C_2O/C_2O^+	990.5	1018.4	1007.3	1000.5	1020.4
C_2O/COC^+	1061.9	1150.1	1120.6	1080.9	1151.7
C_3S/C_3S^+	767.5	1058.8	987.2	778.1	1003.4
C_2S/C_2S^+	909.5	1001.2	964.1	918.1	977.2

Table 5.14. Proton affinities of C_nO and C_nS species calculated including unscaled zero-point vibrational energies.

Molecule	HF /6-31G*	MP2 /6-31G*	MP4SDQ /6-31G* kJ mol^{-1}	HF /6-311G**	MP4SDQ /6-311G**
C_3O/C_3OH^+	535.9	495.4	519.1		
C_3O/HC_3O^+	855.9	866.5	866.0	854.6	872.2
C_2O/C_2OH^+	532.1	432.9	445.5		
C_2O/HC_2O^+	801.5	774.9	773.6	799.6	780.6
C_3S/C_3SH^+	619.2	552.6	596.1		
C_3S/HC_3S^+	910.8	928.6	930.8	911.3	938.0
C_2S/C_2SH^+	644.9	548.0	565.3		
C_2S/HC_2S^+	905.1	853.2	867.4	902.7	874.6

CHAPTER 6

Theoretical Study of $C_6H_4^+$ Formation in Acetylenic Flames.

6.1 Introduction

The chemistry of flames has been of interest to chemists for a long time. Despite all the research on this subject there are still many chemical processes in flames which we do not fully understand.

It has been known for many years that there are significant concentrations of ions in flames. These ions are believed to be generated in a very thin active zone near the flame front via reaction [96]

$$CH(X^2\Pi) + O(^3P) \rightarrow CHO^+ + e \qquad (1)$$

The products from this reaction will go through many secondary ion-molecule reactions in the burnt gas region of the flame before yielding the final species which are H_3O^+, NO^+ and electrons. Many ions in flames have been identified in mass spectrometric sampling experiments and schemes for the processes involved have been proposed [55,56,61].

One of the earliest works on ion-molecule reactions is the study of C_2^+, C_2H^+ and $C_2H_2^+$ with C_2H_2, done by Field et al. in 1957 [51]. Later the studies of acetylenic flames have focused on the possibility that ions derived from acetylene may participate as precusors in soot formation under conditions where large ions were detected [23, 64,114, 129, 139]. The first ion-molecule step for acetylene in flames is :

$$C_2H_2^+ + C_2H_2 \rightarrow C_4H_2^+ + H_2 \qquad (2a)$$

$$\rightarrow C_4H_3^+ + H \qquad (2b)$$

The rate coefficient of this reaction has been measured [69,74] and it was found to be fast (1.41×10^{-9} cm^3 s^{-1}). The $C_4H_2^+$ and $C_4H_3^+$ species can react further with acetylene to form addition products via the reactions:

$$C_4H_2^+ + C_2H_2 \rightarrow C_6H_4^+ \quad (3a)$$

$$C_4H_3^+ + C_2H_2 \rightarrow C_6H_5^+ \quad (3b)$$

These products have been detected in ICR and flow tube experiments and were reported to be long-lived collision complexes ($t \approx 5$ ms) [78]. Later Anicich et al. [4] reported that 89% and 76% of the collision complexes $C_6H_4^+$($t \geq 57$ ms) and $C_6H_5^+$ ($t \geq 18$ ms) reverted back to the reactants as pressures below 1×10^{-6} Torr in ICR experiments. Brill and Eyler [18] reported in ICR experiments that $C_6H_5^+$ in this reaction was composed of two non-interconverting isomers, of which one isomer is able to react further with C_2H_2 while the other isomer is inactive. Although in most experiments $C_6H_5^+$ is taken as the phenylium ion, it is also possible that $C_6H_5^+$ could be acyclic. When the cell pressure was raised to 2×10^{-5} Torr in the ICR experiments, $C_8H_6^+$ and $C_8H_7^+$ were produced through the reactions:

$$C_6H_4^+ + C_2H_2 \rightarrow C_8H_6^+ \quad (4a)$$

$$C_6H_5^+ + C_2H_2 \rightarrow C_8H_7^+$$

$$\rightarrow C_8H_6^+ + H \quad (4b)$$

In these reactions $C_{10}H_8^+$ and $C_{10}H_6^+$ species were also found at low intensity, implies the occurrence of another step in a sequential chain reaction.

In 1976 Vinckier et al. [140] has proposed that an important process of sooting flames is the rapid polymerization of acetylenic species via the reactions:

$$C_{2n}H_{2n+1}^{+} + C_2H_2 \rightarrow C_{2n+2}H_{2n+3}^{+}$$

$$\rightarrow C_{2n+2}H_{2n+1}^{+} + H_2 \quad (5a)$$

$$C_{2n}H_{2n-1}^{+} + C_2H_2 \rightarrow C_{2n+2}H_{2n+1}^{+} \quad (5b)$$

From this scheme, when the reactants are C_2H^+, $C_2H_3^+$ and C_2H_2 we will have the possible products, $C_4H_5^+$, $C_4H_3^+$, $C_6H_5^+$, $C_6H_7^+$ and H_2. However, in most studies of ion-molecule reaction of acetylene, while $C_6H_4^+$ was found to be an important species, $C_4H_5^+$ and $C_6H_7^+$ have not been detected.

Knight et al. [78] reported different rates of reaction with C_2H_2 for $C_6H_4^+$ from $C_4H_2^+ + C_2H_2$ source and $C_6H_4^+$ from a benzene source (1×10^{-11} cm^3 s^{-1} and 7×10^{-11} cm^3 s^{-1}). They also suggested that $C_6H_4^+$ from the two sources are different isomers.

The structure of $C_4H_2^+$ is known to be linear and recently its geometries were reinvestigated in $X^2\Pi_g$ and $A^2\Pi_u$ electronic states by Lecoultre et al. by a laser excitation technique [80]. The structures of $C_6H_4^+$ from the reaction between $C_4H_2^+$ and C_2H_2 have not yet been confirmed, nor has the chemical pathway which leads to this species been established.

Though $C_6H_4^+$ produced in the ion-molecule reaction (3a) can be acyclic or cyclic, the calculations in this chapter would suggest an acyclic structure is more favourable. However Rosenstock et al. [120] have demonstrated that the acyclic $C_6H_4^+$ isomers have significantly higher heats of formation than those benzyne structure and thus should be more reactive.

The object of the present study is to predict the structure of the product $C_6H_4^+$ and establish the pathway of the reaction between C_2H_2 and $C_4H_2^+$ by using ab initio and semiempirical (AM1) methods.

6.2 Method

The ab initio calculation was done with the GAUSSIAN 82 program [11] with 4-31G and 6-31G* basis sets at HF, MP2 and MP4SDQ levels of theory. A convergence difficulty was encountered, especially in calculating isomers of cyclic structure and transition states with 6-31G* basis set. At this stage the semiempirical, AM1 method [41] in the MOPAC program [134] was brought into use, to establish a feasible pathway and locate the transition states before calculations were attempted by the ab initio method.

The optimized structures from ab initio calculations were recalculated in AM1 to compare the two methods. The total energies from AM1 are different from those from ab initio calculations by definition, but the relative energies between species calculated from each method should be comparable.

The harmonic vibrational frequencies from AM1 were calculated by the gradient method of force constants. In the AM1 force calculation the vibrational modes are not assigned to any symmetric species. Only unassigned frequency values could be reported.

Figure 6.1 shows all structures of spicies calculated in this study.

(1)

(2)

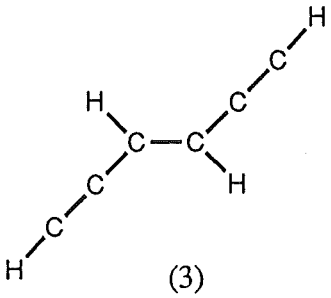

(3)

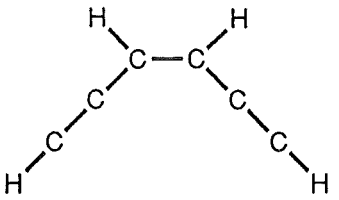

(4)

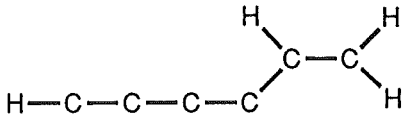

(5)

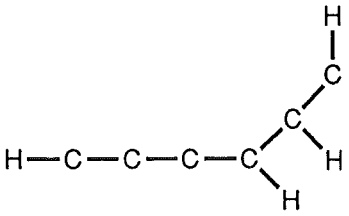

(6)

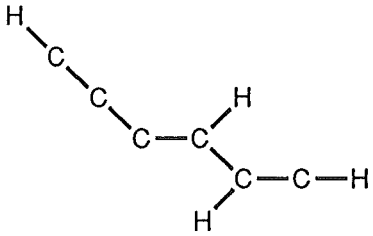

(7)

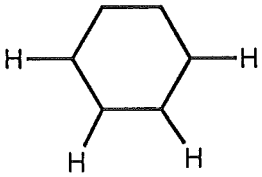

(8)

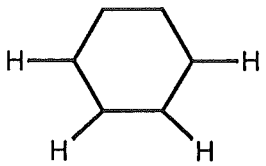

PLANAR (9)

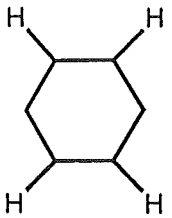

(10)

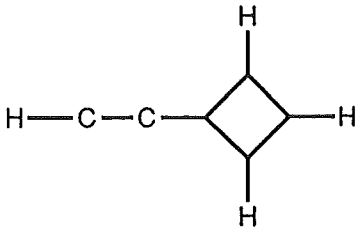

(11)

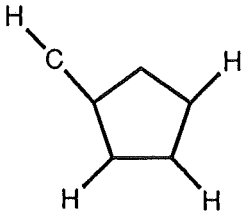

(12)

Figure 6.1 Structures of molecules in AM1 calculations

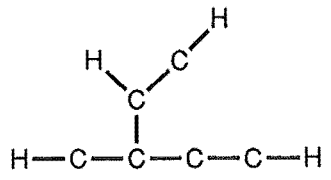

(13)

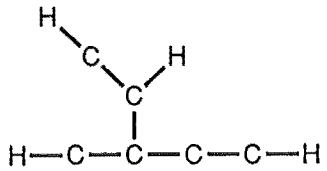

(14)

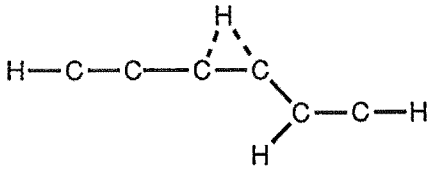

(15)

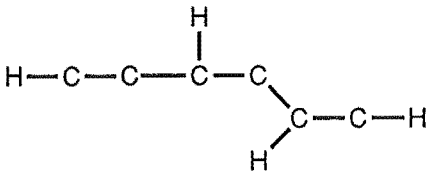

(16)

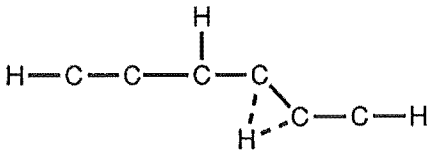

(17)

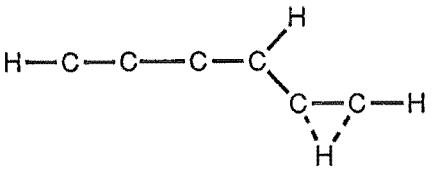

(18)

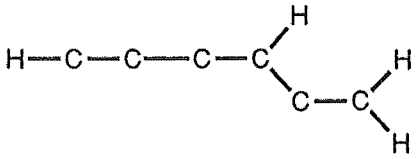

(19)

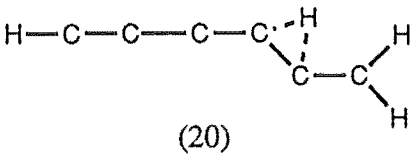

(20)

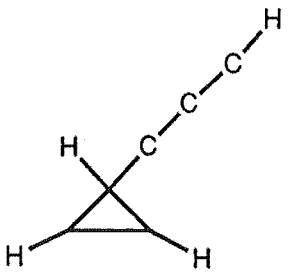

(21)

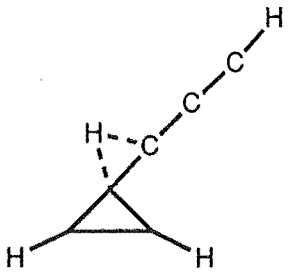

(22)

Figure 6.1 (continued)

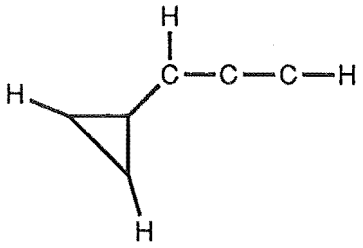

(23)

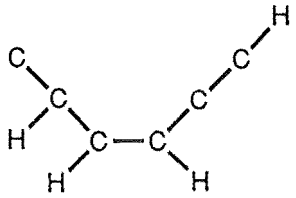

(24)

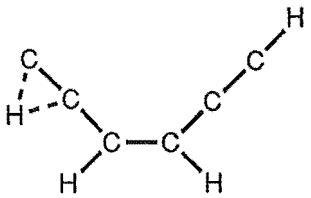

(25)

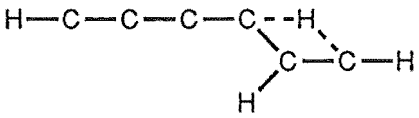

(26)

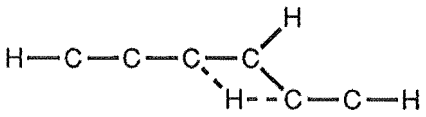

(27)

Figure 6.1 (continued)

6.3 Results and Discussion

The first step of molecular-ion interaction between C_2H_2 and $C_4H_2^+$ is the formation of a $C_6H_4^{+\dagger}$ collision complex (Figure 6.2). The lifetime of this complex in an ICR experiment was determined by Knight et al. [78] and Anicich et al. [4]. In the pressure below 1 X 10^{-6} Torr, 89% of the complex was found to revert back to the reactants [4]. The $C_6H_4^+$ complex initially formed in reaction (3a) can stabilize either by emission of a photon (radiative stabilization) or by collision with another species in which energy is transferred (collision stabilization). Providing an appropriate path on the potential energy surface is available, the resulting $C_6H_4^+$ ion should have a major fraction of the most stable isomers.

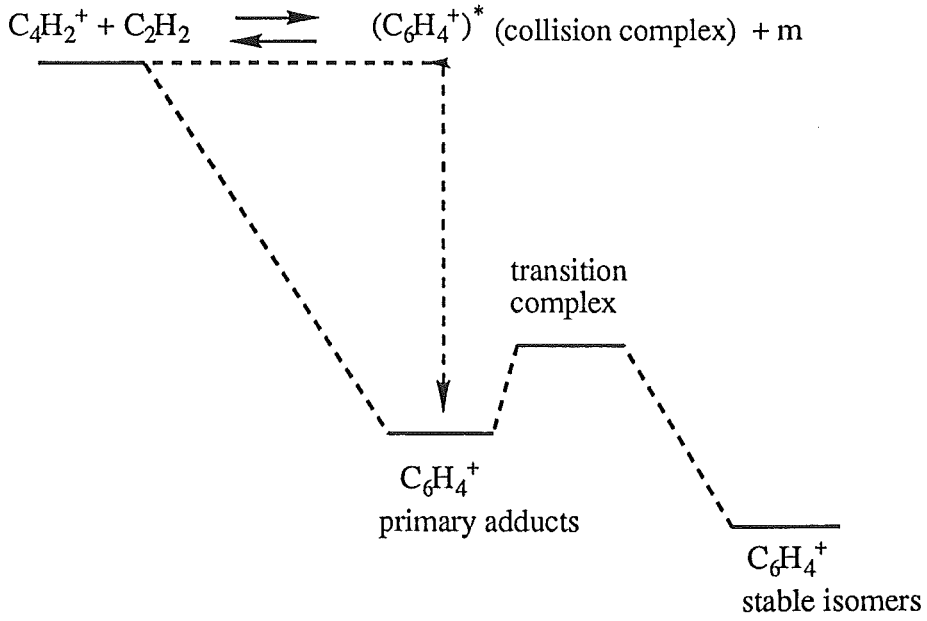

Figure 6.2 Main chemical process of the reaction between C_2H_2 and $C_4H_2^+$

The calculation by GAUSSIAN 82 for $C_4H_2^+$ assigned the terminal carbon atom as positive, whereas the calculation using MOPAC assigned the positive charge to the C_2 carbon atom. Calculations with C_2H_2 bonding to C_1 and C_2 on $C_4H_2^+$, by both methods show that the products from C_1 attack, (6) and (7), are more stable than those from C_2 attack, species (13) and (14).

In AM1 calculations, isomer (6) is more stable than isomer (7) by 31.7 kJ mol^{-1} (37.4 kJ mol^{-1} by the MP4SDQ/6-31G* with GAUSSIAN 82) while isomer (13) is more stable than isomer (14) by 2.0 kJ mol^{-1}.

Isomer (7) and can undergo a 1-3 sigmatotropic proton shift (Figure 6.3) to give stable isomers (3) or (5). The energy of the transition state for the rearrangement from isomer (7) to isomer (3) is found to be less than the energy of $C_6H_4^+ + C_2H_2$ reactants by -8.8 kJ mol^{-1} in AM1 method. When the error of calculation is taken into account (19.3 kJ mol^{-1} for an error of ionization potential of diacetylene) [135], the uncertainty is sufficiently large that the transition state might be higher in energy than the reactants and therefore removing the channel as a possible route for the reaction. The transition state for the process from isomer (7) to isomer (5) was calculated, but the optimization process by AM1 method failed to achieve an optimized structure. This could imply that this pathway is not feasible or that better methods are needed to solve the convergence problem in order to make any conclusions.

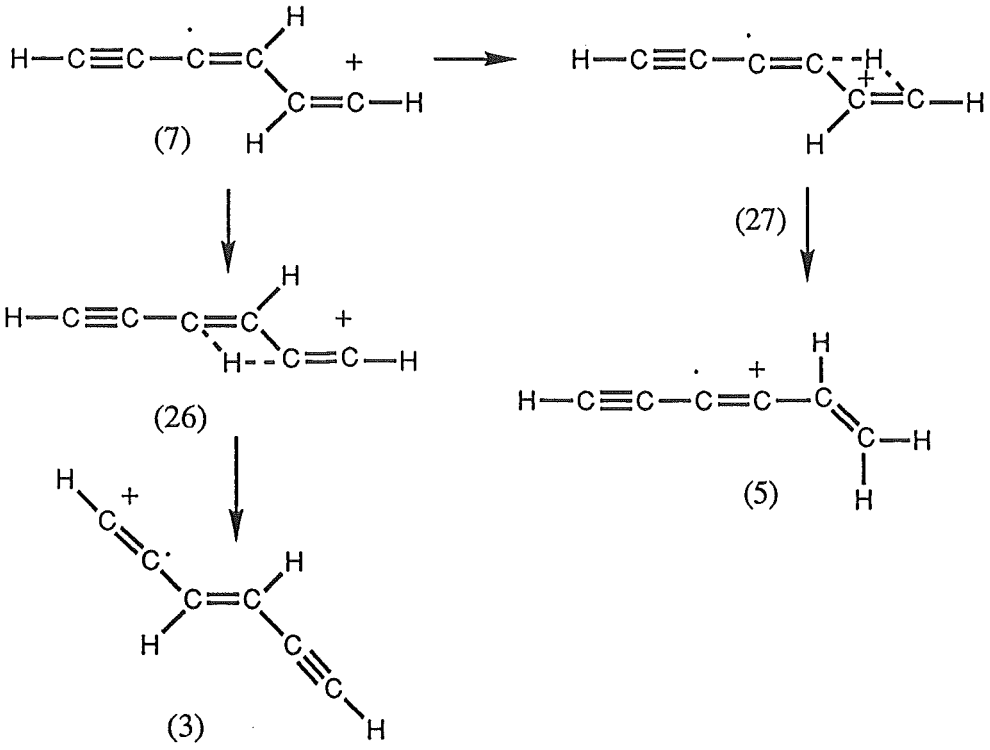

Figure 6.3 1-3 sigmatrotopic proton shift in isomer (7)

Figure 6.4 shows the two pathways by which isomer (7) rearranges through two steps of 1-2 proton shift to give the stable isomers (3) and (5). The energies calculated for these processes are shown in Figure 6.5 and 6.6. From the energy diagrams these two pathway seem very feasible, although they need two steps to complete the reactions whereas only one step is necessary in Figure 6.3.

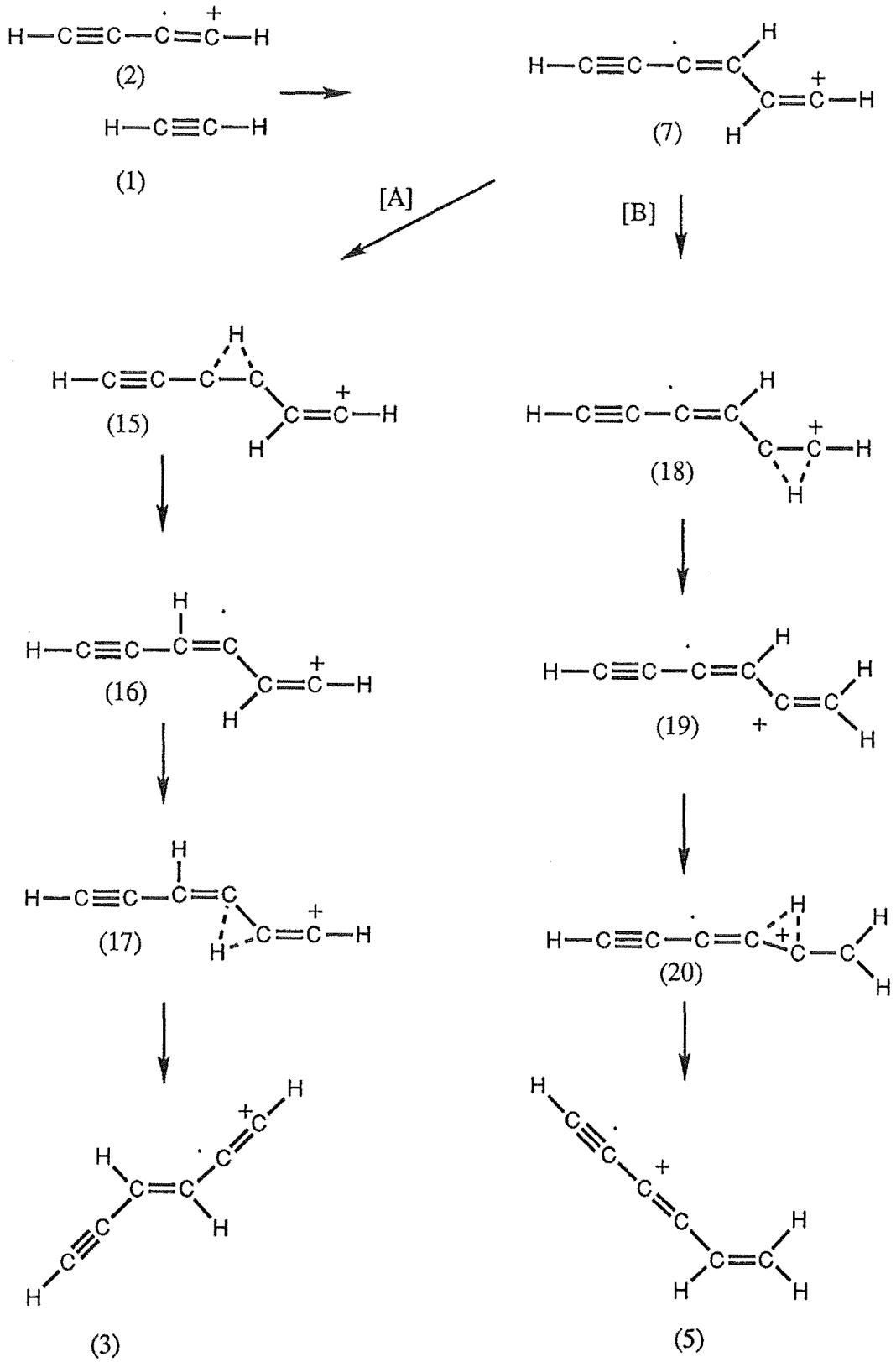

Figure 6.4 1-2 proton shift in isomer (7)

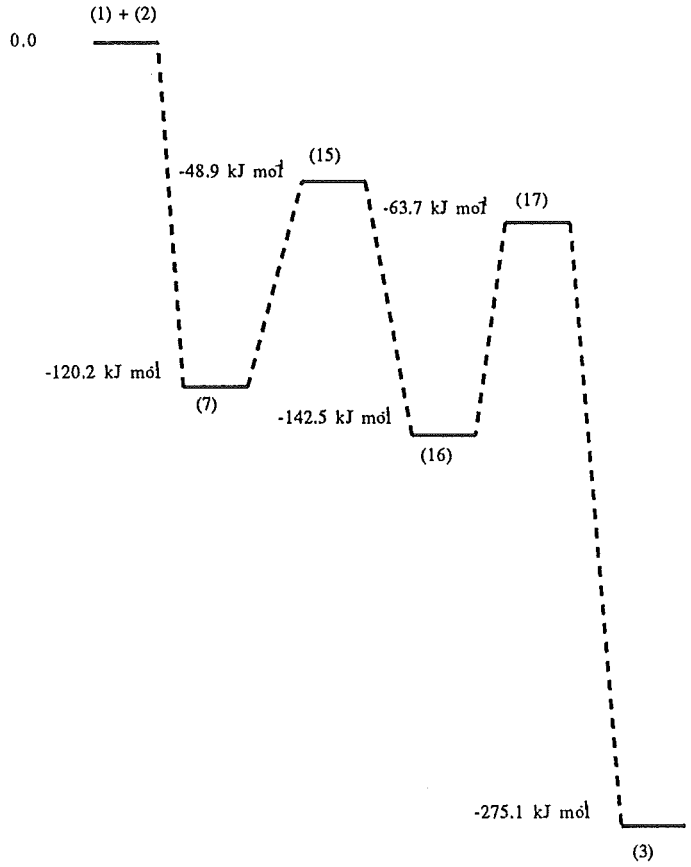

Figure 6.5 Energy diagram for the pathway A

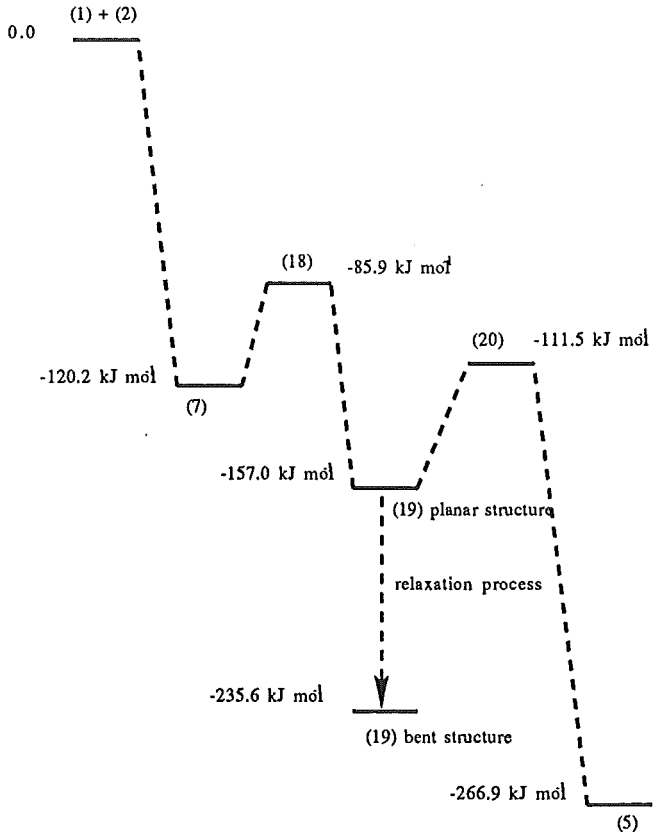

Figure 6.6 Energy diagram for the pathway B

Isomers (6), (13) and (14) can form 3-, 4-, 5-, and 6-membered ring intermediates (Figure 6.7) and then go through other rearrangement processes. Optimizations of these structure isomers converged in AM1 and HF with the 4-31G basis set but had convergence problems when the 6-31G* basis set was used.

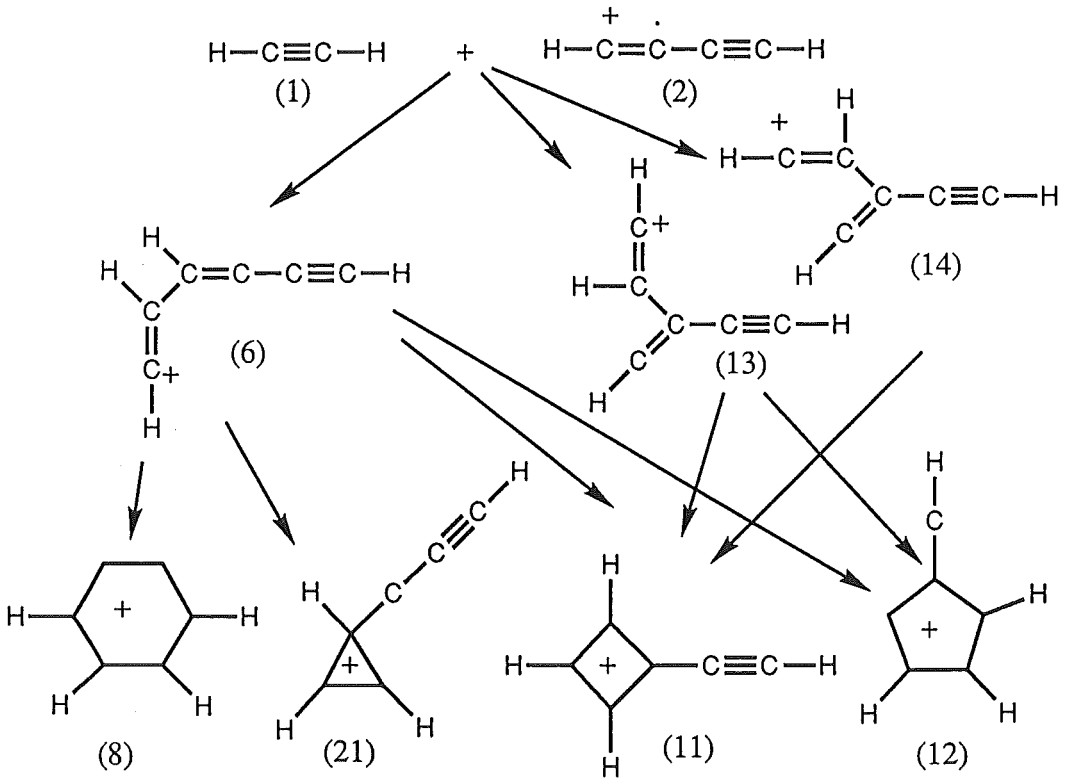

Figure 6.7 The formations of cyclic isomers

The 5-membered ring isomer is quite stable with energies relative to reactant energies of -89.7 and -144.5 kJ mol^{-1} by the AM1 and HF calculations. A force constant calculation in AM1 gives one imaginary harmonic vibrational frequency while calculation in GAUSSIAN 82 for this species does not. The hydrogen atoms rearrangement is not likely to occur in the ring because of the ring strain. In such a case the ring structure can break and go through a process which is shown in Figure 6.8. The energy of the transition state in this process by AM1 was 25.8 kJ mol^{-1} higher than the energy of the reactants, so for this reason this pathway is prohibited.

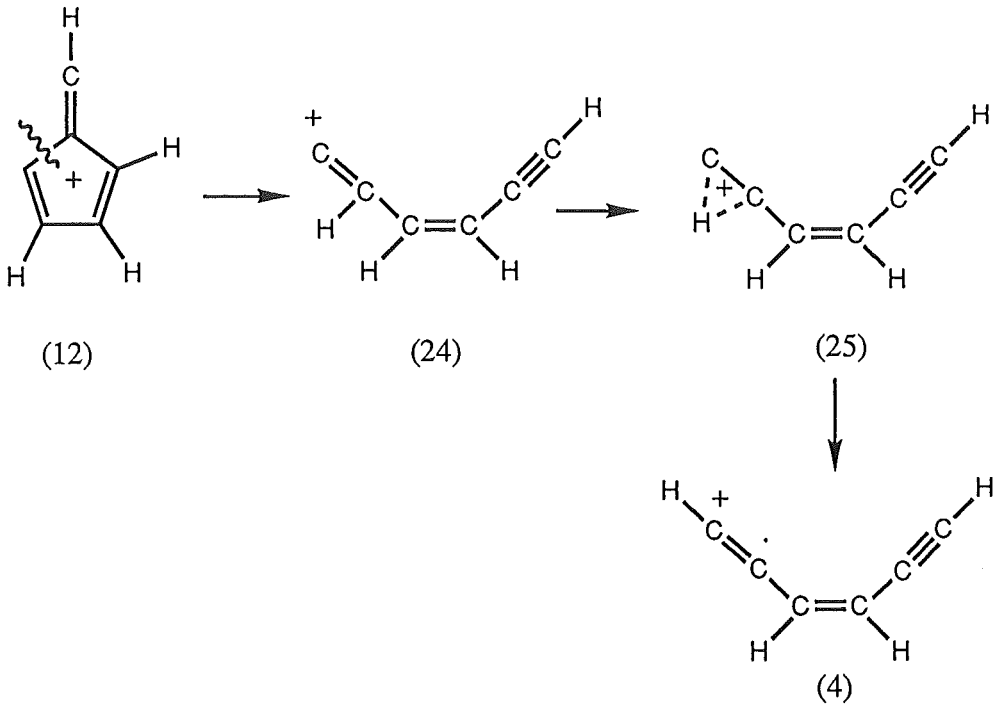

Figure 6.8 Dissociative pathway for 5-membered ring isomer

The 3-membered ring structure (21) has an energy -93.3 kJ mol^{-1} lower than the energy of reactants. The hydrogen shift in the ring was also investigated but was found to be unfeasible because of the high energy of the transition state (32.8 kJ mol^{-1} higher than the energy of reactants). Another proton shift process was considered, from the ring to the carbon atom on the branch chain as shown in Figure 6.9. Although this pathway gives a surprisingly stable product (23), the energy of the transition process, 0.9 kJ mol^{-1} higher than the reactants, makes this pathway also less significant than the acyclic pathway of Figure 6.3.

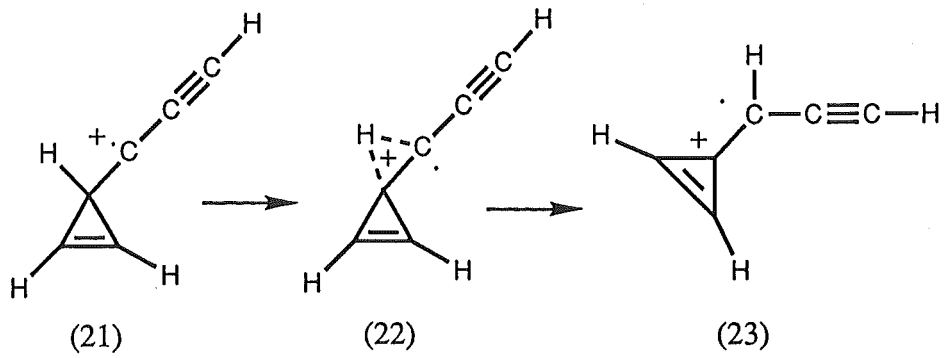

Figure 6.9 Rearrangement process for propene structure isomer

The ortho-benzyne cation structure of $C_6H_4^+$ ((8) in Figure 6.10) has also been considered as a product of the reaction of C_2H_2 and $C_4H_2^+$. The related cyclic phenylium isomer, $C_6H_5^+$, had been assumed to be the isomer generated in experiments and theoretical studies of this isomer have been done at different levels of theory [18,50,130]. Hydrogen atoms in $C_6H_5^+$ were found to undergo rearrangement i.e. 'scrambling process' in the ring. The force constant calculation at the 4-31G level in GAUSSIAN 82 showed that although $C_6H_4^+$ it has a relatively low energy compared to the reactants (-229.2 kJ mol^{-1}), it is a transition structure with one imaginary vibrational frequency. In the AM1 method, it first gave an optimized structure with high gradients, which was reoptimized in a force constant calculation. This led to a new optimized structure and a new value of heat of formation. Two imaginary frequencies were found as a result of this calculation. When the structure was reoptimized and the force constant calculation repeated, the calculation crashed and the SCF could not be achieved. A proposed chemical pathway for the benzyne structure shown in Figure 6.10 also requires the scrambling process of hydrogen atoms. Although the convergence problem in the AM1 calculation of the ortho-benzyne cation occurred, the energy from the HF/4-31G calculations of this isomer and the study the neutral benzyne stability by J.O. Noell and M.D. Newton [99] showed that the ortho-benzyne cation should be more stable than meta- and para-isomers. Hence the pathway shown in Figure 6.10 can be ruled out.

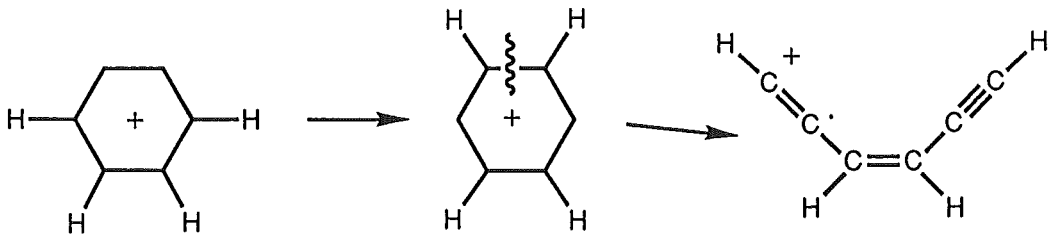

(8) (10) (4)

Figure 6.10 Rearrangement process for benzyne structure isomer

The 4-membered ring structure ((11) in Figure 6.7) was found to be stable (-110.7 and -174.1 kJ mol^{-1} by HF/4-31G and AM1) by both methods but it had a convergence problem when the 6-31G* basis set was used in the HF calculation. If the hydrogen rearrangement in the ring does not occur, this structure will tend to break down and revert back to isomer (6), (13) or (14) as shown in Figure 6.11.

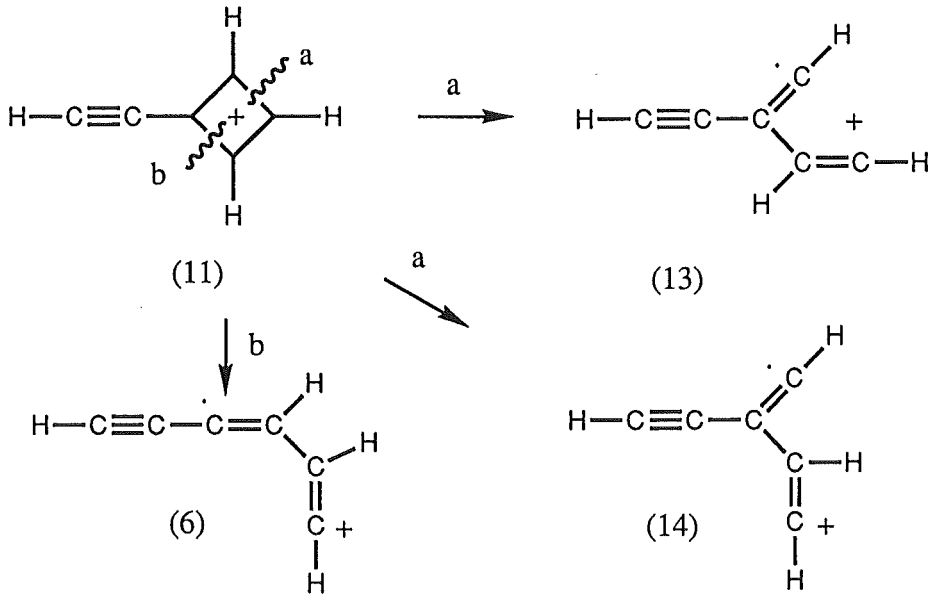

Figure 6.11 Rearangement process for butadienylium structure isomer

In Figure 6.12 AM1 relative energies of important intermediates are shown in order to illustrate their potential in the chemical process between C_2H_2 and $C_4H_2^+$.

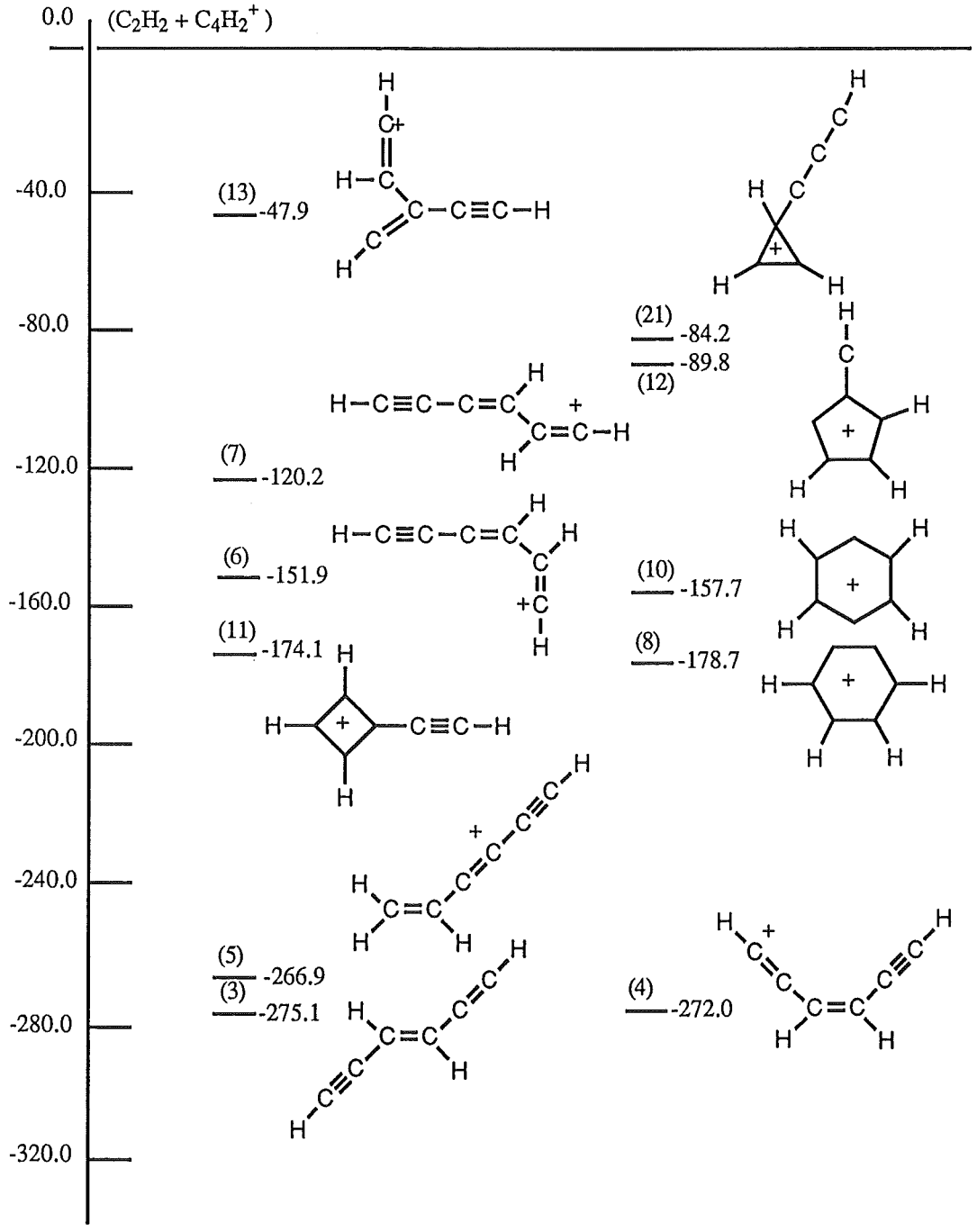

Figure 6.12 AM1 relative energy diagram of $C_6H_4^+$ isomers (kJ mol^{-1})

Figure 6.13 and 6.14 show the optimized structures of $C_6H_4^+$ isomer from AM1 and HF calculations.

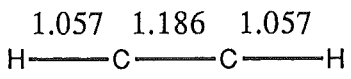

(1)

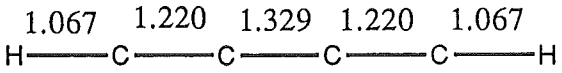

(2)

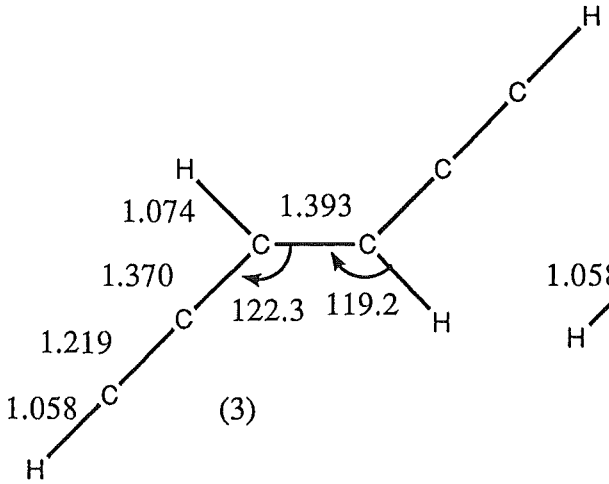

(3)

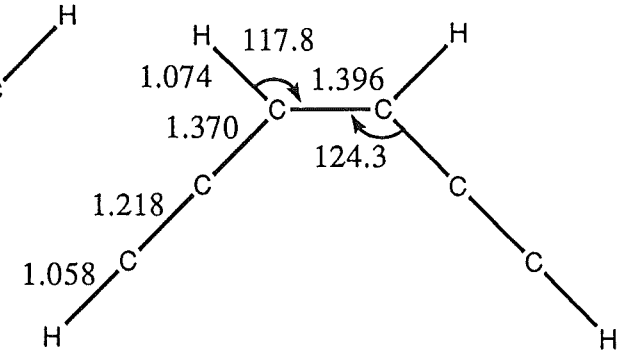

(4)

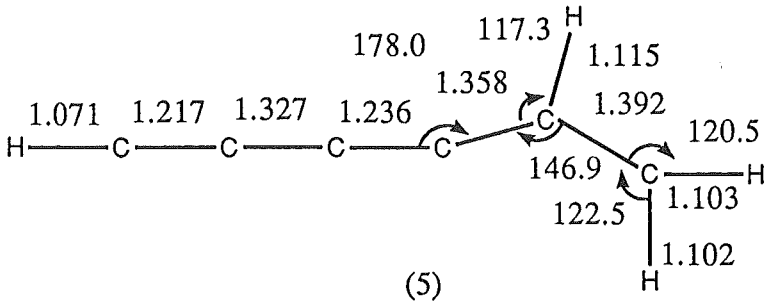

(5)

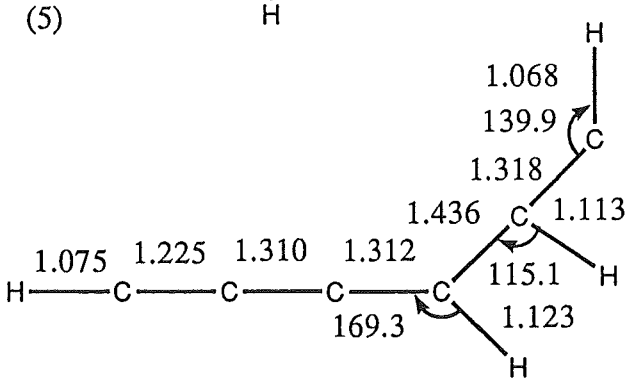

(6)

Figure 6.13 Optimized structures from the AM1 method (Ångstroms and degrees)

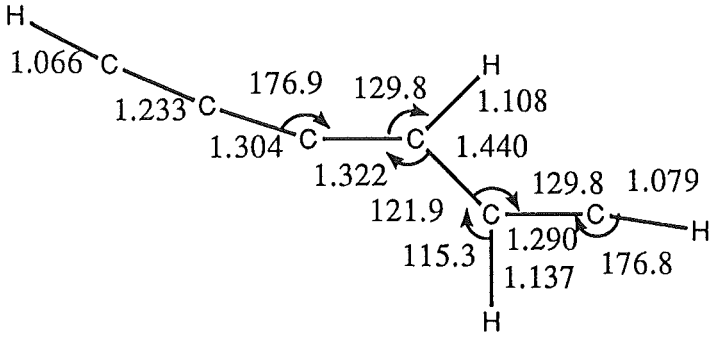

(7)

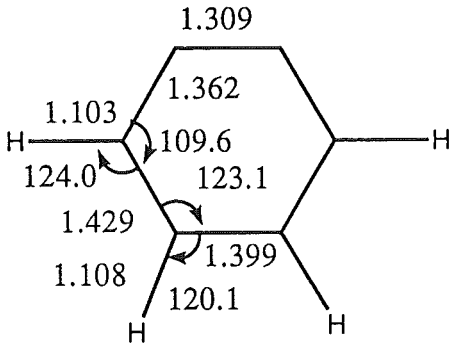

(8)

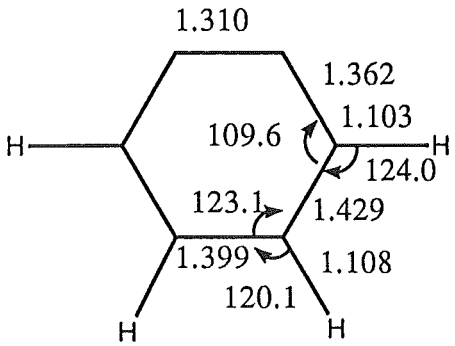

(9) (PLANAR)

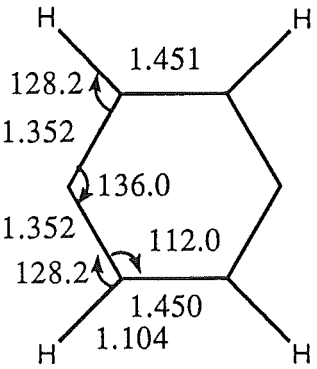

(10)

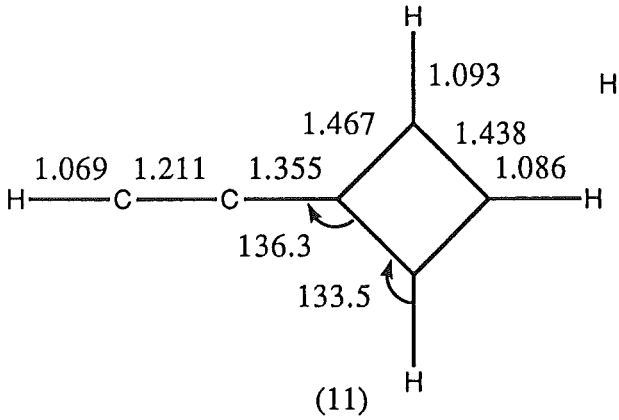

(11)

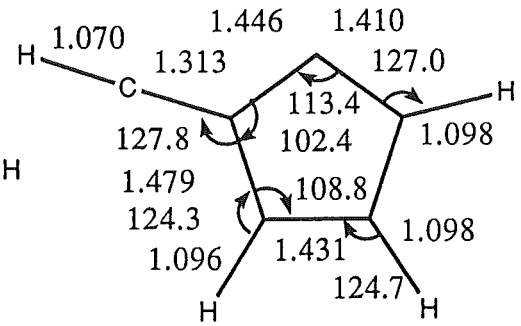

(12)

Figure 6.13 (continued)

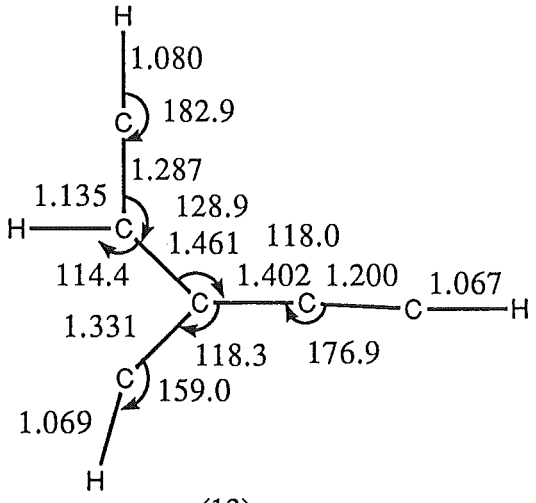

(13)

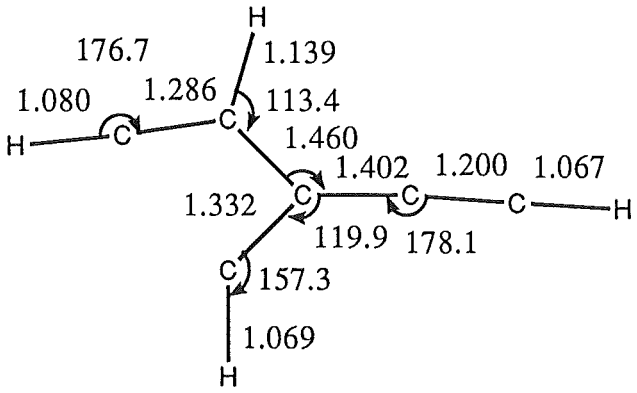

(14)

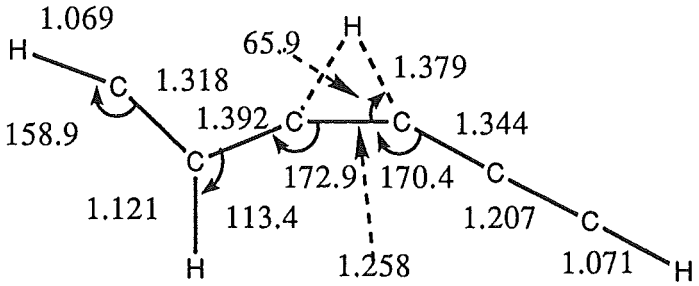

(15)

Figure 6.13 (continued)

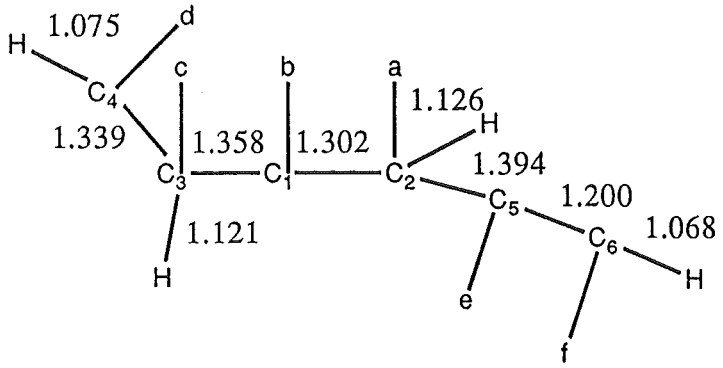

a,b,c,d,e and f are dummy axes

A31b = 90.5, A43c = 44.3
A52a = 114.7, A65e = 90.6
AH6f = 90.1, AH4d = 104.3
AH21 = 62.7, AH31 = 118.1
D31b2 = -176.7, D43c1 = 140.6
D52a1 = -130.3, D65e2 = -178.0
DH6f5 = -179.8, DH4d3 = -163.8
DH2a1 = 121.9, DH31b = 148.9

(16)

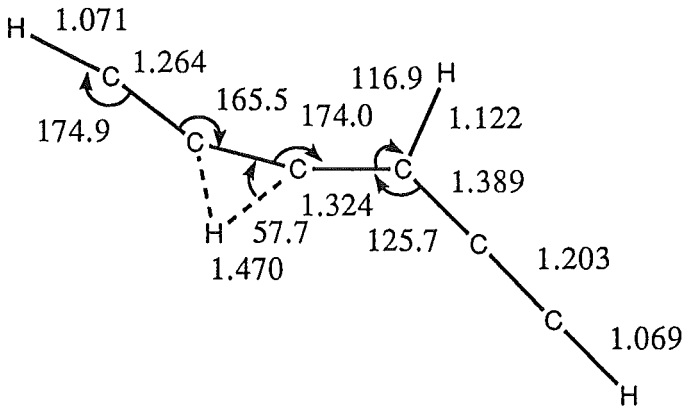

(17) Planar structure

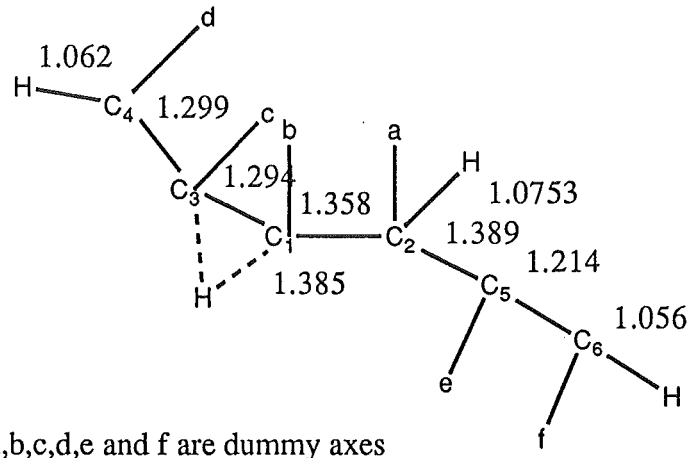

a,b,c,d,e and f are dummy axes
A213 = 169.8, A134 = 170.0, A34H = 172.3
A31H = 57.3 , A12H = 137.7, A56H = 180.0
A125 = 139.1, A256 = 181.3
D21b3 = 170.0, D12a5 = -133.6, D25e6 = -177.9
D12aH = 130.6, Dc31H = -178.2

(17) Non-planar structure

Figure 6.13 (continued)

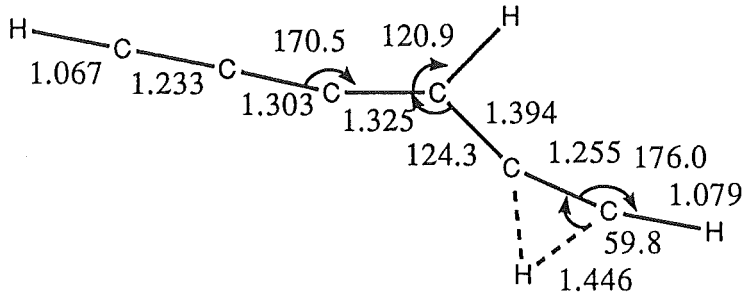

(18)

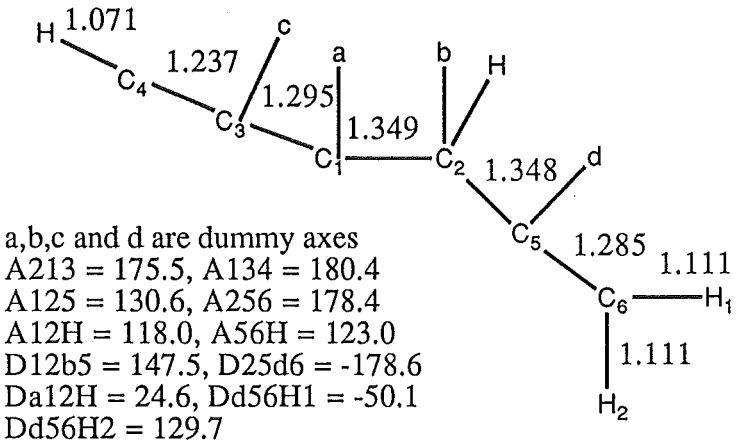

a,b,c and d are dummy axes
A213 = 175.5, A134 = 180.4
A125 = 130.6, A256 = 178.4
A12H = 118.0, A56H = 123.0
D12b5 = 147.5, D25d6 = -178.6
Da12H = 24.6, Dd56H1 = -50.1
Dd56H2 = 129.7

(19)

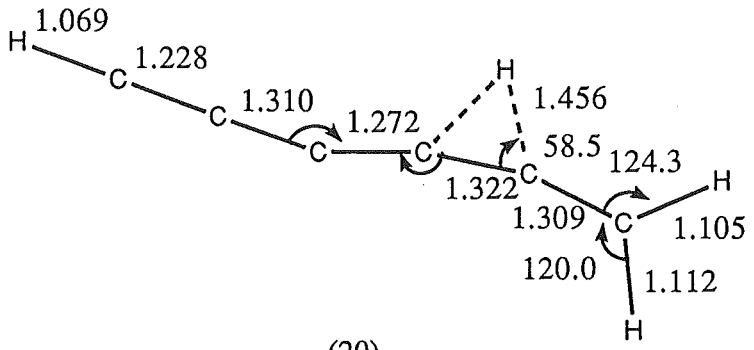

(20)

Figure 6.13 (continued)

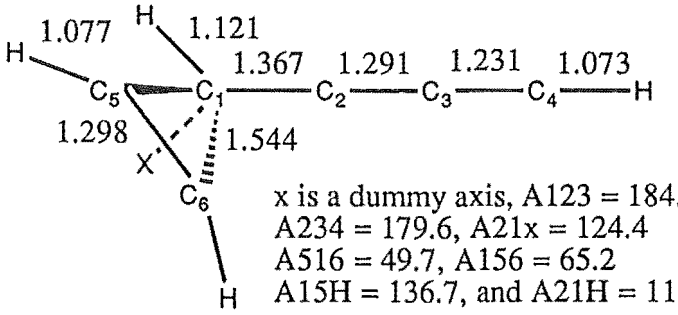

x is a dummy axis, A123 = 184.0
A234 = 179.6, A21x = 124.4
A516 = 49.7, A156 = 65.2
A15H = 136.7, and A21H = 114.2

(21)

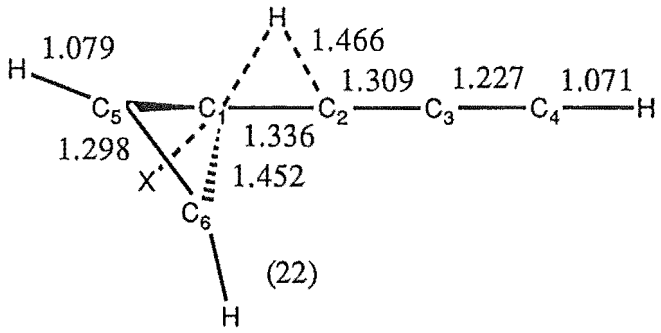

(22)

x is a dummy axis, A123 = 182.0
A234 = 180.9, A21X = 104.6, A516 = 54.8
A156 = 62.6, A15H 144.2, and A12H = 57.7

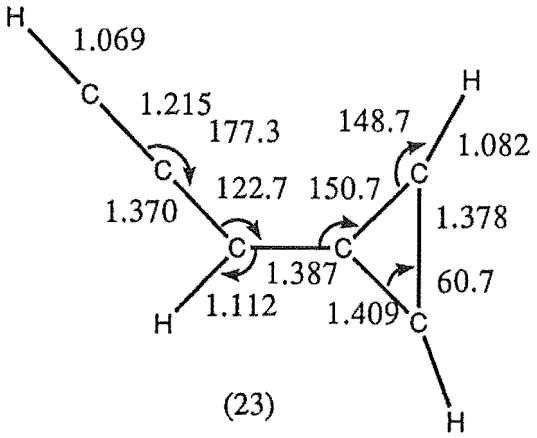

(23)

Figure 6.13 (continued)

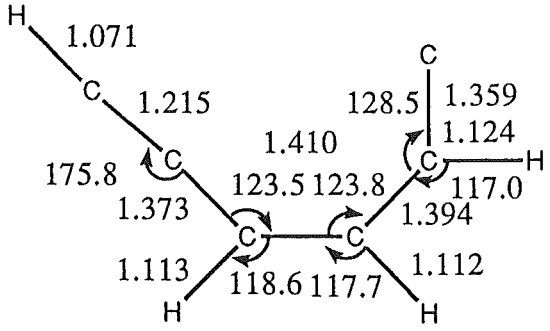

(24)

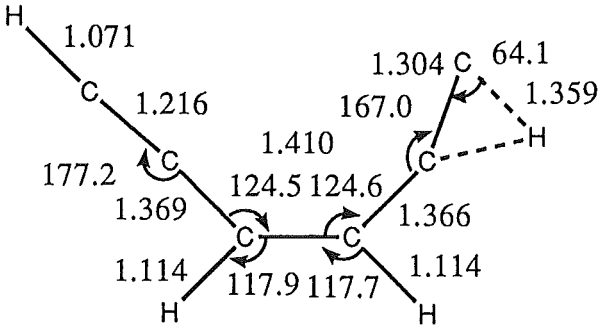

(25)

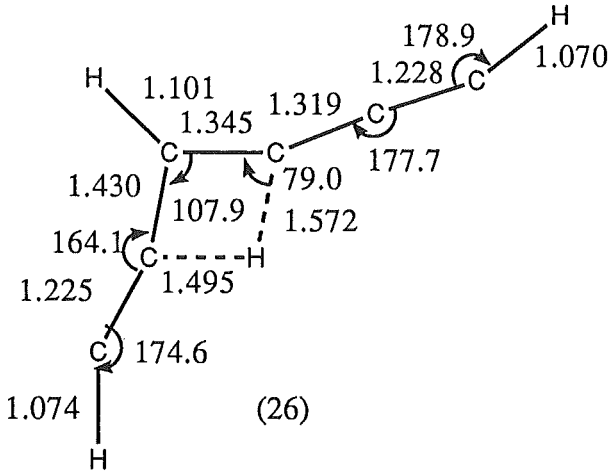

(26)

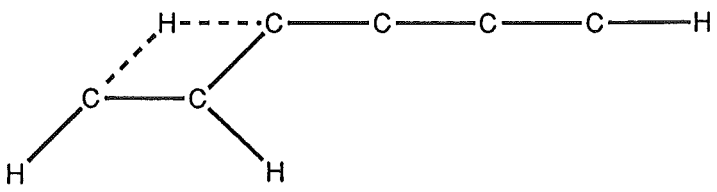

(27)

Figure 6.13 (continued)

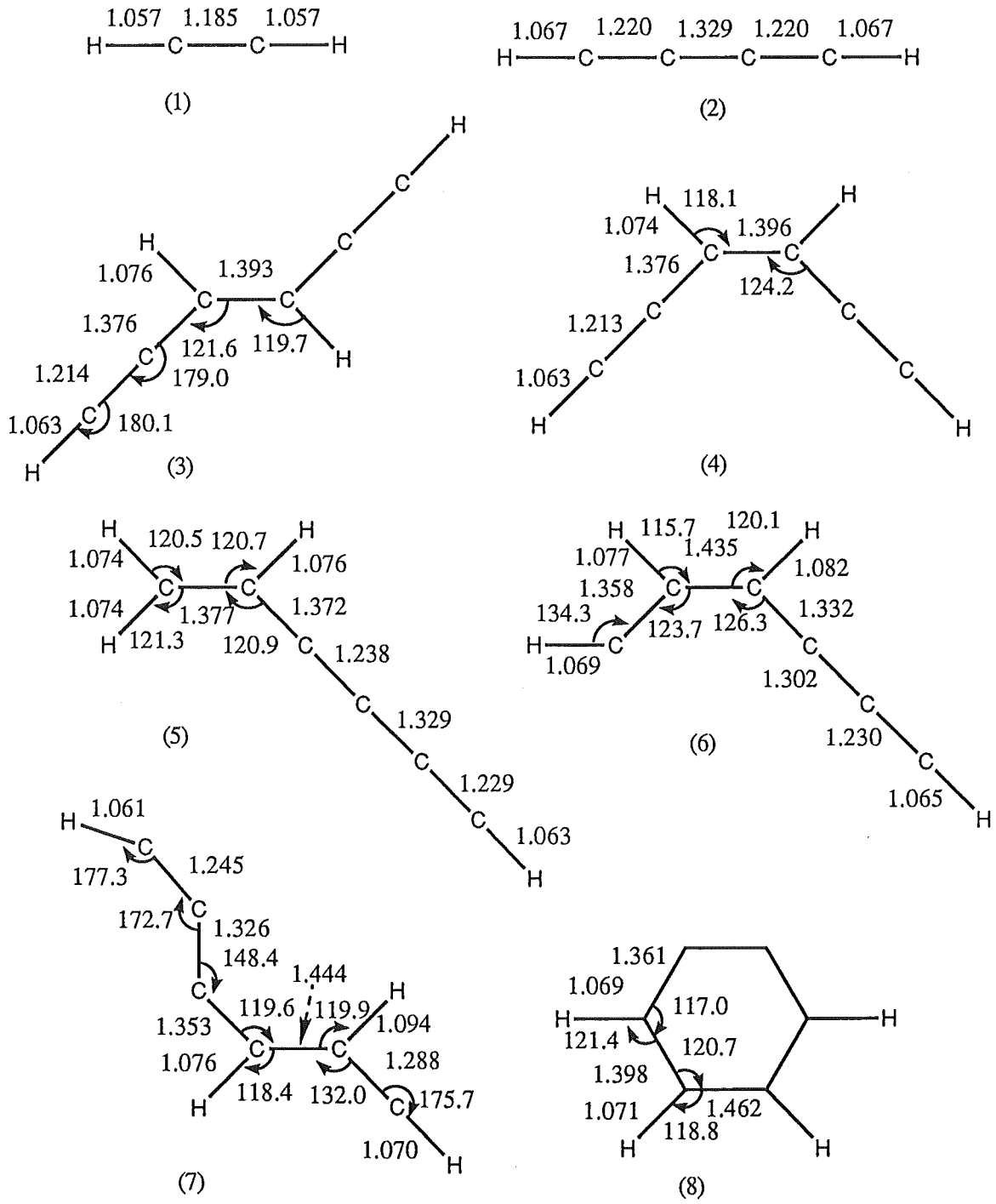

Figure 6.14 Optimized structures (Ångstroms and degrees) from the Hartree-Fock method (1) to (7) using a 6-31G* basis set and (8) to (12) using a 4-31G basis set

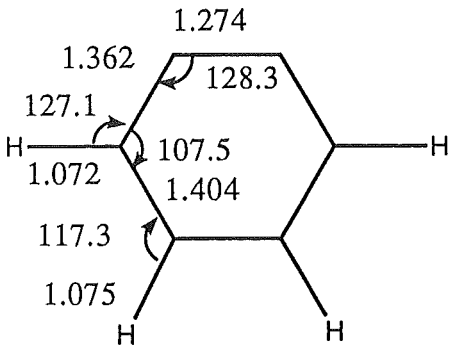

(9)

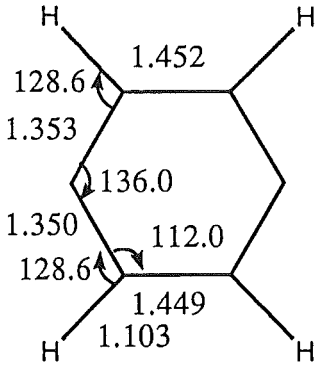

(10)

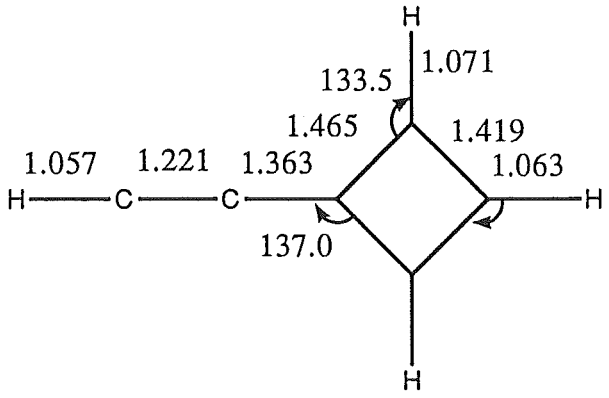

(11)

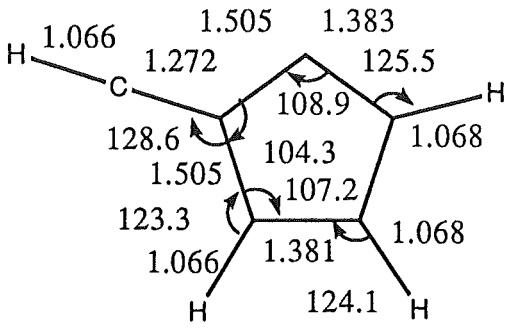

(12)

Figure 6.14 (continued)

Optimized structures of stable $C_6H_4^+$ isomers (1 to 6) from the AM1 method are in better agreement with the optimized structures at the 6-31G* level than with the results from the 4-31G level. For less stable structures, the optimized structures from both methods do differ but not significantly.

The calculated harmonic vibrational frequencies from the ab initio method at the 4-31G level are 6 to 25% higher than the values from AM1.

Table 6.1 contains optimized energies of C_2H_2, $C_4H_2^+$ and $C_6H_4^+$ isomers at 4 different levels of theory by GAUSSIAN 82. The blanks in the table are due to lack of convergence in some levels.

Table 6.2 contains calculated vibrational frequencies and zero-point vibrational energies of C_2H_2, $C_4H_2^+$ and $C_6H_4^+$ isomers by GAUSSIAN 82; blanks in front of the frequencies indicate unassigned vibrational modes.

Table 6.3 contains the relative energies between $C_6H_4^+$ and the reactants, C_2H_2 and $C_4H_2^+$ by GAUSSIAN 82.

Table 6.4, 6.5 and 6.6 contain optimized energies, calculated harmonic vibrational frequencies and relative energies for C_2H_2, $C_4H_2^+$ and $C_6H_4^+$ by the AM1 method.

Table 6.7 gives a comparison between relative energies calculated by MOPAC and GAUSSIAN 82.

Table 6.8 contains a comparison between the AM1 and HF/6-31G* optimized geometries of $C_4H_2^+$ with experimental results from laser excitation spectra by Lecoultre et al. [80]. The AM1 and HF methods give the same structure, which is in agreement with the experimental values.

In Table 6.9 a value of the heat of formation of a $C_6H_4^+$ isomer which was generated from benzonitrile, by A. Maccoll and D. Mathur [90], is compared with calculated values from the AM1 method. Though the authors believed that $C_6H_4^+$ in the experiment was a benzyne cation structure, the AM1 results shows that the value is closer to the value for an acyclic structure.

Table 6.1 GUASSIAN 82 calculated energies of compounds (hartree) with 4-31G and 6-31G* basis sets.

Structure number	HF/4-31G	HF/6-31G*	MP2/4-31G	MP4SDQ/6-31G*
(1)	-76.711413	-76.817827	-76.896447	-77.079999
(2)	-151.964927	-152.178881	-152.285374	-152.652391
(3)	-228.788930	-229.110487	-229.270721	-229.840259
(4)	-228.786737	-229.107975	-229.269010	-229.838363
(5)	-228.797432	-229.116196	-229.252648	-229.831906
(6)	-228.742891	-229.058800	-229.180799	-229.753711
(7)	-228.727656		-229.152477	-229.043744
(8)	-228.756557		-229.247064	
(9)	-228.754945		-229.264116[a]	
(10)	-228.741917			
(11)	-228.765816		-229.229414	
(12)	-228.737594			

[a] This structure has one imaginary frequency.

Table 6.2 Calculated Harmonic Vibrational Frequencies (cm^{-1}) and zero-point vibrational energies of molecules (kJ mol^{-1}) with a 4-31G basis set .

Structure number	Harmonic vibrational frequencies (cm^{-1})			ZPVE (kJ mol^{-1})
(1)	(π_g) 894	(π_g) 894	(π_u) 896	78.6
	(π_u) 896	(σ_g) 2229	(σ_u) 3606	
	(σ_g) 3727			
(2)	(a_u) 211	(b_u) 225	(a_g) 498	100.5
	(b_g) 616	(b_u) 855	(a_g) 867	
	(a_u) 885	(a_g) 1015	(b_u) 2064	
	(a_g) 2467	(b_u) 3549	(a_g) 3555	
(3)	(a") 109	(a') 142	(a') 259	196.2
	(a") 365	(a") 499	(a') 555	
	(a') 571	(a") 814	(a") 817	
	(a') 841	(a') 843	(a") 1013	
	(a") 1078	(a') 1145	(a') 1158	
	(a') 1400	(a') 1460	(a') 1693	
	(a') 2042	(a') 2132	(a') 3355	
	(a') 3362	(a') 3576	(a') 3580	
(4)	(a') 122	(a") 192	(a') 265	196.8
	(a") 371	(a') 485	(a") 520	
	(a') 800	(a") 817	(a") 825	
	(a') 842	(a') 843	(a") 907	
	(a') 974	(a") 1140	(a') 1148	
	(a') 1364	(a') 1595	(a') 1647	
	(a') 2037	(a') 2131	(a') 3351	
	(a') 3365	(a') 3577	(a') 3581	

(5)	(a') 103	(a") 135	(a') 247	194.8
	(a") 342	(a') 598	(a") 553	
	(a') 627	(a") 704	(a') 730	
	(a') 747	(a") 773	(a") 1032	
	(a') 1147	(a") 1175	(a') 1338	
	(a') 1402	(a') 1590	(a') 1679	
	(a') 1849	(a') 2176	(a') 3340	
	(a') 3358	(a') 3455	(a') 3553	
(6)	(a') 109	(a") 149	(a') 275	187.2
	(a") 302	(a") 478	(a') 507	
	(a") 626	(a") 645	(a') 709	
	(a") 838	(a') 894	(a') 966	
	(a") 975	(a') 1051	(a') 1149	
	(a') 1350	(a') 1418	(a') 1542	
	(a') 1715	(a') 2000	(a') 3288	
	(a') 3323	(a') 3453	(a') 3542	
(7)	(a') 102	(a") 110	(a") 238	178.5
	(a') 296	(a') 385	(a') 451	
	(a") 459	(a') 462	(a") 470	
	(a") 587	(a") 836	(a') 864	
	(a") 911	(a') 1053	(a') 1183	
	(a') 1278	(a') 1455	(a') 1629	
	(a') 1661	(a') 1843	(a') 3184	
	(a') 3337	(a') 3483	(a') 3567	
(8)	(b)1339i	(a) 182	(a) 372	199.2
	(b) 406	(a) 647	(b) 794	
	(b) 818	(a) 902	(a) 984	
	(b) 1074	1075	1078	
	(a) 1118	(b) 1225	(a) 1297	
	(b) 1447	(a) 1466	(a) 1520	
	(b) 1598	(a) 1685	(b) 3390	
	(a) 3398	(b) 3410	(a) 3413	

(9)	(b_2) 933i	(b_2) 316	(b_1) 438	205.5
	(a_2) 593	(a_1) 637	(a_2) 777	
	(b_2) 816	(b_1) 836	(a_1) 1043	
	(b_1) 1098	(a_1) 1114	(a_2) 1171	
	(b_2) 1202	(a_1) 1261	(a_1) 1321	
	(b_2) 1367	(b_2) 1528	(b_2) 1575	
	(a_1) 1596	(a_1) 2012	(b_2) 3391	
	(a_1) 3402	(b_2) 3430	(a_1) 3432	
(10)	492	(b_1) 507	(b_2) 567	227.3
	685	(a_1) 812	(b_1) 902	
	(a_2) 1044	(a_1) 1067	(a_2) 1077	
	(b_2) 1137	(a_1) 1161	(a_1) 1239	
	(b_2) 1359	(b_2) 1411	(a_1) 1477	
	(a_1) 1564	(a_2) 1605	(b_2) 1630	
	(b_2) 1861	(b_1) 2791	(b_2) 3392	
	(b_2) 3397	(a_1) 3412	(a_1) 3417	
(11)	(a") 96	(a") 178	(a') 191	193.4
	(a") 452	(a') 515	(a') 645	
	(a") 687	(a") 793	(a') 849	
	(a') 884	(a') 980	(a") 1016	
	(a') 1098	(a') 1178	(a") 1195	
	(a') 1315	(a') 1401	(a') 1459	
	(a') 1522	(a') 1960	(a') 3418	
	(a') 3419	(a') 3496	(a') 3485	
(12)	(a") 192	(a') 273	(a") 504	195.3
	(a") 608	(a") 644	(a') 677	
	(a') 684	(a") 750	(a") 841	
	(a') 896	(a') 950	(a") 984	
	(a') 1079	(a') 1146	(a') 1167	
	(a') 1256	(a') 1396	(a') 1455	
	(a') 1519	(a') 1804	(a') 3427	
	(a') 3441	(a') 3454	(a') 3505	

Table 6.3 The relative energies(zero-point vibrational energy corrected) between reactants, C_2H_2 and $C_4H_2^+$ and $C_6H_4^+$ isomers.

Structure number	HF/4-31G	HF/6-31G*	MP2/4-31G	MP4SDQ/6-31G*
		kJ mol^{-1}		
(1)+(2)	0.0	0.0	0.0	0.0
(3)	-278.505017	-281.625367	-216.306687	-266.108401
(4)	-272.192509	-274.476956	-211.260514	-260.575722
(5)	-302.277259	-298.067795	-170.306777	-245.627376
(6)	-166.611332	-154.902653	+10.803321	-47.857879
(7)	-135.352040	-124.113063	+76.421399	-10.471879
(8)	-190.567825		-151.251202	
(9)	-180.017683		-189.704700	
(10)	-123.972397		-189.665502	
(11)	-220.619215		-110.655410	
(12)	-144.522362			

Table 6.4 Heat of formation and zero-point vibrational energies of molecules by the AM1 method.

Structure number	Heat of formation ($kJ\ mol^{-1}$)	ZPVE ($kJ\ mol^{-1}$)
(1)	229.28295	74.9
(2)	1395.30082	101.3
(3)	1336.46136	189.1
(4)	1339.19890	189.5
(5)	1345.38001	188.3
(6)	1472.62344	176.1
(7)	1504.44753	176.1
(8)	1474.43913	147.3
(9)	1474.43796	
(10)	1448.49825	194.6
(11)	1441.50478	184.9
(12)	1522.10723	188.7
(13)	1573.61918	179.1
(14)	1575.58503	178.9
(15)	1589.49587	162.3
(16)	1474.09835	184.5
(17)	1542.67129	164.4
(18)	1554.21169	160.7
(19)	1461.39857	182.0
(20)	1527.65951	161.5
(21)	1540.42085	166.9
(22)	1630.19707	171.1
(23)	1393.51936	193.3
(24)	1581.06465	184.9
(25)	1659.52674	166.9
(26)	1633.26545	158.9

Table 6.5 The AM1 calculated harmonic vibrational frequencies (cm^{-1}) for $C_6H_4^+$ isomers.

Structure number	Harmonic vibrational frequencies			
(1)	804	805	929	929
	2182	3424	3476	
(2)	247	259	569	585
	786	797	823	835
	1095	1906	2434	3269
	3286			
(3)	82	146	277	389
	458	561	590	828
	829	834	863	864
	973	1149	1210	1274
	1375	1681	2161	2238
	3071	3086	3331	3335
(4)	118	145	288	401
	444	498	767	818
	828	829	863	864
	982	1079	1160	1232
	1453	1678	2145	2248
	3059	3074	3333	3338
(5)	124	151	268	311
	457	542	595	640
	801	824	853	888
	1039	1054	1256	1348
	1455	1646	2124	2382
	3068	3132	3150	3334
(6)	89	131	242	250
	387	530	534	63i
	690	723	787	870
	914	962	1126	1204
	1321	1681	1860	1940
	2887	3095	3232	3359

(7)	90	92	243	296
	375	476	542	632
	686	731	790	852
	867	1030	1106	1238
	1298	1670	1864	1959
	2877	3111	3233	3360
(8)	10160i	151i	344	438
	543	562	742	786
	883	896	971	1006
	1099	1190	1227	1309
	1526	1569	2663	3103
	3106	3120	3130	4551
(9)				
(10)	347	359	521	568
	700	714	819	913
	921	934	1055	1068
	1130	1156	1201	1243
	1388	1437	1639	1825
	3129	3133	3140	3152
(11)	144	164	241	322
	525	570	663	804
	817	852	948	970
	1019	1034	1111	1139
	1334	1374	1697	2184
	3183	3191	3247	3360
(12)	245i	210	372	440
	616	734	819	842
	864	921	991	1049
	1099	1163	1248	1306
	1388	1498	1525	1854
	3178	3182	3194	3301

(13)	98	163	290	296
	396	542	585	642
	666	731	829	845
	866	929	985	1139
	1370	1632	1796	2318
	2891	3225	3314	3385
(14)	77	187	258	302
	437	558	568	652
	671	726	829	846
	863	888	1046	1119
	1355	1647	1782	2312
	2861	3223	3312	3385
(15)	970i	41	138	239
	302	316	479	532
	554	744	797	835
	840	869	877	1161
	1395	1692	2010	2253
	2311	3009	3321	3344
(16)	105	168	225	388
	421	444	572	643
	811	853	864	885
	942	1029	1120	1199
	1395	1684	2100	2347
	2976	3017	3262	3374
(17)	931i	126	136	317
	363	462	505	524
	556	737	770	846
	852	869	972	1144
	1344	1806	1912	2158
	2295	3006	3300	3368
(18)	878i	91	108	218
	301	369	396	530
	598	680	687	787
	818	948	1019	1160
	1307	1853	1879	2014
	2290	3045	3252	3358

(19)	78	203	261	339
	385	427	569	626
	663	860	871	942
	956	1026	1156	1259
	1377	1835	1974	2128
	3043	3047	3102	3318
(20)	1027i	117	136	256
	301	453	457	510
	600	680	745	754
	797	989	1003	1287
	1376	1823	1985	2005
	2209	3063	3130	3339
(21)	113	147	347	388
	476	656	729	779
	834	852	912	919
	923	935	1067	1114
	1260	1810	1942	1961
	3049	3286	3301	3322
(22)	1124i	66	181	380
	396	467	663	713
	793	814	873	910
	918	994	1050	1130
	1346	1773	2031	2125
	2248	3283	3314	3332
(23)	116	150	376	415
	417	610	837	870
	885	920	923	961
	1022	1056	1177	1270
	1386	1606	2095	2247
	3086	3260	3288	3353
(24)	55	107	259	299
	431	482	746	758
	842	856	893	1009
	1078	1141	1180	1243
	1472	1617	1781	2193
	3002	3076	3098	3336

(25)	1226i	120	133	299
	402	438	443	529
	797	834	840	857
	987	1073	1143	1226
	1439	1652	1959	2189
	2280	3065	3081	3339
(26)	1285i	134	168	317
	324	483	493	582
	583	776	792	797
	817	914	995	1112
	1243	1546	1786	1949
	2160	3149	3309	3334

Table 6.6 The AM1 calculated relative energies between C_2H_2 + $C_4H_2^+$ and $C_6H_4^+$ isomers (kJ mol^{-1}).

Structure number	Δ(Heat of formation)
(1) + (2)	0.0
(3)	-275.11706
(4)	-271.99607
(5)	-267.13292
(6)	-151.89309
(7)	-120.21862
(8)	-178.72973
(9)	
(10)	-157.65082
(11)	-174.14616
(12)	-89.77810
(13)	-47.90043
(14)	-45.93605
(15)	-48.89690
(16)	-142.45152
(17)	-63.67370
(18)	-85.87173
(19)	-156.99707
(20)	-111.51377
(21)	-93.32169
(22)	-47.90043
(23)	0.90647
(24)	-213.77194
(25)	-34.66159
(26)	25.78001
(27)	-8.84092

Table 6.7 Order of relatives energies (kJ mol^{-1}) for $C_6H_4^+$ isomers with $C_2H_2^+$ $C_4H_2^+$, compared between the AM1 and the Hartree-Fock method.

Structure number	Energy (AM1)	Structure number	Energy (HF)
(3)	-275.11706	(3)	-266.10741[a]
(4)	-271.99907	(4)	-260.52946[a]
(5)	-267.12444	(5)	-245.57661[a]
(8)	-178.72973	(11)	-220.61922[b]
(11)	-174.14616	(8)	-190.56783[b]
(10)	-157.64566	(6)	-166.62963[b]
(6)	-151.88811	(12)	-144.52236[b]
(7)	-120.21862	(7)	-135.33015[b]
(12)	-89.77810	(10)	-123.97239[b]

[a] MP4SDQ/6-31G* level
[b] HF/4-31G level

Table 6.8 Optimized geometries $C_4H_2^+$ (Ångstroms) from AM1, HF/6-31G* and an experiment.

method	C-H	C-C	C-CH
AM1	1.067	1.329	1.220
HF/6-31G*	1.067	1.329	1.220
experiment[a]	1.046	1.346	1.234

[a] Reference 80

Table 6.9 Comparison of the heats of formation of some isomers of $C_6H_4^+$ from the AM1 method with experiment.

Structure number	Heat of formation (kJ mol^{-1})
(3)	1336.46
(4)	1339.20
(5)	1345.54
(8)	1474.44
(10)	1428.89
experiment[a]	1304 ± 3

[a] Reference 90

6.4 Conclusion

The reaction between C_2H_2 and $C_4H_2^+$ had been studied by two molecular orbital methods, Hartree Fock and AM1. The pathway of the probable products was established by considering the energies required in the pathway together with available data from ICR experiments. From this study the two most feasible processes are the pathways which involve acyclic isomers in a 1-2 proton shift processes. The processes that involve cyclic isomers are prohibited by the activation energies required. This conclusion should be treated with great caution however because the results from GAUSSIAN 82 show some fluctuations in relative energies and also because of the difficulty in obtaining convergence when a larger basis set was used. Most of the isomers showed high gradient values in the AM1 calculations which led to unreal optimized structures. These problems lead us to suggest that the potential surface of this reaction should be nearly flat. More experiment results and higher levels of theory are needed to understand this reaction properly.

CHAPTER 7

Valence Bond Study of the BH_2 Radical

7.1 Introduction

Valence-bond theory (VB) was formulated during the same period as molecular orbital theory (MO) [127] and has been often used qualitatively to describe the electronic structure of molecules. Although it can give a clear physical interpretation of such phenomena as charge transfer or spin pairing, this method has been much less used than molecular orbital theory because of the 'non-orthogonality' problem and the exponential growth of the size of the calculation when the size of the molecule increases. The first problem was solved by the biorthogonalization technique of Prosser and Hagstrom [115]; and the latter has been improved by the implementation of more efficient algorithms.

BH_2 is a small unstable molecule whose structure was first determined by Herzberg and Johns from a spectrum observed during flash photolysis of borine carbonyl [67]. Only a small number of theoretical studies [8,9,42,130] have been made for BH_2. This could be because the predicted geometries of the ground state agrees with the original interpretation of the electronic spectrum by Herzberg and Johns, which is not the case for the ground state of CH_2. Because of the suitable size and lack of VB calculation for the molecule, we chose to use the VB calculation to investigate features of the ground state bonding in this molecule (BH_2, $^2A_1$ $1a_1^2$ $2a_1^2$ $1b_2^2$ $3a_1$) with natural orbitals and hybrid orbitals. A comparison is made between the results from VB and with different levels MO calculations.

7.2 Method

In this study, the best orbital energy basis sets [46,104] were used. A 10s6p/2s1p contracted basis was used for boron orbitals and a 6s/1s contracted basis set with an optimized scale factor of 1.34 was used for the hydrogen orbitals. The values of exponent and coefficient of the basis set are given in Table 7.1. All calculations were performed on an IBM PC /AT microcomputer.

Table 7.1 Exponent and coefficient values of best orbital energy basis set used for boron and hydrogen atoms in this study.

Exponent	Coefficient 1s	2s	2p
Boron			
0.09402	0.001461	-0.489065	
0.28368	-0.005148	-0.595390	
0.82562	0.055946	-0.030148	
2.47699	0.371716	0.173234	
6.69825	0.418145	0.108288	
19.10235	0.216546	0.048748	
59.18759	0.074495	0.015416	
209.55715	0.019099	0.003920	
921.45590	0.003719	0.0000749	
6149.2302	0.000480	0.0000097	
0.16141			0.296070
0.46335			0.497379
1.43230			0.256922
5.07051			0.075577
22.28259			0.015345
148.38187			0.002006
Hydrogen			
0.16141	0.296070		
0.46335	0.497379		
1.43230	0.256922		
5.07051	0.075577		
22.28259	0.015345		
148.38187	0.002006		

The valence bond program used in this study derives from a work on BeH_2 followed by MacLagan and Schunelle [88] . The computation scheme in the program was as follow:

(i) Evaluation of one- and two-electron integrals. All one-and two-electron integrals were calculated by version 5 of the Micromol program [28]. The integrals were rounded to six decimal places. The scale factor for the basis set on hydrogen was optimized by GAMESS program version 3.0 [124] for the use in this study.

(ii) Input of details of all determinant to be used in the study

(iii) Evaluation of **H** and **S** matrices between all input determinants by using the Prosser-Hagstrom biorthogonalization method to evaluate cofactors and then applying Lowdin's formulae [87].

(iv) Input of details of configuration determinants to be studied.

(v) Solve the eigenvalue equation (**H**-ES) **C** = 0

The table below shows that in the ground state ($^2A_1$) BH_2 has a bent structure with a bond angle between 120.0° and 135.0°.

Table 7.2 The full VB electronic energies (hartree) for the ground state of BH_2

θ (degree)	r (bohr)		
	2.25	2.35	2.45
120.0	-25.75402	-25.75664	-25.75400
135.0	-25.75549	-25.75755	-25.75448
150.0	-25.75224	-25.75401	-25.75056
165.0	-25.74790	-25.74934	-25.74556
180.0	-25.74257	-25.74370	-25.73959

In the VB calculation with natural orbitals, 100 determinants of 21 configurations were used to form the wavefunction. The $1s^2$ core on boron atom was kept unchanged ('frozen-core approximation'). This approximation should not affect the shape of the potential surface, as has been demonstrated in for NH_3 [102]. The molecule is placed on the plane yz with z as the principle axis. Through out this study, p_x orbital was excluded from all calculations because of its geometry. Optimization of geometries was achieved by varying parameters until the energy was a minimum. The B-H bond was determined to within 0.01 au. for the bond length and 0.1 degree for the bond angle. The frozen-core hybrid VB calculation involved 21 combinations of the same spin from 58 determinants which were used to represent all seven configurations for B^0, B^-, B^+, B^{-2} and B^{+2}. Hybrid orbitals were used in order to investigate the relationship between nuclear bond angle and hybrid angle. The calculation with hybrid orbitals tended to require fewer determinants than the calculation with natural orbitals to obtain the same energy value.

Three orthogonal hybrid orbitals used in this calculation are defined as:

$$l_1 = -\alpha s - \sqrt{1-\alpha^2}.(2p_z) \qquad (7.1)$$

$$b_1 = 1/\sqrt{2}\,[-\sqrt{1-\alpha^2}.(2s) + (2p_y) + \alpha(2p_z)] \qquad (7.2)$$

$$b_2 = 1/\sqrt{2}\,[-\sqrt{1-\alpha^2}.(2s) - 2(p_y) + \alpha(2p_z)] \qquad (7.3)$$

where $\alpha = \cot \theta/2$ (7.4)

l_1 and b_1 and b_2 are lone-pair and bonding orbitals respectively. The quantity θ is the angle between the two hybrid orbitals, b_1 and b_2. A set of calculation was performed at R_{B-H} = 2.340 a.u. for bonding angles between 100° to 160° in which a was optimized. The calculations on the configurations with neutral and charged boron atoms were performed to investigate the contribution from each configuration.

The molecular orbital calculation was performed with the same basis set. The HF and MP4SDQ calculations were done on GAUSSIAN 90 [53]. The geometries from HF were used in frozen-core CI calculation on Gamess version 3.0 [124] in order to verify the energies from VB calculations.

7.3 Results and Discussion

Table 7.3 shows that the VB method gives a lower optimized energy than the result from the single determinant MO method. This is not unexpected because, in the VB method electron correlation was included through the VB structures while it was neglected in the single-determinant MO method.

Table 7.3 Optimum geometries and corresponding energies for $^2A_1$ ground state of BH_2 from different methods and basis sets.

Method	r (Å)	θ (deg)	Energy (hartree)
STO-3G[a]	1.161	123.5	
DZCI[b]	1.211	129.4	-25.79078
SJ[c]	1.204	128.6	
SJ CI[c]	1.204	128.6	
DZ[d]	1.190	129.0	-25.74006
DZd[d]	1.197	129.5	-25.81634
DZdCI[d]	1.197	129.5	-25.81634
DZdp[d]	1.189	128.1	-25.75254
DZdpCI[d]	1.189	129.5	-25.83321
HF[e]	1.216	130.3	-25.72827
MP4SDTQ[e]			-25.76063
Single excited CI[e]			-25.73063
Double excited CI[e]			-25.76172
Triple excited CI[e]			-25.76200
Quadruple excited CI[e]			-25.76232
Full CI[e]			-25.76232
full VB[e]	1.238	129.9	-25.75791
hybrid VB[e]			-25.73997
experiment[f]	1.181	131	

[a] Reference 42
[b] Reference 9
[c] Reference 130
[d] Reference 8
[e] This study
[f] Reference 67

In a 'build-up' study, it took only the linear combination of four VB configurations to give a lower energy than the MO energy. The lower energy from the MP4SDQ, perturbation theory calculations agree with the values from CI calculations. From the nature of the two methods, this is predictable. The energy from VB method which used the combination of hybrid orbitals is poorer than the natural VB method but the energy is slightly better than the single determinant MO method because of the smaller number of configurations used in the hybrid wavefunction. The optimized geometry of BH_2 from the VB method give good agreement in bond angle value with the experiment and with other theoretical studies but not in the bond length. The inflexibility of the 10s6p/2s1p basis set could be a reason for the poor bond length but even the MO method with the same size of the basis set gave better geometry of the molecule. This raises a question about the optimization method which was employed in this study.

From the configuration calculation in Table 7.4, the lowest energy configuration is $2sp_yp_z$ on neutral boron atom. The most surprising result is the large contribution from B^- and B^{-2} configurations as $2s^2p_yp_z$, $2sp_y^2p_z$, $2sp_yp_z^2$ and $2s^2p^2p$. This was also observed in the study of CH_2 by MacLagan [88] but not to the extent found in this study. The configurations $2sp_y$, $2sp_z$ and p_yp_z from B^+ are also important but configurations from B^{2+} have only a small contribution.

Table 7.4 Configuration energies for BH_2 at R_{B-H} = 1.238 Ångstrom and HBH = 129.9 degrees.

Charge on B atom	No	Configuration	Configuration energy (hartree)
0	1	$1s^2 2s^2 p_y h_1 h_2$	-25.30958
	2	$1s^2 2s^2 p_z h_1 h_2$	-25.28262
	3	$1s^2 2sp_y^2 h_1 h_2$	-24.94609
	4	$1s^2 p_y^2 p_z h_1 h_2$	-25.00230
	5	$1s^2 p_z^2 h_1 h_2$	-25.26724
	6	$1s^2 p_y p_z^2 h_1 h_2$	-25.06702
	7	$1s^2 2sp_y p_z h_1 h_2$	-25.63569
+1	8	$1s^2 2s^2 h^2 h$	-24.88564
	9	$1s^2 2sp_y h^2 h$	-25.00677
	10	$1s_2 2sp_z h^2 h$	-25.23124
	11	$1s^2 p_y p_z h^2 h$	-25.10685
	12	$1s^2 p_y^2 h^2 h$	-24.41221
	13	$1s^2 p_z^2 h^2 h$	-24.72159
-1	14	$1s^2 2s^2 p_y p_z h$	-25.49802
	15	$1s^2 2sp_y^2 p_z h$	-25.40083
	16	$1s^2 2sp_y p_z^2$	-25.19768
	17	$1s^2 2s^2 p_y^2 h$	-25.06600
	18	$1s^2 2s^2 p_z^2 h$	-25.15860
	19	$1s^2 p_y^2 p_z^2 h$	-24.81817
-2	20	$1s^2 2s^2 p^2 p$	-25.27628
+2	21	$1s^2 2sh_1^2 h_2^2$	-24.81886

A build-up study was performed for the first ten natural orbital configurations. The first configuration has the lowest energy and the others are added successively in such a way that the resultant energy is a minimum. In the table below, the study shows that although the energies of configurations 11, 12 and 15 are not favoured on their own, they still make a significant contribution.

Table 7.5 Valence-bond 'build-up' study of BH_2 with natural orbitals

Configuration[a] include	Position of configuration in table of increasing configuration energies	Energy (hartree)
7	1	-25.63560
+14	2	-25.68343
+15	3	-25.70737
+1	4	-25.72666
+2	5	-25.73946
+20	6	-25.74350
+11	11	-25.74666
+6	12	-25.75101
+4	15	-25.75332
+5	7	-25.75441
E_{MO}		-25.72827

[a] Number refer to configurations given in Table 7.4

Table 7.6 shows the energies of each combination which are functions of the spin operator. One unexpected result is that the lowest energy combination is one of the B^- configurations. The B^- configurations were also found to be important in the natural orbital calculations. Chemical intuition suggests that the result from natural orbitals, of which $2sp_yp_z$ were the lowest configuration, is more acceptable. The result from hybrid orbitals needs more investigation.

Table 7.6 Valence-bond study on the ground state of BH_2: configuration energies (hartree).

No	B S	B M_S	Configuration	|Ci|	Population	Configuration energy
B^0						
1	3/2	3/2	$1s^2lb_1b_2h_1h_2$	0.1887	0.1423	-25.39878
2	3/2	1/2		0.1792	0.1325	-25.27345
3	3/2	-1/2		0.1650	0.0845	-25.16236
4	1/2	1/2		0.0000	0.0000	-24.82792
5	1/2	1/2		0.1453	0.1211	-25.31988
6	1/2	1/2	$1s^2l^2bh_1h_2$	0.0631	0.0059	-25.05035
7	1/2	-1/2		0.0451	0.0040	-25.00572
B^+						
8	1	1	$1s^2lbh^2h$	0.0455	0.0357	-25.29474
9	1	1		0.0156	0.0003	-24.40054
10	0	0		0.1106	0.0701	-25.05600
11	0	0		0.0206	0.0002	-24.32629
12	0	0	$1s^2b_1b_2h^2h$	0.0266	0.0005	-24.29289
13	1	1		0.0192	0.0002	-24.57346
B^-						
14	1	1	$1s^2lb^2bh$	0.0300	0.0005	-24.64260
15	0	0		0.0199	0.0003	-25.58543
16	0	0		0.2783	0.2449	-25.52733
17	0	0		0.2225	0.15812	-25.28674
BH^+H^-						
18	1/2	1/2	$1s^2l^2bh^2$	0.0109	0.0004	-23.83142
19	1/2	1/2		0.0299	0.0024	-24.71203
20	1/2	1/2	$1s^2lb_1b_2h^2$	0.0041	0.0001	-24.24843
21	1/2	1/2		0.0040	0.0001	-24.23295

The 'build-up' study with hybrid orbitals was conducted with the same criteria that used with natural orbitals. Table 7.7 shows that seven combinations of configurations are required to give a lower energy than the MO calculation.

Table 7.7 Valence-bond 'build-up' study of BH_2 with hybrid orbitals

Configuration[a] include	Position of configuration in table of increasing configuration energies	Energy (hartree)
16	1	-25.52733
17	5	-25.59639
1	2	-25.63160
2	6	25.67722
3	7	-25.70267
5	3	-25.72094
10	8	-25.72969
6	9	-25.73273
7	10	-25.73459
8	4	-25.73515
E_{MO}		-25.72827

[a] Number refer to configurations given in Table 7.6

In both natural-orbital and hybrid-orbital calculations, the configurations from B^- surprisingly have low energies and a large contribution in lowering energies of the 'build-up' wavefunctions. The study of the change of hybrid orbitals angle when the bond angle vary gave the expected result. This study it shows that the hybrid angles follow the changes of the bond angle although the optimized hybrid angles and the optimized bond angle do not coincide. This behaviour is the same as the 'orbital stasis' of AH_2 reported by MacLagan et al. [89].

Table 7.8 Energies of BH_2 at maximum hybrid angle at different bond angles.

Bond angle (deg)	Maximum hybrid angle (deg)	Energy (hartree)
100.0	117.3	-25.72352
110.0	120.3	-25.73268
120.0	123.5	-25.73789
125.0	125.5	-25.73929
130.0	128.1	-25.74002
135.0	130.0	-25.74019
140.0	134.1	-25.73990
150.0	142.4	-25.73841
160.0	153.4	-25.73646

Calculated charges on each atom are shown in Table 7.9. The negative charge on boron atom support the important of the contribution from B^- configurations.

Table 7.9 Calculated charge density from the MO calculations.

Theory	B	H
Mulliken Population Analysis[a]	-0.36015	0.18008
Lowdin Population Analysis[a]	-0.25727	0.12863
Mulliken Population Analysis[b]	-0.37827	0.18913

[a] Full CI on GAMESS program
[b] HF on GAUSSIAN 90

7.4 Conclusion

The VB calculation was performed for the $^2A_1$ ground state BH_2 molecule. The optimized bond length and bond angle from this method are 1.238 Å and 129.9 °. The calculated bond length is significant larger than founded by studies and experimental result. The energy from the full VB calculation is in a good agreement with other studies, although it is higher than the energies obtained from the MP4SDQ and the CI method. The hybrid orbital calculations give poorer energy values than the full VB calculation. The 'build-up' study with natural orbitals shows the covalent $1s^2 2sp_y p_z h_1 h_2$ is the most important configuration, while the calculation with hybrid orbitals suggests that the most important configuration is $1s^2 1b^2 b$. The B^- structures are more important than expected.

Acknowledgments

My Gratitude to the following people cannot be adequately expressed for their contributions during my four and a half years study in New Zealand. I am especially indebted to Dr. R.G.A.R. Maclagan for his patient supervision of my research and to the New Zealand government and the Ministry of External Relations & Trade for a scholarship.

I am grateful to Prof. L.F. Phillips for his proof-reading of my thesis which turned my English into English and to his wife, Mrs. P. Phillips for her great hospitality during these years.

A special thank goes to Mrs. E.M. Ross for her English tutorials in my second year which helped to reduce my initial communication difficulties.

I am also indebted to Mr. S.T. Grice and his family for his help in my research and our wonderful friendship, to Dr. M.J. McEwan for helpful discussions on gaseous chemistry, to Dr. B. Williamson for providing a harmonic vibrational frequencies program, to Drs. A.D. Abell, P.J. Steel and Mr. A. Burritt who spent time talking with me on 'organic chemistry' parts in my work and to Miss W. Marsh for her advice on the editing and printing processes.

I would like to thank Mr. D.Q. McDonald for his great encouragement and many delightful discussions ranging from music to computers.

Finally, I would like to thank my parents whose love and dreams make my life meaningful, my friend Lay Keok for her valuable friendship, Audri and Sue for taking me to the mountains and lakes and letting me have a part in their family and Thai farmers who are poor as ever but still grow rice to feed me and others.

References

1. N.G. Adams and D. Smith, *Chem. Phys. Lett.*, 54 (1978) 530.
2. D. Alexander, *New Scientist*, 126 (1990) 61.
3. J. Almof and K. Faegri, *Theor. Chim. Acta.*, 96 (1986) 447.
4. V.G. Anicich, A.D. Sen, W.T. Huntress, and M.J. McEwan, *J. Chem. Phys.*, 93 (1990) 7163.
5. P. Ausloos and S.G. Lias, *Int. J. Mass spectrom. Ion Processes*, 58 (1984) 165.
6. K.D. Bayes, *J. Chem. Phys.*, 52 (1970) 1093.
7. K.H. Becker and K.D. Bayes, *J. Chem. Phys.*, 48 (1968) 653.
8. S. Bell, *J. Chem. Phys.*, 68 (1978) 3015.
9. C.F. Bender and H.F. Schaefer, *J. Mol. Spectrosc.*, 37 (1971) 423.
10. R.C. Bingham, M.J.S. Dewar, and D.H. Lo, *J. Am. Chem. Soc.*, 97 (1975) 1285.
11. J.S. Binkley, M.J. Frisch, D.J. Defrees, K. Raghavachari, R.A. Whiteside, E.M. Fludde, and J.A. Pople, GAUSSIAN 82, Carnegie-Mellon University, Pittsburgh, (1983).
12. J. S. Binkley, J. A. Pople and W. J. Hehre, *J. Am. Chem. Soc.*, 102:3 (1980) 939.
13. C. E. Blom and C. Altona, Mol. Phys., 31 (1976) 1377.
14. M. Born and J.R. Oppenheimer, *Ann. Physik*, 84 (1927) 457.
15. P. Botschwina, H. Schramm and P. Sebald, in press.
16. G. Bouchoux, J.P. Flament, Y. Hoppiliard, J. Tortajada, R. Flammang, and A. Maquestiau, *J. Am. Chem. Soc.*, 15 (1989) 5561.
17. (a) S.F. Boys and F. Bernardi, *Mol. Phys.*, 19 (1970) 553; (b) B. Liu and A.D. McLean, *J. Chem. Phys.*, 59 (1973) 4557; (c) Z. Latajka, and Scheiner, *Chem. Phys. Lett.*, 105 (1984) 435; (d) D.W. Schwenke and D.G. Truhlar, *J. Chem. Phys.*, 82 (1985) 2418.
18. F.W. Brill and J.R. Eyler, *J. Phys. Chem.*, 85 (1981) 1091.
19. L. Brillouin, *Actualities Sci. Ind.*, 71 (1934) 159.
20. R.D. Brown and E.H.N. Rice, *J. Am. Chem. Soc.*, 106 (1984) 6475.

21 R.D. Brown, F.W. Eastwood, P. Elmes, and P.D. Godfrey, *J. Am. Chem. Soc.*, 105 (1983) 6496.

22. R.D. Brown, P.D. Godfrey, D.M. Cragg, E.H.N. Rice, W.M. Irvine, P. Friberg, H. Suzuki, M. Ohishi, N. Kaifu, and M. Morimoto, *Ap. J.*, 297 (1985) 302.

23. E.M. Bulewicz, D.G. Evans, and P.J. Padley, *Symp. (Int.) Combust., [Proc.]*, 14th, 1975 (1975) 1461.

24. F. Cacace, G. Ciranni, and P. Giacomello, *J. Am. Chem. Soc.*, 104 (1982) 2258.

25. C.F. Chabalowski, R.J. Buenker, and S.D. Peyerimhoff, *J. Chem. Phys.*, 84 (1986) 268.

26. T. Clark, "A Handbook of Computational chemistry", John Willey and Sons, Inc., New York, (1985).

27. D.L. Cooper, J. Gerratt, and M. Raimondi, *Adv. Chem. Phys.*, 69 (1987) 319.

28. S.M. Cowell, R. Amos, N.C. Handy, and A.R. Marshall, MICROMOL MARK III, Department of theoretical chemistry, University of Cambridge, 1986.

29. C.A. Deakyne, M. Meot-Ner, T.J. Buckley, and R. Metz, *J. Chem. Phys.*, 86 (1987) 2334.

30. J. P. Declaux and P. Pyykko, *Chem. Phys. Lett.*, 29 (1974) 534.

31. D.J. DeFrees and A.D. McLean, *J. Comp. Chem.*, 7 (1986) 321.

32. D.J. DeFrees and A.D. McLean, *J. Chem. Phys.*, 82 (1985) 333.

33. R.L. DeKock and W. Weltner, *J. Am. Chem. Soc.*, 93 (1971) 7106.

34. J. E. Del Bene, H.D. Mettee, M.J. Frisch, B.T. Luke, and J.A. Pople, *J. Phys. Chem.* 87 (1983) 3279.

35. C. Devillers and D.A. Ramsay, *Can. J. Phys.*, 49 (1971) 2839.

36 M.J.S. Dewar, *J. Am. Chem. Soc.*, 74 (1952) 3341.

37. M.J.S. Dewar and Theil, *J. Am. Chem. Soc.*, 99 (1977) 4899.

38 M.J.S. Dewar, E.G. Zoebisch, E.F. Healy, and J.J.P. Stewart, *J. Am. Chem. Soc.*, 107 (1985) 3902.

39. M. J. S. Dewar, G. L. Grady,, D. R. Kuhn and K. M. Merz, *J. Am. Chem. Soc.*, 106 (1984) 6771.

40. Ibid, *J. Am. Chem. Soc.*, 106 (1984) 6773.

41. M.J.S. Dewar, E.G. Zoebisch, E.F. Healy, and J.J.P. Stewart, *J. Am. Chem. Soc.*, 107 (1985) 3902.

42. J.D. Dill, P.R. Scheleyer, and J.A. Pople, *J. Am. Chem. Soc.*, 93 (1971) 5339.

43. K. D. Dobbs and W. J. Hehre, *J. Comput. Chem.*, 7 (1986) 359.

44. V.M. Donnelley, W.M. Pitts, and J.R. McDonald, *Chem. Phys.*, 49 (1980) 289.

45. V.M. Donnelley and L. Pasternack, *Chem. Phys.*, 39 (1979) 427.

46. F.B. v. Duijneveldt, "Gaussian Basis Sets for The Atoms H - Ne for Use in Molecular Calculations", IBM Reasearch Laboratory report, 1971.

47. M. Dupuis, J. Rys, and H.F. King, *J. Chem. Phys.*, 65 (1976) 111.

48. J. R. Durig, C. M. Whang, G. M. Attia, and Y. S. Li, *J. Mol. Spectrosc.*, 108 (1984) 240.

49. D.W. Ewing, *J. Am. Chem. Soc.*, 111 (1989) 8809.

50. J.R. Eyler and J.E. Campana, *Int. J. Mass Spectrom. Ion Processes*, 55 (1983/1984) 171.

51. F.H. Field, J.L. Franklin, and F.W. Lampe, *J. Am. Chem. Soc.*, 79 (1957) 2665

52. J.L. Franklin, Y. Wada, P. Natalis, and P.M. Nierl, *J. Phys. Chem.*, 70 (1966) 2353.

53. M.J. Frisch, M. Head-Gordon, G.W. Trucks, J.B. Foresman, H.B. Schlegal, K. Raghavachari, M.A. Robb, J.S. Binkley, C. Gonzalez, D.J. Defrees, D.J. Fox, R.A. Whiteside, R. Seeger, C.F. Melius, J. Baker, R.L. Martin, L.R. Kahn, J.J.P. Stewart, S. Topiol, and J.A. Pople, GAUSSIAN 90, Gaussian, Inc., Pittsburgh, PA, 1990.

54. G.A. Gallup, R.L. Vance, J.R. Collins, and J.M. Norbeck, *Adv. Quat. Chem.*, 16 (1982) 229.

55. J.M. Goodings, D.K. Bohme, and Chun-Wai Ng, *Combust. Flame*, 36 (1979) 27.

56. J.M. Goodings, D.K. Bohme, and Chun-Wai Ng, *Combust. Flame*, 36 (1979) 45.

57. G.A. Gray, *J. Am. Chem. Soc.*, 90 (1968) 6002.

58. S. Grigoras and T. H. Lane, *J. Comput. Chem.*, 8 (1987) 84.

59. N.H. Haese and R.C. Woods, *Chem. Phys. Lett.*, 91 (1982) 190.

60. G.G. Hall, *Proc. Roy. Soc. (London)*, A205 (1951) 541.

61. A.N. Hayhaurst and D.B. Kittelson, *Combust. Flame*, 31 (1978) 37.

62. W.J. Hehre, L. Radom, P.v.R. Schleyer, and J.A. Pople, "Ab initio Molecular Orbital Theory", John Willey and Sons, Inc., New York.

63. For a discussion, see reference 62, p. 193 ff.

64. R.J. Heinsohn and P.M. Becker, "Effects of Electric Field in Flames" in "Combustion Technology, Some Modern Developments", H.B. Palmer and J.M. Beer, Ed., Academic Press New York, 1974.

65. W. Heitler, and F. London, *Z. Phys.*, 44 (1927) 455.

66. E. Herbst, D. Smith, and N.G. Adams, *Astron. Astrophys.*, 138 (1984) L13.

67. G. Herzberg and J.W.C. Johns, *Proc. R. Soc. (London) Ser.*, A 298 (1967) 142.

68. B.A. Hess Jr., W.D. Allen, D. Michalska, L.J. Schaad, and H.F. Schaefer, *J. Am. Chem. Soc.*, 109 (1987) 1615.

69. W.T. Huntress, *Astrophys. J.* (Suppl. Ser.), 33 (1977) 495.

70. S. Huzinaga, J. Andzeim, M. Klobukoswaki, E. Radzio-Andzelm, Y. Sakai, and H. Tazewaki., "Gaussian Basis Sets for Molecular Calculations", Elsevier, New York, 1984.

71. W.M. Irvine, "Astrochemistry ", ed. M.S. Vardya and S.P. Tarafdar (Dordrecht:Reide), 1986, p.245.

72. W.M. Irvine, P. Friberg, N. Kaifu, K. Wanaguchi, Y. Kitamura H.E. Matthews, Y. Minh, S. Saito, N. Ukita, and S. Yamamoto, *Ap. J.*, 342 (1989) 871.

73. M.E. Jacox, D.E. Milligan, N.G. Moll, and W.E. Thompson, *J. Chem. Phys.*, 43 (1965) 3734.

74. J.K. Kim, V.G. Anicich, and W.T. Huntress, *J. Phys. Chem.*, 81 (1977) 1798.

75. K.S. Kim, H.F. Schaefer, L. Random, J.A. Pople and J.S. Binkley, *J. Am. Chem. Soc.*, 105 (1983) 4148.

76. H. Kimmel and C. R. Dillard, *Spectrochim. Acta*, Part A 24A (1968) 909.

77. J.S. Knight, C.G. Freeman and M.J. McEwan, *J. Am. Chem. Soc.*, 108 (1986) 1404.

78. J.S. Knight, C.G. Freeman, and M.J. McEwan, *J. Phys. Chem.*, 91 (1987) 3898.

79. H.W. Kroto, C. Kirby, D.R.M. Walton, L.W. Aveny, N.W. Broten, J.M. Macleod, and T. Oka, *Astrophys. J.*, 219 (1978) L133.

80. J. Lecoultre, J.P. Maier, and M. Rosslein, *J. Chem. Phys.*, 89 (1988) 6081.

81. I.N. Levine, "Quantum Chemistry", 3rd ed., Allyn and Bacon, Boston, 1983.

82. For a discussion, see I.N. Levine, "Quantum Chemistry", 3rd ed., Allyn and Bacon, Boston, 1983, p. 172-192.

83. I. W. Levine and H. Schiffer, *J. Chem. Phys.*, 43 (1965) 4023.

84. G.N. Lewis and M. Randall, "Thermodynamics" , revised by K.S. Pitzer and L. Brewer, McGraw-Hill, New York, 1961.

85. S.G. Lias, J.E. Bartmess, J.F. Liebman, J.L. Holmes, R.D. Levin, and W.G. Mallard, *J. Phys. Chem. Ref. Data*, 17, Supplement 1 (1988)

86. F.P. Lossing and J.L. Holmes, *J. Am. Chem. Soc.*, 106 (1984) 6917.

87. P.-O. Lowdin, *Phys. Rev.*, 97 (1955) 1474, 1490, and 1509.

88. R.G.A.R. MacLagan, and G.W. Schnuelle, *J. Chem. Phys.*, 55 (1971) 5431.

89. R.G.A.R. MacLagan, *Mol. Phys.*, 41 (1980) 1471; I.J. Doonan and R.G.A.R. MacLagan, *Theor. Chim. Acta* , 50 (1978) 87; R.G.A.R. MacLagan, and G.W. Schnuelle, *Theor. Chim. Acta* , 46 (1977) 165; R.G.A.R. MacLagan, and H.D. Todd, *Theoret. Chim. Acta*, 34 (1974) 19.

90. A. Maccoll and D. Mathur, *Org. Mass Spectrom.*,16 (1981) 261.

91. H.E. Matthews, W.M. Irvine, P. Friberg, R.D. Brown, and P.D. Godfrey, *Nature*, 310 (1984) 125.

92. M. Meot-Ner (Mauter), *J. Am. Chem. Soc.*, 100 (1978) 4694.

93. M. Meot-Ner (Mauter) and Z. Karpas, *J. Phys. Chem.*, 90 (1986) 2206.

94. M. Meot-Ner (Mauter), Z. Karpas,and C.A. Deakyne, *J. Am. Chem. Soc.*, 108 (1986) 3913.

95. W. Meyer, *J. Chem. Phys.* 58 (1973) 1017.

96. W.J. Miller, *Symp. (Int.) Combust., [Proc.]*, 14th, 1972 (1973) 307.

97. C. Mϕller and M.S. Plesset, *Phys. Rev.*, 46 (1934) 618.

98. A. Murakami, *Ap. J.*, 357 (1990) 288.

99. J.O. Noell and M.D. Newton, *J. Am. Chem. Soc.*, 101 (1979) 51.

100. W. Pauli, *Z. Physik*, 31 (1925) 765.

101. S. Petrie, J.S. Knight, C.G. Freeman, R.G.A.R. Maclagan, M.J. McEwan, and P. Sukeaw, *Int. J. Mass. Spectrom. Ion Processes*, 105 (1991) 43.

102. A. Pipano, R.R. Gilman, and I. Shavitt., *Chem. Phys. Lett.*, 5 (1970) 285.

103. K.S. Pitzer, "Quantum Chemistry" , Prentice-Hall, Englewood Cliffs, NJ, 1961.

104. R. Poirier, R. Kari, and I.G. Csizmadia, "Handbook of Gaussian Basis sets", Elsevier, Amsterdam, 1985.

105. J.A. Pople, *J. Chem. Phys.*, 90 (1989) 5622.

106. J.A. Pople, D.P. Santry, and G.A. Segal, *J. Chem. Phys.*, 43 (1965) s129.

107. J.A. Pople and G.A. Segal, *J. Chem. Phys.*, 43 (1965) s136.

108. J.A. Pople, D.L. Beveridge, and P.A. Dobosh, *J. Chem. Phys.*, 47 (1967) 2026.

109. J.A. Pople and R.K. Nesbet, *J. Chem. Phys.*, 22 (1954) 571.

110. J.A. Pople, H.B. Schlegel, R. Krishnan, D.J. DeFrees, J.S. Binkley, M.J. Frisch, R.A. Whiteside, R.F. Hout Jr., and W. J. Hehre, *Int. J. Quant.Chem. Symp.*,15 (1981) 269.

111. J.A. Pople, M. Head-Gordon, D.J. Fox, K. Raghavachari and L.A. Curtiss, *J. Chem. Phys.*, 90 (1989) 5622.

112. C. Pouchan, G. Lespes and A. Dargelos, *J. Phys. Chem.*, 92 (1988) 28.

113. C. Pouchan, A. Dargelos and M. Chaillet, *J. Chim. Phys.*, 75 (1978) 595.

114. G.P. Prado and J.B. Howard, *Adv. Chem. Ser.*, No. 166, chapter 10 (1978).

115. F. Prosser, and S. Hagstrom, *Int. J. Quantum chem.*, 2 (1968) 89.

116. M. Raimondi, M. Simonetta, and G.F. Tantardini, *Comp. Phys. Rep.*, 2 (1975) 171.

117. A.B. Raksit, H.J. Schiff and D.K. Bohme, *Int. J. Mass Spectrom. Ion Processes*, 56 (1984) 321.

118. C.C.J. Roothaan, *Rev. Mod. Phys.*, 23 (1951) 69.

119. (a) C.C.J. Roothan, *Rev. Mod. Phys.*, 32 (1960) 179; (b) J.S. Binkley, J.A. Pople, and P.A. Dobosh, *Mol. Phys.*, 28 (1974) 1423.

120. H.M. Rosenstock, R. Stockbauer, and A.C. Parr, *J. Chim Phys. Phys.-Chim. Biol.* 77 (1980) 745.

121. S. Saito, K. Kawaguchi, S. Yamamoto, M. Ohishi, H. Suzuki, and N. Kaifu, *Ap. J.*, 317 (1987) L115.

122. S.M. Schildcrout and J.L. Franklin, *J. Am. Chem. Soc.*, 92 (1970) 251.

123. H. Schlager and F. Arnold, *Planet. Space Sci.*, 33 (1985) 321.

124. M.W. Schmidt, K.K. Baldridge, J.A. Boatz, J.A. Jensen, S. Koseki, M.S. Gordon, K.A. Nguyen, T.L. Windus, S.T. Elbert, *QCPE Bulletin*, 10 (1990) 52.

125. W. Schneider and W. Thiel, *J. Chem. Phys.*, 89 (1987) 923.

126. E. Schroedinger, *Ann. Physik*, 79 (1926) 361.

127. M. Simonetta, "Forty Years of Valence Bond Theory in Structural Chemistry and Molecular Biology", Freeman, San Francisco, 1968.

128. K.C. Smyth, S.G. Lias, and P. Ausloos, *Conbust. Sci. Technol.*, 28 (1982) 147.

129. M. Speranza, M.D. Sefcik, J.M.S. Henis, and P.P. Gaspar, *J. Am. Chem. Soc.*, 99:17 (1977) 5583.

130. V. Staemmler and M. Jungen, *Chem. Phys. Lett.*, 16 (1972) 187.

131. R.H. Stanley, J.E. Klecker, and J.L. Beauchamp, *J. Am. Chem. Soc.*, 98 (1976) 2081.

132. J.J.P. Stewart, *J. Comput. Chem.*, 10 (1989) 221.

133. J.J.P. Stewart, *J. Comput. Chem.*, 10 (1989) 209.

134. J.J.P. Stewart, *J. Computer-Aided Mol. Des.*, 4 (1990) 1.

135. J.J.P. Stewart, QCPE, No. 455, version 6.0, (1990).

136. J.K. Terlouw, J.L. Holmes, and F.P. Lossing, *Can. J. Chem.*, 61 (1982) 1722.

137. C. Thomson and B.J. Wishart, *Theor. Chim. Acta*, 31 (1973) 347.

138. R.J. Van Zee, G.R. Smith, and W. Weltner, *J. Am. Chem. Soc.*, 110 (1988) 609.

139. A.A. Viggiano, F. Howorka, D.L. Albritton, F.C. Fehsenfeld, N.G. Adams, and D. Smith, *Ap. J.*, 236 (1980) 492.

140. C. Vinckier, M.P. Gardner, and K.D. Bayes, Symp. *(Int.) Combust., [Proc.]*, 16th, 1976 (1977) 881.

141. J. Vogt and J.L. Beachamp, *J. Am. Chem. Soc.*, 97 (1975) 6682.

142. S.P. Walch, *J. Chem. Phys.*, 72 (1980) 5679.

143. G. R. Wilkinson and M. K. Wilson, *J. Chem. Phys.*, 25 (1956) 784.

144. E. B. Wilson, J. C. Decius, P. C. Cross," Molecular Vibrations", McGraw-Hill, New York, 1955.

145. H. Wincel, S. Wlodek, and D.K. Bohme, *Int. J. Mass Spectrom. Ion. Processes*, 84 (1988) 69.

146. H. Wincel, R.H. Fokkens, and N.M.M. Nibbering, *Int. J. Mass Spectrom. Ion Processes*, 91 (1989) 339.

147. Y. Yamaguchi and H. F. Schaefer III, *J. Chem. Phys.*, 73 (1980) 2310.

148. S. Yamamoto, S. Saito, K. Kawaguchi, N. Kaifu, H. Suzuki, and M. Ohishi, *Ap. J.*, 317 (1987) L119.

149. The values of the sum of thermal energies were 54.3, 20.8 and 20.7 kJ mol^{-1} for C_3O, CO, and C_2 respectively.

150. The HF/6-311G**/MP2/6-311G**, MP2/6-311G** and MP4/6-311G**/MP2/6-311G** energies were -150.49925, -150.95005 and -150.91399 hartrees respectively.

151. The values of the sum of thermal energies were 47.3 and 14.7 kJ mol^{-1} for C_3S and CS respectively.

Physical Constants and Conversion Factors

Raw Constants

0.52917706 Ångstrom = 1 Bohr

$1.6605655 \times 10^{-27}$ Kilograms = 1 Atomic Mass Unit

4.803242×10^{-10} ESU = 1 Electron Charge

Planck's Constant = 6.626176×10^{-34} Joule-Seconds

Avogadro's Number = 6.022045×10^{23}

4.184 Joules = 1 Calorie.

4.359814×10^{-18} Joules = 1 Hartree

Speed of Light = $2.99792458 \times 10^{10}$ cm-sec^{-1}

Boltzmann Constant = 1.38066×10^{-23} Joules-Kelvin^{-1}

Inverse Fine Structure Constant = 137.03602

Molar Volume of Ideal Gas at 273.15 K = 0.02241383 meter^3

Conversion Factors

Electron Mass = 0.910953×10^{-30} Kilograms

1822.8880 Electron Mass = 1 Proton Mass

627.5095 KCal-Mol^{-1} = 1 Hartree

23.06035 KCal-Mol^{-1} = 1 Electron-Volt

2.541765 Debye = 1 Bohr-Electron

42.2547 KM-Mol^{-1} = 1 Debye^2-Ångstrom^{-2}-AMU^{-1}

5.82587×10^{-3} cm^{-2}-Atm^{-1} = 1 Debye^2-Ångstrom^{-2}-AMU^{-1}

(at standard temperature and pressure)

219474.7 cm^{-1} = 1 Hartree$^{-1/2}$-Bohr^{-1}-AMU$^{-1/2}$

Glossary of Symbols

Symbol	Meaning
H	One-electron matrix
F	Two-electron or Fock matrix
ϕ	Atomic orbital
μ, ν, λ, σ	Atomic orbital indices
ψ	Molecular orbital
i, j, k, l	Molecular orbital indices
A, B	Atomic indices
α	Alpha spin
β	Beta spin
ξ	Atomic orbital exponent
S	Overlap matrix
P	Density matrix
s, p_x, p_y, p_z	s, p_x, p_y and p_z atomic orbitals
(expression)	Dirac integral symbols
$(\mu\nu \mid \lambda\sigma)$	Two-electron integral
$(\mu \mid \nu)$	Overlap integral
$\delta_{\lambda\sigma}$	Kronecker delta, 1 if $\lambda = \sigma$
	otherwise 0
ε_i	Eigenvalues
Z	Nuclear or core charge